NTNU – Trondheim
Norwegian University of
Science and Technology

Wave Impact Forces on complex structures during lowering through the splash zone

Anders Selvåg

Subsea Technology
Submission date: June 2013
Supervisor: Sverre Steen, IMT
Co-supervisor: Mikal Dahle, Technip Norge AS

Norwegian University of Science and Technology
Department of Marine Technology

NTNU Trondheim
Norwegian University of Science and Technology
Faculty of Engineering Science and Technology
Department of MarineTechnology

M.Sc. thesis 2013

for

Anders Selvåg

Wave Impact Forces on complex structures during lowering through the splash zone

With increasing use of advanced subsea processing of the well stream of offshore oil and gas production, the problem of forces on structures being lowered through the wavy surface offshore is of increasing importance.

The candidate shall perform an analysis of the forces on the subsea compression module to be installed on the Åsgard Field. The analysis shall be based on calculations with Orcaflex and Sima to be performed by the candidate, as well as on experimental results from BGO First. The experimental results shall be analyzed and compared with the results of the numerical analyses. On the basis of the comparison, the validity of the numerical tools shall be discussed. Furthermore, recommendations for further work required to obtain the design loads shall be given.

The work is done in cooperation with Technip.

The candidate should in his report give a personal contribution to the solution of the problem formulated in this text. All assumptions and conclusions must be supported by mathematical models and/or references to physical effects in a logical manner.
The candidate should apply all available sources to find relevant literature and information on the actual problem.

The report should be well organised and give a clear presentation of the work and all conclusions. It is important that the text is well written and that tables and figures are used to support the verbal presentation. The report should be complete, but still as short as possible.

The final report must contain this text, an acknowledgement, summary, main body, conclusions, suggestions for further work, symbol list, references and appendices. All figures, tables and equations must be identified by numbers. References should be given by author and year in the text, and presented alphabetically in the reference list. The report must be submitted in two copies unless otherwise has been agreed with the supervisor.

The supervisor may require that the candidate should give a written plan that describes the progress of the work after having received this text. The plan may contain a table of content for the report and also assumed use of computer resources.

From the report it should be possible to identify the work carried out by the candidate and what has been found in the available literature. It is important to give references to the original source for theories and experimental results.

The report must be signed by the candidate, include this text, appear as a paperback, and - if needed - have a separate enclosure (binder, diskette or CD-ROM) with additional material.

Supervisor : Professor Sverre Steen
Start : 14.01.2013
Deadline : 10.06.2013

Trondheim, 10.01.2013

Sverre Steen
Supervisor

ABSTRACT

New oilfields are discovered further from land, at great depths and in harsh environments. Subsea developments of such fields are economical and preferred choice for operators today. One of the challenges is to process the well stream subsea. Statoil are continuously developing the technology and are going to launch the world's first subsea processing facility, the Åsgard Subsea Compression station. This facility requires maintenance and repair even in rough weather, to avoid economic losses. For marine operations dedicated to this task, dynamic responses are crucial in order to assess the safety level during lifts and work on deck.

The main objective of this thesis is to reduce the uncertainties related to numerical analysis of the wave impact process on the subsea compression modules. The wave impact on complex structures is in reality a complicated process considering the wave kinematics and the involved forces. Two programs, SIMO and Orcaflex, have been used to give an estimation of forces involved in the wave impact process on the complex compression module.

A model test focusing on the splash zone crossing phase was proposed and approved. The aim is to estimate the actual maximum forces in the splash zone and compare the forces against results obtained from the numerical simulations. The module was subjected to regular waves using three environmental conditions in four different elevations.

The numerical comparison between SIMO and Orcaflex shows that the main differences occur when the structure is suspended above the mean sea level. In these elevations the slamming forces are large which is believed to be the root cause of the observed differences. Orcaflex's and SIMO's calculation of slam forces are different and will give different results.

The comparison between the model test and the numerical analysis in SIMO and Orcaflex indicates that the numerical prediction of forces is conservative in most cases. In cases where the numerical models were not conservative, the involved forces are not very large and that the model test wave was not representing the regular wave theory in a sufficient way.

The comparison of forces in elevation 1 & 2 proved that Orcaflex's estimation of slam forces are conservative, when the slamming coefficient is based on slamming tests. The slamming forces in SIMO gives a good estimation of the forces compared to the model test results. As the modules are submerged the slam forces are less governing and Orcaflex's estimation is in many cases closer to the forces obtained in the model tests compared to SIMO.

ACKNOWLEDGEMENTS

This work has been carried out under the supervision of Professor Sverre Steen, at the Norwegian University of Science and Technology. His contributions have been highly appreciated.

I would like to dedicate a special thanks to the Technip office in Stavanger, for continuous guidance and contributions. Rafael, Loic Ingrid and Xiao, your help has been highly valued. A special thanks to Leif Kaare Adolfsen and Mikal Dahle for sending me off to France to take part in the model testing.

I would also like to thank Mariann Morvik for her proof reading and her patience during the final weeks.

CONTENTS

Figure List:

List of Tables:

NOMENCLATURE

General rules:

- Symbols are generally defined where they appear the first time, and will not be repeated a second time.
- All matrixes are represented by bold face characters

Abbreviations:

6D	-	Six dimensions
3D	-	Three dimensional
BGO	-	Bassin de Génie Océanique
COG	-	Center Of Gravity
DOF	-	Degrees Of Freedom
DNV	-	Det Norske Veritas
FFT	-	Fast Fourier Transform
FK	-	Froude-Krylov
IMR	-	Inspection, Maintenance and Repair
KC	-	Keulegan-Carpenter
NTNU	-	Norwegian University of Science and technology
MATLAB	-	Matrix laboratory
MSL	-	Mean Sea Level
PW	-	Proportion Wet
PVC	-	Polyvinyl chloride
ROV	-	Remotely Operated Vehicle
SIMO	-	Simulation of marine Operations
SHS	-	Special Handling System
WBM	-	Wagner's based method
ÅSC	-	Åsgard Subsea Compression

Roman symbols:

A	-	Drag area
a	-	Amplitude of motion
A_{Box-X}	-	Total area of module in x-direction
A_{CS}	-	Beam cross section area
a_E	-	Fluid acceleration relative to the earth
$\mathbf{a_L}$	-	Wave particle acceleration in local strip coordinate system, $[x,y,z]^T$
A_I	-	Inner beam area
A_{ij}	-	Added mass in local X or Y, per unit length
A_w	-	Slam area
a_x	-	Acceleration component in x-direction
A_x	-	Projected area in x-direction for each structural element
AM_x	-	Added mass in x-direction for each structural element (incl. plates)
B	-	With of beam
C_a	-	Drag coefficient
C_e	-	Water exit slam coefficient ($C_s/2$)
$\mathbf{C_l}$	-	distributed linear drag for strip, $[x,y,z]^T$

C_m	-	Added mass coefficient
C_s	-	Water entry slam coefficient
$\mathbf{C_q}$	-	distributed quadratic drag for strip, $[x,y,z]^T$
d	-	Water depth
D_n	-	Drag diameter
E(z)	-	Exponential decay term
F_s	-	Slam force
$\mathbf{F_{W,S}}$	-	wave force on strip, $[x,y,z]^T$
g	-	Acceleration of gravity
h	-	Distance between the instantaneous surface elevation and strip origin in global Z-direction. Time
H	-	Height of beam
ID_{Beam}	-	Beam equivalent inner diameter
k	-	Wave number, $k = \frac{\omega^2}{g}$
L	-	Length of line
M	-	Model mass, in kg
$\mathbf{m_a}$	-	distributed added mass of strip, $[x,y,z]^T$
n	-	Unit vector normal to the water surface
OD_{Beam}	-	Beam equivalent outer diameter
PW	-	Proportion wet
S	-	Drag surface
S_s	-	Slam Area
T	-	Time
$\boldsymbol{U_S}$	-	current flow velocity in local strip coordinate system, $[x,y,z]^T$
V_n	-	Component of buoy velocity normal to the surface
V_N	-	Fluid velocity normal to the body
V_M	-	Volume of displaced fluid
V_{PW}	-	Proportion wet
V_r	-	Fluid velocity relative to the body
V_{ref}	-	Reference volume
V_S	-	submerged volume per strip length, calculated up to z = 0
V_s	-	Water entry speed
$\mathbf{v_S}$	-	wave particle velocity in local strip coordinate system, $[x,y,z]^T$
v_x	-	Velocity component in x-direction
$\dot{\boldsymbol{x}}_{\boldsymbol{S}}$	-	strip velocity in local strip coordinate system, $[x,y,z]^T$

Greek symbols:

β	-	Direction of wave propagation, β = 0 corresponds to wave propagation along the positive x-axis.
ζ	-	Wave elevation
ζ_a	-	Wave amplitude
π	-	The constant 3.1419…
Φ	-	Wave potential
ϕ_ζ	-	Wave component phase angle
ρ	-	Seawater density
ω	-	Wave angular frequency
Δ	-	Mass of the fluid displaced by the body

CHAPTER 1

Introduction

1.1 BACKGROUND

New oilfields are discovered further from land, at great depths and in harsh environments. Subsea developments of such fields are economical and preferred choice for operators today. Statoil is one of the main contributors to developing new technology to the subsea industry. Statoil's goal is to be able to develop all elements required for a remote controlled subsea factory by 2020 (Statoil, 2012). New developments such as subsea compression extend the expected lifetime of the field, as well as the recovered oil and gas (Statoil, 2013). These solutions require maintenance and repair even in rough weather, to avoid economic losses. For marine operations dedicated to this task, dynamic responses are crucial in order to assess the safety level during lifts and work on deck.

Traditionally, marine operations have been carried out based on practical marine experience. This is still an important aspect of the operation, but as structures become larger and more complex an accurate estimation of the dynamic responses is needed. Analytical programs such as Orcaflex and Simulation of Marine Operations (SIMO) are used for such purposes. The main challenge when analyzing complex structures is to build a numerical model which will accurately represent the full scale model. Programs such as these do not include all hydrodynamic effects such as, interaction between the structural members and hydroelasticity (See section Assumptions for details). These effects will contribute to a difference between the real life measurements and the numerical models. It is assumed that these differences will increase as the structure becomes more complex.

Challenges connected to marine operations in rough weather and accurate numerical simulations emerged when the Åsgard Subsea Compression (ÅSC) project started. The subsea modules are very large and heavy, and the margin for error in the numerical models had to be small if the project was going to be successful.

1.2 ÅSGARD FIELD

The oil, gas and condensate field Åsgard lies on Haltenbanken, a field located 200 km north west of Trondheim. This area is known for its harsh weather conditions. Åsgard is one of the most developed fields on the Norwegian continental shelf, with 52 wells drilled through 16 different templates. With a water depth ranging from 250–325 meters, floaters are used to produce the fields. The production ship Åsgard A produces oil, Åsgard B is a floating gas production platform and Åsgard C is a storage ship for condensate gas (Statoil, 2013).

The Åsgard field has for several years experienced what operators fear; a pressure loss and decreasing production. If the production continues without the subsea compressor the natural pressure from the wells will be too low to maintain a stable gas and condensate flow. Even in the early stages of production it was decided that the Åsgard field would be a suitable place to develop the world's first subsea compression facility. This was due to its location and the importance of the Åsgard field's contribution to Norway's gas export.

The ÅSC is expected to add 15 years to the producing life and improve recovery from the field with 278 million barrels of oil equivalent. This is achieved by compressing and separating the condensate and gas from the well production subsea, and boost gas back into the flow lines for transport to Åsgard B, 40 kilometers away. The compression process requires a big processing facility even on land. The subsea compression facility will measure 75m x 45m x 20m. The facility consists of two identical compressor trains with 6 different process modules in each train. Each of the modules has its own task and needs to be replaced quickly to avoid production shutdown (Dahle, 2012). The compression process is given in Appendix 1

Figure 1 Illustration of the facility's dimensions. Here at Ullevål Stadium. (Source: Technip 2012)

After several years of testing Statoil selected a compact horizontal centrifugal compressor, delivered by MAN Diesel & Turbo. The compressor has active magnetic bearings and an 11.5 megawatt (MW) motor. The compressor proved reliable and has the necessary capabilities (Knott, 2011). Maintenance is expected after ~2.5 years but large gas compressors on land have a reputation of being temperamental and might be replaced at an earlier stage (Knott, 2013).

The compressor module has a complex supporting structure and is one of the heaviest lifts connected to the ÅSC station. The module will weigh 333 Te and measure 10 meters

high, 8 meters wide and 11 meters long, according to the latest weight report from Aker Solutions (AkerSolutions, 2012). Due to the weight and large hydrodynamic forces in the splash zone the compressor module is suitable for a comparison task.

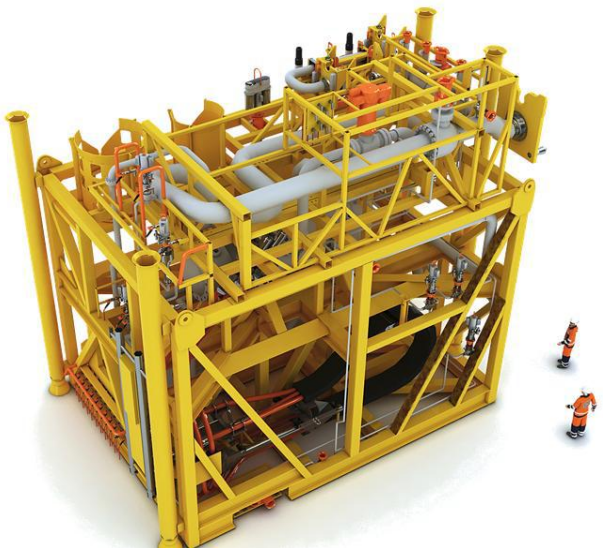

Figure 2 Illustration of the compressor modules dimensions

1.3 MARINE OPERATIONS

Technip Norge was awarded the contract for all marine operations connected to the compression facility by Statoil. The contract entailed that the requirements for the subsea facility downtime should not be less than for a topside plant. The requirement for a topside plant is more than 95% producing time, which is equivalent to 347 days per year (Dahle, 2012).

What if one of the modules breaks down? The short response time means that any repair or intervention must be possible to carry out in rough weather conditions. Based on weather reports from that area the requirement of 95% up-time would indicate that the marine operations must be carried out in 4m-5m Hs. Due to the large and heavy modules, the capacity is exceeded for all current IMR assets today.

The goal of deploying modules in such conditions will not be possible to achieve with today's methods for lifting through the splash zone. A new type of marine operation handling system needed to be invented. Technip has developed the Special Handling System (SHS) which is capable of such lifts, see figure 3. SHS is a crane which controls the modules in all degrees of freedom.

Figure 3 The SHS system attached to North Sea Giant (Source: (Tecnip_Aagard_B_Final, 2012))

1.4 THE SPECIAL HANDLIG SYSTEM

The Special Handling System (SHS) is shown in figure 4 and consists of a tower structure which has the ability to rotate around the tower axis. The tower is equipped with two cursor rails and two main lift winches with a wire routed between them. The sliding frame (2) is attached to the rails using the sliding pads (1) and can slide up and down on the tower and onto the preinstalled cursor rails on the vessel's side, see figure 5. The damping frame (4) and the dampers (3 & 5) will allow for movements up to 10 degrees in roll and pitch when the module is suspended in the tower. The docking frame (6) is equipped with release mechanisms to detach the lifting beam (7) and the upper adapter frame (8). The upper adapter frame is able to mount the 6 different modules using 6 customized lower adapter frames (10). The upper and lower adapter frame is welded together. The guide pins (9) guide the adapter frame into the docking frame. A detailed description of the frame assembly is given in Appendix 2.

The module is connected to the lower adapter frame through 4 pad eyes with hydraulic locking. The adapter frame will be attached to the module during seabed deployment.

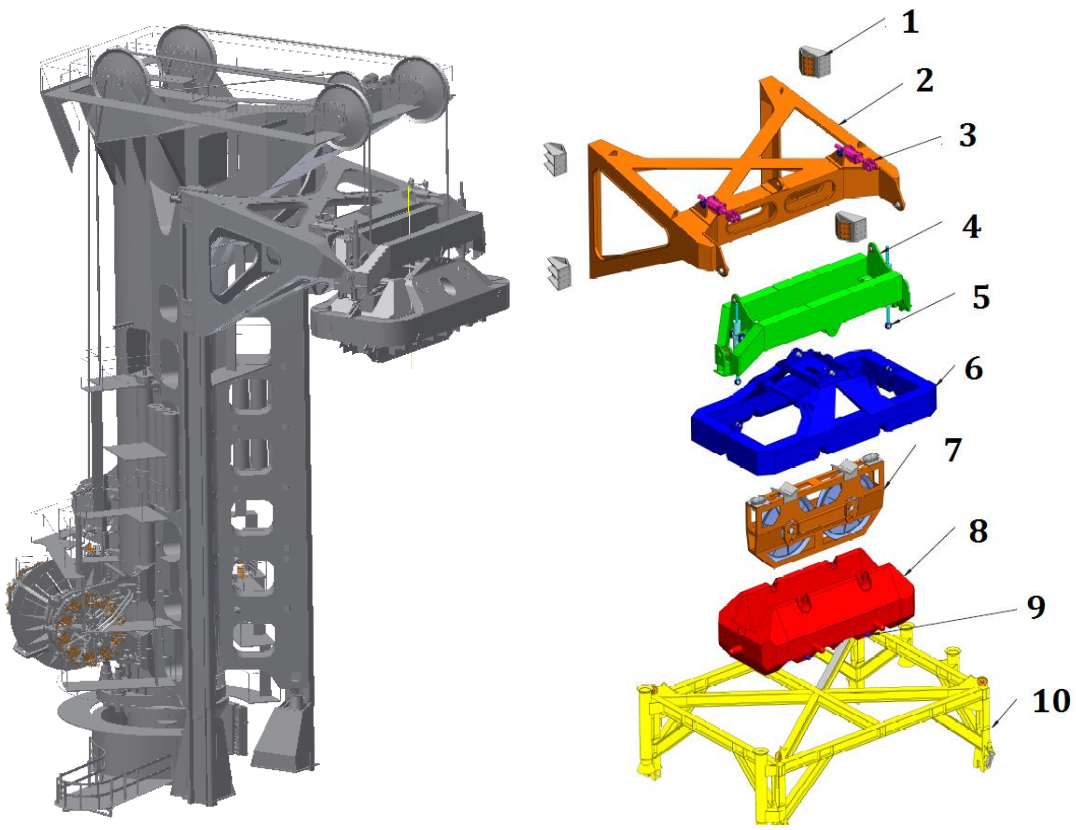

Figure 4 The SHS tower (left), the SHS lifting frame (right)

1.4.1 SHS Deployment procedure

The tower will pick up the module on deck and attach it to the tower structure trough the sliding frame and the customized adapter frame, see figure 5. The module will be lifted from deck and swung over the side. The module and the sliding frame will be lowered on the cursor rails and further down onto the vessels rails. This will allow for a deep deployment of the module. The docking frame will release the lifting beam and all frames below, when the module is suspended below the vessel, as shown in figure 5. All frames below the lifting frame will follow the module down to the seabed (Tecnip_Aagard_B_Final, 2012)

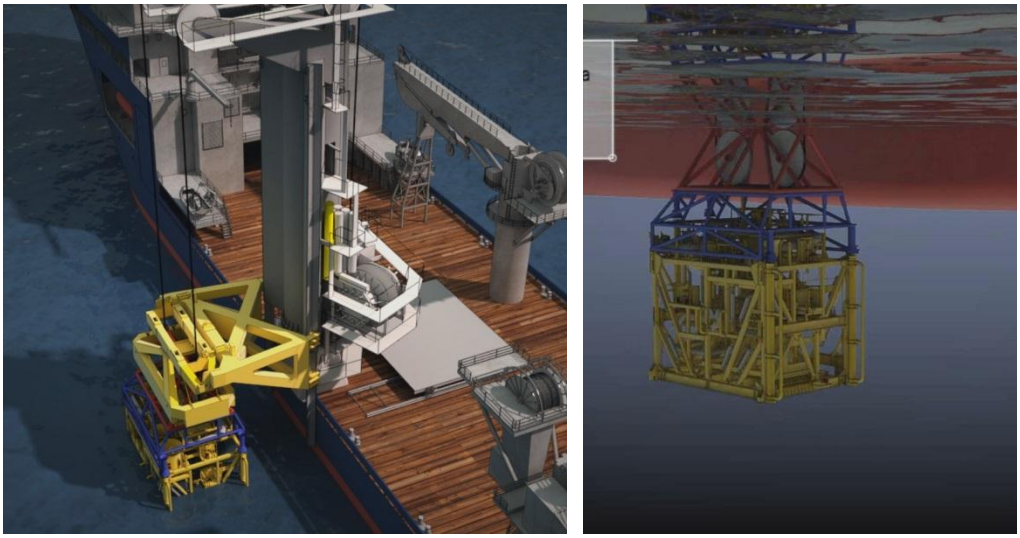

Figure 5 The compressor module partly submerged (left) and fully submerged (right) when connected to the SHS.

The module is lowered with an approximate speed of 0.5 m/s. The active heave compensator is activated during landing. The module is landed inside the Åsgard template using preinstalled guideposts and ROV operated guide wires. The four pad eyes disconnect the module from the frame and allow retrieval of the adapter frames.

Note: The SHS is under constant development. The presented description is dated 21.05.2013

1.5 NUMERICAL SIMULATIONS OF MARINE OPERATIONS

Technip is using Orcaflex to analyze the marine operations connected to the SHS operations. Orcaflex is a marine dynamics program developed by Orcina and considered a reliable program within the offshore industry for most types of dynamic marine systems.

SIMO is developed and maintained by Marintek and is a trusted program for prediction of forces in the splash zone. The program is mainly developed for complex marine operations and station keeping.

These programs handle the numerical calculations in different ways (See Comparison theory), and in some cases the results will give different operational limits. Are the programs able to predict reliable dynamic responses in the splash zone crossing phase? Concerns have been raised by recognized scientists within the marine technology field such as O. Faltinsen (Technip, 2013). O. Faltinsen recommends that the numerical simulation should be compared against results from a model tests under similar conditions. If the numerical solution underestimates the hydrodynamic forces, actions must be taken to prevent accidents during operations with the SHS. The main focus in this thesis is to investigate differences in the results from numerical simulations in Orcaflex and SIMO against results from model testing. By doing so an estimation of the uncertainties related to the numerical simulation can be established.

1.6 PREVIOUS WORK

All structural elements in the splash zone are affected by hydrodynamic forces and loads. In lifting operations structures may be subjected to impulsive vertical loads several times larger than those experienced by continuously submerged elements. The need to estimate all hydrodynamic loads accurately are crucial to achieve a safe working condition for both personnel and equipment involved in the SHS lifting operation. A solid understanding of the wave impact process on the basis of theoretical and experimental analysis is needed on order to compare and predict results. Most of the theoretical studies are based on common objects such as pipes and plates, and is not directly applicable when analyzing the compressor module, but used to interpret problems related to hydrodynamics and the wave impact process on the compressor module.

1.6.1 Theoretical studies

Wagner (1932) developed an analytical solution for the initial impact of beams and wedges on a calm free surface. The expression provided good results for small dead rise angels. This method was used by R.J. Baarholm and O. Faltinsen to develop a generalized Wagner's based method (WBM) for solving the impact process of a wave that reaches the deck at the front end of a platform and propagates downstream along the length of the deck. To validate the theory experiments were carried out (Baarholm, 2001).

The Kaplan theory was presented at the Offshore Technology Conference, in Houston Texas 1992. His method combines the momentum- and drag- force analysis. The result is a time varying vertical force which gives a good prediction of the initial stages of the impact. The analytical results where compared briefly with existing field data and indicated that the variation showed a large discontinuity when the plate was fully submerged (Kaplan, 1992).

Fall 2012, the author of this thesis, carried out a wave impact study on perforated plates. Two analytical approaches were used to estimate the vertical forces on the plate, one by SIMO and calculations in MATLAB based on Kaplans theories. The results indicated that by using the Kaplan theory the results were conservative compared to the SIMO results. These differences were believed to originate from the depth dependent hydrodynamic coefficients input in SIMO, as well as some difference in the slamming calculations (Selvåg, 2012).

A preliminary comparison between SIMO and Orcaflex were carried out by Ingrid Angvik at Technip Norge AS. The analyzed object was a simple beam submerged with different depths hanging by a wire. The conclusion when comparing the results were that SIMO are generally less conservative than OrcaFlex. The differences were largest when the analyzed beam was in the splash zone. In a few cases SIMO has the largest forces, but in these cases the increased wire tension happened over time (Angvik, 2012).

1.6.2 Experimental studies

R.J. Baarholm and O. Faltinsen have carried out experimental studies of the wave impact underneath decks of offshore platforms. The experimental work was carried out at MARINTEK laboratories. The comparison between experiments and analytical solutions shows that both the magnitude and the duration of the positive force peak are well

predicted. However during the water-exit phase the WBM overestimates the F_{Min} and underestimates the duration of the impact process. The free surface becomes strongly deformed as the wave is propagating along the deck, and is believed to be one of the contributing factors to inaccurate results (Baarholm, 2001).

Slamming related experiments have been carried out to predict the wave impact forces on circular cylinders involving the use of a slamming coefficient. Theoretical models have indicated that the maximum slamming coefficient is $C_S = \pi$ [(Campbell, 1980) & (Sarpkaya, 1978)] while experiments show that there is considerable degree of scatter in the estimated slamming coefficient. Based on experiments carried out by Sharpkaya an empirical formulation stating that the slamming coefficient,C_S, lies between 0.5 and 1.7 times the theoretical value (Sarpkaya, 1978). His estimations depend strongly on the risetime and the natural frequency of the cylinder (Sarpkaya, 1978).

An experimental study was carried out by Bureau Veritas Research Department (Hauteclocque, 2009) to measure slamming effects on solid and perforated mudmats. The experiments show that when using the solid mudmat with trapped air underneath the initial vertical force was smaller compared to the perforated mudmat with no air cushion. SIMO and Orcaflex use potential flow theory to calculate slamming forces. Several important hydrodynamic phenomenons are neglected when using this theory. It is assumed that the pressure is constant and equal to atmospheric pressure on the free surface. This is not the case when a flat structure hits the free surface. This process will in some cases create an air cushion under the structure which will reduce the pressure. In the current versions of SIMO and Orcaflex air cushion is not accounted for, hence the slam force will always decrease with perforated plates or structures.

1.7 OUTLINE OF THESIS

The thesis is mainly divided into three parts, an experimental study, a numerical comparison of forces in SIMO and Orcaflex, and a final comparison between the experimental study and the numerical simulations.

The first part is the experimental study of forces in regular waves in chapter 4 and the estimation of global coefficients in chapter 5. The experimental setup is described and the findings are discussed.

The second part is the numerical comparison. Chapter 6 describes how the model is made in the numerical programs and a comparison of the numerical results is discussed. In addition, some cases are presented where the force contributions have been separated to provide a better understanding of the governing forces.

The third part is chapter 7. This chapter will contain the comparison of the maximum and minimum values in the experimental study and the numerical simulations. Some relevant cases have been studied to analyze the wave impact process more closely. General trends and possible error sources is discussed.

Finally, the main conclusions and suggestions for further work is presented in chapter 8

CHAPTER 2

Theory

The numerical simulations are based on assumptions related to wave particle kinematics and fluid force estimation on objects. A general understanding of the theory behind the programs is important to be able to analyze the results and compare data against results obtained from the model test. This chapter will highlight important theory related to the solution of the wave impact forces.

Orcaflex and SIMO theory is presented. A small comparison of the theory is presented to better understand the main differences in the force calculation in the two programs.

The model test has been carried out using Stokes 5^{th} waves. Due to limitations in SIMO, waves according to Airy's theory have been used in the numerical simulation. The two regular wave theories have been compared to understand the fluid particle behavior and how this may impact the final comparison between the numerical simulation and the model test.

2.1 ORCAFLEX THEORY

Orcaflex is a frequently used program within the offshore industry due to its graphical- and easy-to-use interface. The program has the capabilities to analyze a number of marine operations such as pipelay-, riser- and splash zone analysis. Orcaflex is a non-linear time domain finite element program developed by Orcina. The program use "lumped mass" elements and "6D-bouys", to simulate structural elements such as beams, pipes and plates. The elements will simplify the mathematical formulation and reduce the overall computational time. The hydrodynamic forces are calculated based on an extended version of the Morison equation and cross flow assumptions. The theory is written according to the Orcaflex Manual, version 9.6a (Orcina, 2013).

2.1.1 Environment

The "Single Airy" wave is used in the Orcaflex calculations. This theory is extended to account for wave kinematics for points above the mean water level. The Single Airy wave theory, in Orcaflex, is described by the following wave potential:

$$\Phi_0 = \frac{\omega\zeta_a}{k}\frac{\cosh k(z+d)}{\sinh kd}\sin(kx-\omega t) \tag{5.1}$$

Where:

ζ_a	-	Wave amplitude
Φ	-	Wave potential
ω	-	Wave angular frequency
k	-	Wave number, $k = \frac{\omega^2}{g}$
d	-	Water depth
t	-	Time

When describing waves and wave induced responses the surface elevation, ζ, is used as a reference. The surface elevation is given by:

$$\zeta = \zeta_a \cos(kx-\omega t) \tag{5.2}$$

Where:

ζ	-	Wave elevation

The horizontal particle velocity v_x in an undisturbed wave field propagating in the positive x direction is given by the formula at position (x,z) at time, t, as:

$$v_x = \zeta_a E(z)\omega\cos(\omega t-\phi-kx) \tag{5.3}$$

$$a_x = \zeta_a E(z)\omega^2\sin(\omega t-\phi-kx) \tag{5.4}$$

Where:

v_x	-	Velocity component in x-direction
a_x	-	Acceleration component in x-direction
E(z)	-	Exponential decay term

The E(z) is an exponential decay term that simulates a decrease in the fluid velocity and acceleration as the point (x,z) goes deeper i.e, z>0.

The linear potential flow theory is limited to the mean water level and does not calculate accelerations and velocities above the mean water line. To cover points above the free surface Orcaflex allows for artificial stretching of the wave kinematics. For comparison purposes “Vertical Stretching” is used, i.e. for z<0 the E(z) term is left unchanged and according to the linear potential flow theory. Above mean water level z>0, E(z) is replaced by E(0).

2.1.2 Force models

The hydrodynamic load formulation is presented for line elements. The line element will be the main element used to describe loads on the structure.

The slamming loads are calculated using a 6D-bouy and will be presented in the following sections. The 6D-buoy element hydrodynamic calculation for drag inertia and buoyancy is given in the Orcaflex manual.

2.1.2.1 Bodies

Two types of elements are used to simulate the hydrodynamic and structural properties for the compressor module; line elements and 6D buoy elements. The total force on the module is a sum of all contributions. The lines will represent the structural elements and the 6D buoys will account for other contributions such as slam force, weight, buoyancy etc.

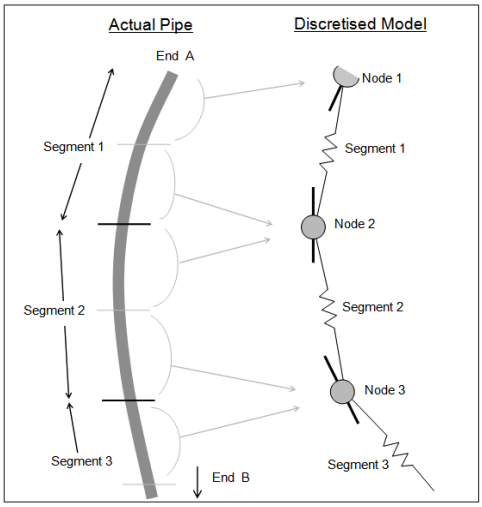

Figure 6 Illustration of the line setup in Orcaflex (Source: Orcaflex manual)

The line consists of several massless segments with nodes attached at each end, as shown in figure 6. The segments will model the axial and torsional stiffness of the line. For properties such as drag, mass, weight and buoyancy the segment properties are divided and assigned to each node. All fluid related forces are applied at the nodes.

The 6D-buoy is treated as a body with the ability to move in 6 degrees of freedom. The 6D-bouy is assigned to the model to account for additional hydrodynamic properties such as drag, slam force, weight, buoyancy, etc. The buoy can be assigned with only one property for example weight to calibrate the center of gravity (COG). Three different types of buoys can be used; lumped buoy, spar buoy and towed fish. Lumped buoy is used in the current analysis. The lumped buoy can be specified without a reference to a specific geometry.

2.1.2.2 Buoyancy forces

The buoyancy force for line elements is acting in the global Z-direction and applied at each node. The node will represent two half segments and will allow for the varying wetted length up to the instantaneous free surface. The force is scaled using the proportion wet, see section 2.1.3.

$$F_B(t) = \rho g * V_{PW} \tag{5.5}$$

Where:

V_{PW} - Proportion wet
ρ - Seawater density

2.1.2.3 Wave excitation forces on line elements

Orcaflex uses an extended form of the Morison equation to account for the movement of the body. The hydrodynamic forces, F_W, are calculated per unit length along each line according to strip theory. The hydrodynamic force on line element consists of two force components, one related to the inertia force F_i and the second to the water particle velocity F_d, drag.

$$F_W = F_I + F_D \tag{5.6}$$

Inertia force:

$$F_I = \Delta a_E + C_m \Delta a_E \tag{5.7}$$

Where:

Δ - Mass of the fluid displaced by the body
a_E - Fluid acceleration relative to the earth
C_m - Added mass coefficient

The inertia force, F_I, is consisting of two force contributions. One is the hydrodynamic force acting on the displaced fluid in the absence of the body (Froude-Krylov component), and one additional force due to the accelerated water particle induced by the presence of the body (added mass component).

To account for free flooding guideposts and pipes, the line contents can be specified as "Free-Flooding". The flooding is according to the instantaneous water surface and the content is according to the properties set for sea water. Additional inertia forces due to the trapped water are accounted for in the analysis.

Drag force:

$$F_D = \frac{1}{2} \rho V_r |V_r| C_a A \tag{5.8}$$

Where:

V_r	-	Fluid velocity relative to the body
C_a	-	Drag coefficient
A	-	Drag area

The drag is calculated by using the cross flow principle, and by using the local line coordinates the fluid velocities will act parallel or normal to the line. The drag and added mass coefficients in different directions can be implemented to account for rectangular beams and plates. The drag coefficients are specified as constant in this analysis.

2.1.2.4 Slam force

The slam force is applied to the numerical model by inserting lumped 6D buoys. The formulation of the slam force is similar to the recommended practice in DNV-RP-H103 (Det Norske Veritas, 2011). The 6D-buoys calculates forces for both water entry and water exit.

$$F_{S,Entry} = \frac{1}{2}\rho\, C_s\, A_w\, |V_n|^2\, n \tag{5.9}$$

$$F_{S,Exit} = -\frac{1}{2}\rho\, C_e\, A_w\, |V_n|^2\, n \tag{5.10}$$

Where:

V_n	-	Component of buoy velocity normal to the surface
C_s	-	Water entry slam coefficient
n	-	Unit vector normal to the water surface
C_e	-	Water exit slam coefficient = $C_s/2$
A_w	-	Slam area

The calculation of slam force in Orcaflex differs from the DNV in one way. The slam force in Orcaflex is applied normal to the water surface by using the unit normal vector, allowing for a horizontal slamming component. In DNV-RP-H103 the forces will only act in the vertical direction.

The slam force contribution acts at the same point as the wave excitation force, i.e. the center of the wetted volume. In the idealized slamming theory, the duration of slamming pressure measured in one place is in the range of milliseconds. This means that the slamming force should be applied immediately. For a lumped buoy the slam force is ramped up to 110% of its full value over the first 10% of the buoys passage through the surface. The ramping is shown in the figure 7.

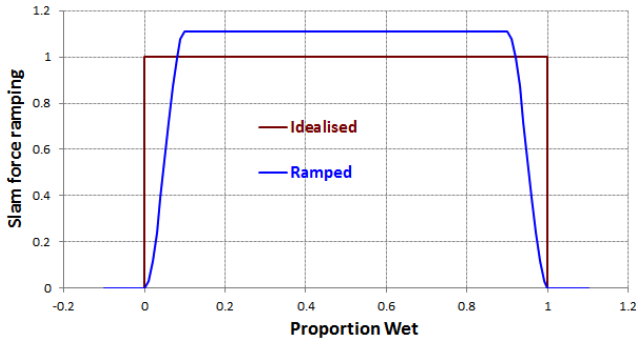

Figure 7 The ramping of slam forces in Orcaflex (Source: Orcaflex Manual)

Orcaflex includes water exit slam forces to account for additional loads when a body exits the free surface. The force generated during the water exit is often assumed negligible but included in the Orcaflex calculations (Orcina, 2013).

2.1.3 Surface piercing objects

For surface piercing objects, the hydrodynamic forces and hydrostatic pressure is calculated depending on how much the object is submerged. All lines in Orcaflex are divided into segments with a node at each end, see figure 8. The amount of submerged segments scales the proportion wet for each line.

Orcaflex has developed a solution to the problem when using the segment centerline. This method will not converge when the segment is tangent to the surface. By using a diagonal line across the segment combining the lowest point and the dry end, the diagonal line will switch ends as the segment passes through the tangential position. By applying this method the forces are assigned to the appropriate node and the proportional wet will vary continuously.

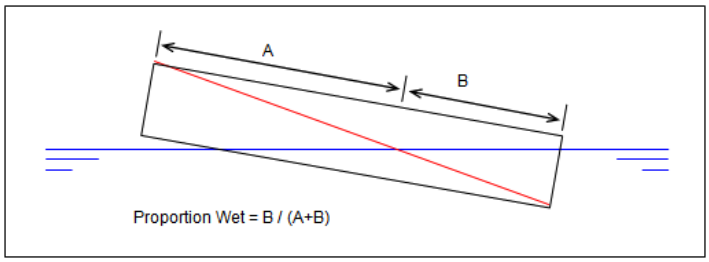

Figure 8 Illustration of method calculating the proportion wet

2.1.4 Numerical integration

Two integration methods can be selected in Orcaflex. An implicit integration scheme based on a generalized α integration described by (Hulbert, 1993). This method solves the system equation at the end of each time series. Additional information is given in the Orcaflex manual (Orcina, 2013).

2.2 SIMA THEORY

SIMA is used to estimate the wave impact force on the module. This is a program developed by MARINTEK and is a graphical representation of SIMO (Simulation of Marine Operations). SIMO is a time domain simulation program for study of motions and station keeping of multi body systems. The program allows non-linear effects to be included in the wave frequency range. The program is based on potential flow theory which assumes that oscillation amplitudes of the fluid and the body are small relative to the cross-sectional dimensions of the body.

This chapter will highlight important aspects connected to SIMO's force calculations. All theory is written according to the SIMO User Manual and SIMO Theory Manual (SIMO Project team, 2004) & (SIMO Project team, 2010).

2.2.1 Environment

For a regular wave setup in SIMO, linear wave potential theory is used. The undisturbed wave field is determined by the wave potential, Φ_0, which will define a long crested sinusoidal wave. The wave potential is written according to Airy's theory:

$$\Phi_0 = \frac{\zeta_a g}{\omega}\frac{\cosh k(z+d)}{\cosh kd}\cos\left(\omega t - kx\cos\beta - ky\sin\beta + \phi_\zeta\right) \tag{5.11}$$

Where:

g	-	Acceleration of gravity
β	-	Direction of wave propagation, β = 0 corresponds to wave propagation along the positive x-axis.
ϕ_ζ	-	Wave component phase angle

The wave potential can be extracted at the coordinates x, y and z.

The surface elevation ζ, is used as a reference when calculating hydrodynamic forces on "slender Elements" and "Fixed Body elements". The surface elevation, ζ, is given by:

$$\zeta = \zeta_a \sin\alpha \tag{5.12}$$

Where:
$\alpha = \omega t + \phi_p + \phi_\zeta$.
$\phi_p = -kx\cos\beta - ky\sin\beta$.

The horizontal velocity and the acceleration for a wave propagating along the positive x-axis in the undisturbed wave field are given as:

$$v_x = \zeta_a \omega \frac{\cosh\left(k(d+z)\right)}{\sinh(kd)}\sin\left(\omega t - kx + \phi_\zeta\right) \tag{5.13}$$

$$a_x = \zeta_a \omega^2 \frac{\cosh\left(k(d+z)\right)}{\sinh(kd)}\cos\left(\omega t - kx + \phi_\zeta\right) \tag{5.14}$$

For wave particle velocity and accelerations above the mean water level, z<0, values for z = 0 is used, see details in section 2.1.1 (Orcaflex). Full review of the wave particle velocities and accelerations can be found in SIMO theory manual.

2.2.2 Force models

2.2.2.1 Bodies

Two main types of bodies are used in this analysis. These can be defined as “large volume body” and “small volume body”. These bodies are used in combination to obtain a model for comparison purposes. One “large volume body” is used and fixed in space. “Small volume bodies”, such as “Slender Elements” and “Fixed body elements”, are attached to the larger body. The calculated forces on the small volume bodies are transferred to the “large volume body”.

The loading on the small volume bodies are described using depth-dependent hydrodynamic coefficients. This is used where the viscous hydrodynamic forces are important and subjected to small diffraction forces. The small volume bodies can be divided into two groups; “Slender elements” and “Fixed body elements”. Both elements are completely rigid and will not deflect in any way when subjected to wave forces. In this analysis the “Slender elements” are used to simulate the beams and pipes, and “Fixed body elements” is used to simulate the plating.

2.2.2.2 Wave excitation forces

The hydrodynamic force on a small volume body is calculated based on Morison’s formula. The external load on the slender element is divided into four contributions:

$$\boldsymbol{F_{TOT,body} = F_{b,\sum ds} + F_{G,\sum ds} + F_{W,\sum ds} + F_{S,\sum ds}} \tag{5.15}$$

- Buoyancy forces (F_b)
- Gravity forces (F_g)
- Wave forces (F_w)
- Slamming forces (F_S)

The force contribution from each strip is summed up for each slender element, making one resulting force. The total force acting on the body is the sum of all resulting forces.

Gravity forces are not accounted for in this analysis.

2.2.2.3 Buoyancy forces

The buoyancy force acts in the positive global Z-direction through the center of buoyancy of the element. By using Depth-Dependent hydrodynamic coefficients the volume can be adjusted as a function of submergence.

$$F_b(t) = \begin{bmatrix} 0 \\ 0 \\ \rho g V \end{bmatrix} \tag{5.16}$$

Where:

V - submerged volume

The buoyancy force is integrated up to the still water level. For elements crossing the surface the buoyancy from z = 0 to z = ζ is an adjustment to the Froude-Krylov force.

2.2.2.4 Wave forces

The wave force is acting through the center of buoyancy for each strip. The direction of the load vector is defined by the local coordinate system for each slender element.

The following equation is describing the wave force on a strip used in SIMO.

$$\begin{aligned} \boldsymbol{F_{W,S}} = (\rho V_S + \boldsymbol{m_a})\boldsymbol{a_L} + \boldsymbol{C_q}\{(\dot{\boldsymbol{x}}_{\boldsymbol{S}} - \boldsymbol{U_S} - \boldsymbol{v_S})|\dot{\boldsymbol{x}}_{\boldsymbol{S}} - \boldsymbol{U_S} - \boldsymbol{v_S}|\} \\ + \boldsymbol{C_l}(\dot{\boldsymbol{x}}_{\boldsymbol{S}} - \boldsymbol{U_S} - \boldsymbol{v_S}) \end{aligned} \tag{5.17}$$

Where:

$\mathbf{F_{W,S}}$ - wave force on strip, $[x,y,z]^T$

V_S - submerged volume per strip length, calculated up to z = 0

$\boldsymbol{U_S}$ - current flow velocity in local strip coordinate system, $[x,y,z]^T$

$\mathbf{m_a}$ - distributed added mass of strip, $[x,y,z]^T$

$\mathbf{a_L}$ - wave particle acceleration in local strip coordinate system, $[x,y,z]^T$

$\mathbf{C_q}$ - distributed quadratic drag for strip, $[x,y,z]^T$

$\dot{\boldsymbol{x}}_{\boldsymbol{S}}$ - strip velocity in local strip coordinate system, $[x,y,z]^T$

$\boldsymbol{v_S}$ - wave particle velocity in local strip coordinate system, $[x,y,z]^T$

$\mathbf{C_l}$ - distributed linear drag for strip, $[x,y,z]^T$

The first term contains the Froude-Krylov and diffraction force. The diffraction force represents change in the undisturbed pressure field due to the presence of a body. The second term describes the quadratic drag term of the Morrison formula. The third term represents the linear drag and is not accounted for in this analysis.

The wave kinematics in SIMO is calculated based on the Fast Fourier Transform (FFT). The FFT assumes that the body has the same position during the simulation. The method pre-generates wave kinematics at the surface at all relevant horizontal positions, and makes depth correction to the actual depth at each time step.

Free flooding of structural elements is accounted for by including the trapped water in the added mass input. The additional added mass is calculated based on the trapped water per meter.

Note: The rate of change in added mass is used as slam force input. By including trapped water in the added mass input the slam force on the free flooded structural elements may be over predicted. This will only influence horizontal elements. Only vertical free flooded elements are used in the current analysis.

2.2.2.5 Slam force

The slamming force is related to the change in added mass with time. The slamming force is expressed in local strip coordinates.

$$\boldsymbol{F_{S,S}} = -\frac{\partial \mathrm{m_s}}{\partial \mathrm{t}}\dot{\boldsymbol{x}}_{\boldsymbol{S}} = -\frac{\partial \mathrm{m_s}}{\partial \mathrm{t}}\frac{\partial \mathrm{h}}{\partial \mathrm{t}}\dot{\boldsymbol{x}}_{\boldsymbol{S}}$$

$$= \frac{\partial}{\partial \mathrm{h}}\begin{bmatrix} \mathrm{m_{h,x(h)}} & 0 & 0 \\ 0 & \mathrm{m_{h,x(h)}} & 0 \\ 0 & 0 & \mathrm{m_{h,x(h)}} \end{bmatrix}\frac{\partial \mathrm{h}}{\partial \mathrm{t}}\mathrm{v_r} \qquad (5.18)$$

Where:

h	-	Distance between the instantaneous surface elevation and strip origin in global Z-direction.
$\frac{\partial \mathrm{m_s}}{\partial \mathrm{t}}$	-	Time derivative of the added mass

The slamming is connected to the added mass and therefore strongly dependent on the added mass depth dependent hydrodynamic coefficients.

2.2.3 Depth-dependent hydrodynamic coefficients

Depth-dependent coefficients are defined in SIMO for all horizontal elements. This is done to account for the effect of the free surface as the elements are being submerged through the splash zone. The coefficients are defined based on the vertical distance from the free surface elevation, ζ.

Pipes: The added mass depth-dependent coefficients used for cylinders are based on and simplified using DNV-RP-C205 (Det Norske Veritas, 2010). The variation of m_a with depth of submergence h from free surface to the center of the cylinder (dm_a/dh) is shown in the figure and table below:

Table 1 Pipe Depth-dependent Hydrodynamic coefficients

Pipe: Depth-dependent hyd. coefficients		
Vert. pos.	**Rel. vol.**	m_a
[m]	[m^3]	[RAM]
-1.00 *r	0.00	0.00
0.0	0.50	0.50
1.00*r	1.00	0.65
3.00*r	1.00	1.00

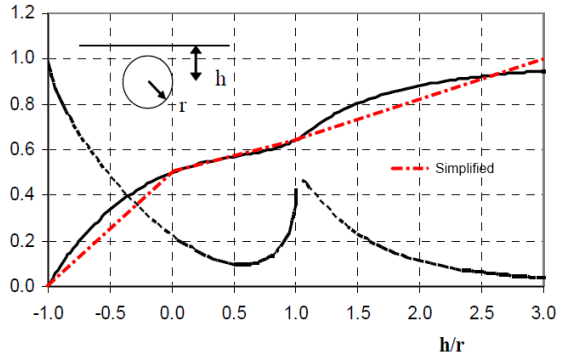

Figure 9 The varying added mass of pipes and beams in the vicinity of the free surface (Source DNV)

Plates: The coefficients used for plates are based on recommendations from Marintek (Sandvik, 2012). The added mass variation with depth close to the free surface is shown in the figure and table below:

Table 2 Plates Depth-dependent Hydrodynamic coefficients

Plate: Depth-dependent hyd. coefficients		
Vert. pos.	**Rel. vol.**	m_a
[m]	[m^3]	[RAM]
-0,2	0.00	0.00
0.0	0.50	0.50
0.8	1.00	0.65
1.5	1.00	1.00

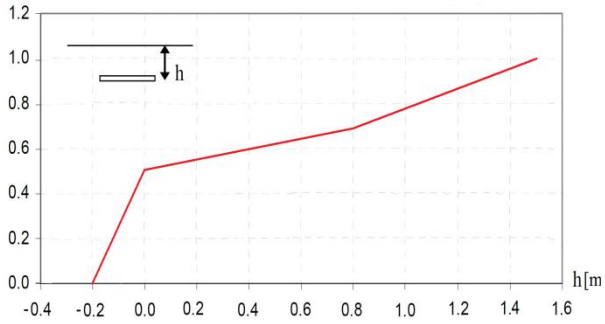

Figure 10 The varying added mass of plates in the vicinity of the free surface (Source: Anders Selvåg)

Note: The vertical position in SIMO is reversed compared to the values given in table 1 and 2.

2.2.4 Numerical integration

Three integration methods for motions can be selected in SIMO. The 3rd order Runge Kutta approximates the solutions of the initial value problem, which evaluates the integrand three times per step. Formulas are given in SIMO Theory manual, (SIMO Project team, 2010). Fast Fourier Transforms is used to calculate wave particle motions and forces due to wind and waves.

2.3 THEORY COMPARISON

SIMO and Orcaflex are different in the way they handle the input data and force calculations. Some of the differences related to the calculation of the wave impact process are highlighted here:

2.3.1 Buoyancy and gravity

Table 3 Buoyancy and gravity calculations

Buoyancy and gravity calculations		
Load on element:	**SIMA**	**Orcaflex**
Gravity	mg	mg
Buoyancy	$\rho g V'$	$\rho g V_{WV}$

The gravity force is subtracted from the final results in both Orcaflex and SIMO. Both programs calculate the gravity forces using distributed mass input for each line element.

In SIMA two methods are given for the calculations of the buoyancy force. For horizontal elements the predefined depth-dependent hydrodynamic coefficients are used for each strip, giving a vertical varying buoyancy force over the element. For vertical elements the buoyancy is calculated based on the submerged part of the element, i.e. for each submerged strip.

Orcaflex lines consist of nodes. For a surface piercing element the nodes affected by the free surface, i.e. proportion wet, is included in the buoyancy calculations, see section 2.1.3 for details.

2.3.2 Inertia

Table 4 Inertia calculations

Inertia calculations		
Load on element:	**SIMA**	**Orcaflex**
Inertia (Froude-Krylov)	$\rho V_S \boldsymbol{a_L}$	Δa_E
Inertia (Added mass force)	$\boldsymbol{m_a a_L}$	$C_m \Delta a_E$

The Froude-Krylov and added mass force is calculated the same way, using the mass of the fluid displaced by the body and the added mass input. The difference is that the calculation is based in different coordinate systems. SIMO is using the wave particle acceleration in $[X, Y, Z]^T$ on the local submerged strip coordinate system.

Orcaflex applies the earth relative coordinate system and calculates the inertia forces based on the PW of each line. Orcaflex uses the added mass coefficient C_m and the mass of the fluid dispersed by the body, Δ, to calculate the added mass.

By deducing the inertia components one finds that they are equal (Greco, 2012).

2.3.3 Drag

Table 5 Drag calculations

Drag calculations		
Load on element:	**SIMA**	**Orcaflex**
Quadratic damping	$\boldsymbol{C_q \lvert V_r \rvert V_r}$	$\frac{1}{2}\rho C_a A\ V_r \lvert V_r \rvert$
Linear damping	$\boldsymbol{C_L V_r}$	$\frac{1}{2}\rho C_l A\ V_r \lvert V_r \rvert$

SIMO calculates the quadratic drag using the distributed drag input in each flow direction and the relative wave particle velocity in the local strip coordinates [X, Y, Z]^T. The quadratic drag can be adjusted using the depth dependent hydrodynamic coefficients.

The drag force calculations in Orcaflex applies drag coefficients $C_{a,x}$, $C_{a,y}$ and $C_{a,z}$ and the drag areas given for each line element. The fluid velocity relative to the line V_r is divided into three velocity components V_N, V_X and V_Y which gives a force contribution in each local direction using the diameter assigned to the respective line. The formulas are based on the amount of the proportion wet. The standard formulation is given below:

$$F_{DX} = PW(\frac{1}{2}\rho(D_n L)C_{a,x}\, V_N \lvert V_X \rvert \tag{5.19}$$

Where:

PW	-	Proportion wet
D_n	-	Drag diameter
L	-	Length of line
V_N	-	Fluid velocity normal to the body

Linear drag is not accounted for in this analysis.

2.3.4 Water entry slam force

Table 6 Slam force calculations

Slam force calculations		
Load on element:	**SIMA**	**Orcaflex**
Slamming	$\boldsymbol{F_{S,S} = -\frac{\partial \mathrm{m_s}}{\partial \mathrm{t}}\dot{x}_S = -\frac{\partial \mathrm{m_s}}{\partial \mathrm{t}}\frac{\partial \mathrm{h}}{\partial \mathrm{t}}\dot{x}_S}$	$\frac{1}{2}\rho\ C_s\ A_w\ \lvert V_n \rvert^2\ n$

Slamming is applied in Orcaflex by using a lumped buoy while in SIMO the slamming loads is included in the force calculations for "slender elements". Some differences in the calculations are present.

In Orcaflex, a slamming coefficient and a slamming area are defined (Orcina, 2013). The slamming force is assumed to be constant over the height of the lifted structure, except for

some ramping at the bottom and the top. The component V_n is the lumped buoy velocity relative to the fluid component. By using the unit normal vector, *n*, Orcaflex calculates the slam forces normal to the water surface elevation. This implies that the slamming forces will have a horizontal component.

In SIMO, the slamming force is estimated from the rate of change in the added mass in the vertical direction as the object is submerged, see section 2.2.2.5. This indicates that all horizontal slamming contributions are based on the vertical added mass change. In addition the depth dependent volume and hydrodynamic coefficients can be defined in SIMO. The rate of change of added mass can therefore be linear or non-linear over the height of the lifted structure, while it is constant in Orcaflex.

2.3.5 Water exit slam force

Table 7 Water exit slam force calculations

Slam force calculations		
Load on element:	**SIMA**	**Orcaflex**
Water exit slam	–	$\frac{1}{2}\rho\,(C_s/2)\,A_w\,\lvert V_n\rvert^2\,n$

Orcaflex includes the water exit slam forces in the lumped 6D-bouy calculation. This is done to account for vertical forces related to additional added mass in heave, as the structure is exiting the water. The water exit slam coefficient is considered to be 50% of the water entry slamming coefficient, according to DNV-RP-H103 (Det Norske Veritas, 2011).

In SIMO these forces are neglected. If a slender element exits the water the time derivative of the added mass, $\frac{\partial \mathrm{m_s}}{\partial \mathrm{t}}$, is equal to zero, i.e. no water exit force is present.

2.4 REGULAR WAVE THEORY

In the numerical simulation and in the model tests, regular wave theory is used. The mathematical formulations of the regular waves are based on two different theories, Airy's and Stokes 5th. The model test is conducted using transfer functions to generate waves, similar to the Stokes 5th regular wave theory. Due to limitations in SIMO regular waves according to Airy's theory is used in the numerical simulations.

The fluid particle behavior is studied to achieve a solid understanding of the differences in the regular wave theories. This study is needed to compare the model test against results from the numerical analysis.

2.4.1 Airy's wave theory

Airy's wave theory was published in the 1841 by George Biddell Airy. His theory is used today to describe a linear propagating gravity wave in fluids (Airy, 1841).

The surface elevation has a simple sinusoidal shape. Underneath the surface the fluid particle motion are in orbital motion, circles for deep water waves with the radius of the circles decreasing with increasing depth. The fluid velocity and acceleration calculations are limited up to the mean sea level, see section 2.1.1.

Airy's wave theory is limited to small amplitude waves and cannot replicate waves in shallow water. The linearized theory will give a rough estimate of a natural propagating wave and the associated forces.

2.4.2 5th Order Stokes wave

The 5th order Stokes wave theory was developed by John D. Fenton in 1985. The theory describes a nonlinear wave with a high and short wave crest and long and shallow trough. The periodic wave is calculated based on the actual wave steepness as the expansion parameter. Stokes 5th replicates a real propagating wave in a good way (Fenton, 1985).

The Stokes 5th order wave theory is accurate for waves shorter than 10 times the water depth.

2.4.3 Comparison

Compared to a real wave, the Stokes 5th theory produces better kinetics and pressures than the Airy's wave theory (Fenton, 1985). Both theories have limitations in the wave amplitude. The Stokes 5th theory is applicable up to breaking waves, $H/\lambda = 0.142$, for deep water waves. The Airy's wave theory is limited to small amplitude waves i.e. $H/2 \lambda << 1$.

The fluid particle velocities and accelerations are compared to better understand the potential differences between the model test and the numerical simulations. A wave with a period of 7 seconds and wave amplitude of 2.5 meters has been analyzed. Orcaflex has been used to produce the fluid particle properties.

2.4.4 Wave elevation

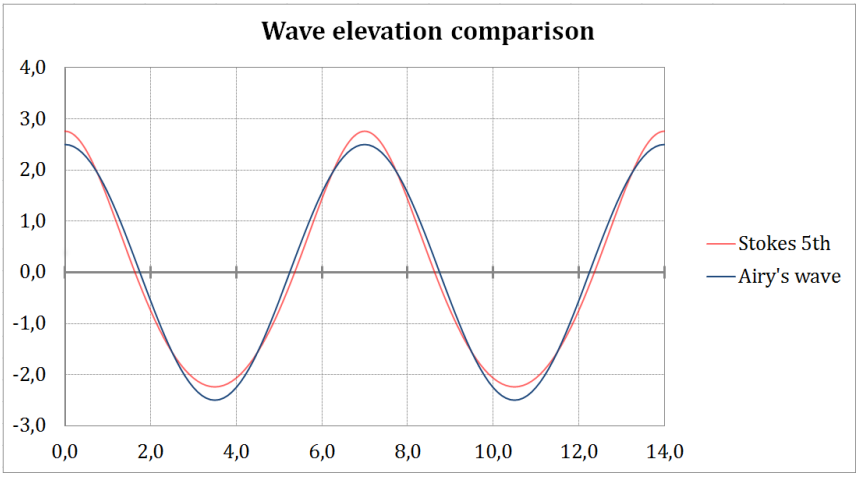

Figure 11 Comparison of wave elevation

The Stokes 5th wave has according to theory a steeper wave crest and a flatter wave trough compared to the Airy's wave. As a result the Stokes 5th wave has a slightly higher wave crest and a shallower wave trough.

2.4.5 Wave particle kinematics

The maximum and minimum values for the horizontal and vertical velocities and accelerations have been extracted. The results are presented in table 8.

Table 8 Wave particle kinematics is Stokes 5th and Airy's theory

	X Velocity		Z Velocity		X Acceleration		Z Acceleration	
	Max	**Min**	**Max**	**Min**	**Max**	**Min**	**Max**	**Min**
Stokes 5th	1.76	-1.78	1.77	-1.77	1.58	-1.58	1.81	-1.36
Airy's	1.83	-1.83	1.83	-1.83	1.64	-1.64	1.64	-1.64
Difference	-3.92 %	-2.67 %	-3.29 %	-3.29 %	-3.38 %	-3.38 %	10.27 %	-17.34 %

For the horizontal components and the vertical velocity the difference between the maximum and minimum values are not greater than 3.92%. For the vertical acceleration component the differences are larger. -17.34% separates the minimum vertical acceleration between Stokes 5th and the Airy's wave.

2.4.6 Conclusion

Two different wave theories are used in the numerical analysis and the model test. This may lead to inaccuracies when comparing forces on the structure. The differences in the wave elevation will affect the wetted area and the time varying buoyancy force. In general terms, the Airy's wave theory will generate larger forces on an element compared to using Stokes 5th wave kinematics. Based on the comparison of the vertical acceleration component it is assumed that the vertical added mass force in the model tests is larger in

the water entry phase and smaller in the water exit phase compared to the numerical simulations.

Note: The wave kinematics in the generated model waves may not replicate the Stokes 5th kinematics in a accurate way. This comparison will give a rough indication of differences that may be expected.

CHAPTER 3

Modeling and test setup

The compressor module is analyzed using two methods, the first method is a model test where the structure is scaled and fabricated accordingly. The second one is a method where the structure is built numerically. The numerical analyses are carried out in two different programs, Orcaflex and SIMO. To obtain comparable results, the modeling and test setup has to be as similar as possible.

This chapter will give a general introduction to the test setup and the fabrication/modeling of the compressor module. The chapter will provide a better understanding of the test and reasons for choosing test parameters.

3.1 MODELING:

The compressor module consists of a large number of structural elements and internal components. Replicating the model in detail is a time consuming job, both in the numerical simulation and in the model fabrication.

The full scale module from Aker solutions is scaled down to 1/10 and simplified. All simplifications to the model are presented in figure 12. The alterations to the model are believed not to affect the global hydrodynamic properties of the structure to any significant degree. All simplifications on the compressor module are made by Oceanide and are applied to the numerical model.

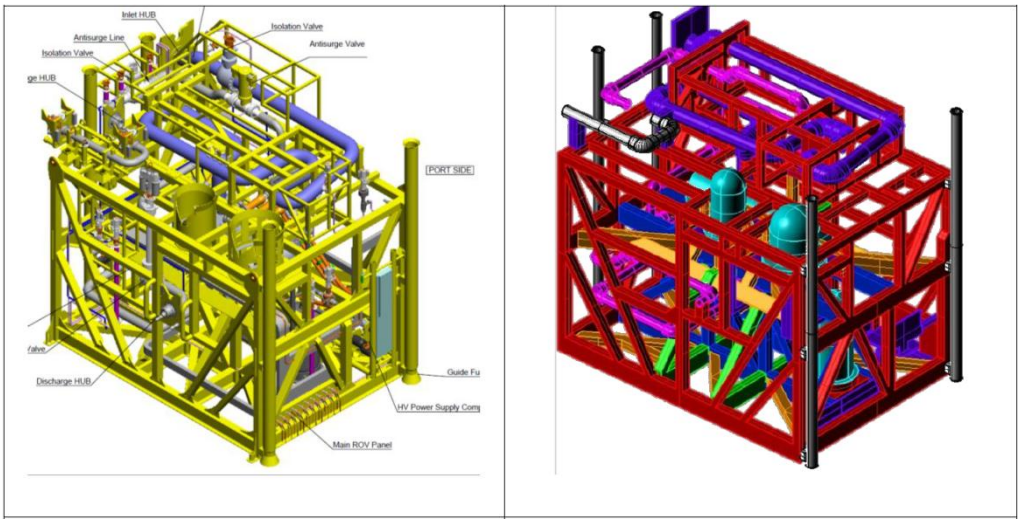

Figure 12 Illustration of the compressor module by Aker Solutions (left). The simplified compressor module by Oceanide (right) (Source: Oceanide)

3.2 SIMULATION OF SPLASH ZONE CROSSING PHASE

A common criterion for normal lifting operations is that a downward load should always be present in the crane wire and lifting slings to prevent snap loads, ref (Det Norske Veritas, 2011). The SHS will lower the modules using a sliding frame and a damping frame to prevent large movements on the module. This method will lead to large shear forces on the structure and on the frame assembly connecting the module to the tower cursor rails. When the compressor module is lowered through the splash zone several elevations can limit the operation, with respect to different governing parameters, such as tension at pad eyes and moments in the docking frame.

The modules are lowered with an approximate velocity of 0.1 m/s. At this low pay-out rate the relative velocity of the module is considered negligible, due to the wave particle velocity $v_z \gg v_{Pay-out}$. In order to find the vertical level at which the largest dynamic forces can be expected, a stepwise lowering analysis of the modules from air to fully submerged, have been carried out by Technip (Technip, 2013). The lowering analysis has been carried out using Orcaflex.

The structure has been analyzed from 8.5 meters above to -21.5 meters below MSL, while subjected to regular waves, according to Airy's theory, in 30 minutes. The elevation spacing has been set to 1 meter. Forces have been measured at several points to ensure that all governing parameters are taken into account.

Table 9 Summary of lowering analysis. (Source: Technip Norge, by Chen Xiao)

	Elevation [m]											
Elevation [m]	2.5	1.5	0.5	-0.5	-2.5	-3.5	-4.5	-5.5	-6.5	-7.5	-8.5	-9.5
Max effective tension [KN]	4188,9	4369,8	4511	4584	5124	5379	5575	5998,9	6342,16	6558	6540	6483
Min effective tension [KN]	1972,4	1799	1554	881,5	-76,2	-565	-1162	-1751	-2259,9	-2484	-2609	-2559
Max end force LX [KN]	2279,2	2763,3	3862	4288	4628	5090	5166	4961,9	4625,69	4235	3867	3551
Max end force LY [KN]	525,11	642,13	842	1045	1000	1033	1029	979,16	885,224	762,9	644,3	535
Max end force LZ [KN]	4188,9	4369,8	4511	4584	5124	5379	5575	5998,9	6342,16	6558	6540	6483
Max end moment LX [KN.m]	5263,8	6220,9	7558	8694	8593	8102	7286	6340,7	5433,99	4481	3681	3138
Max end moment LY [KN.m]	24417	27915	35274	37616	35757	36749	35527	33638	31245,9	28707	26359	24354
Max end moment LZ [KN.m]	909,51	1170,3	2278	1845	1930	1557	1469	1201,1	1086,21	913,2	784,9	665
Max effective tension at padeye [KN]	1896,1	2016,2	2154	2281	2074	1974	1861	1746,4	1885,56	1960	1976	1928
Max end force LX at padeye [KN]	583,15	705,27	988,1	1091	1189	1287	1293	1255,3	1170,71	1070	976,5	896,3
Max end force LY at padeye [KN]	150,88	185,01	259,5	294,8	298,4	294	279,6	258,78	228,145	200	169,3	141,1
Max end force LZ at padeye [KN]	1896,1	2016,2	2154	2281	2074	1974	1861	1746,4	1885,56	1960	1976	1928

A summary of the lowering analysis is given in table 9. Four elevations have been chosen for the numerical analysis and the model test, based on the maximum and minimum forces and moments. Measured from the bottom of the module the compressor elevations are; 2m, 0m, -3.75m and -7.75m as illustrated in figure13.

Elevation 1, 2 meters above mean sea level, has been included in the model test to insure that all slamming loads are captured.

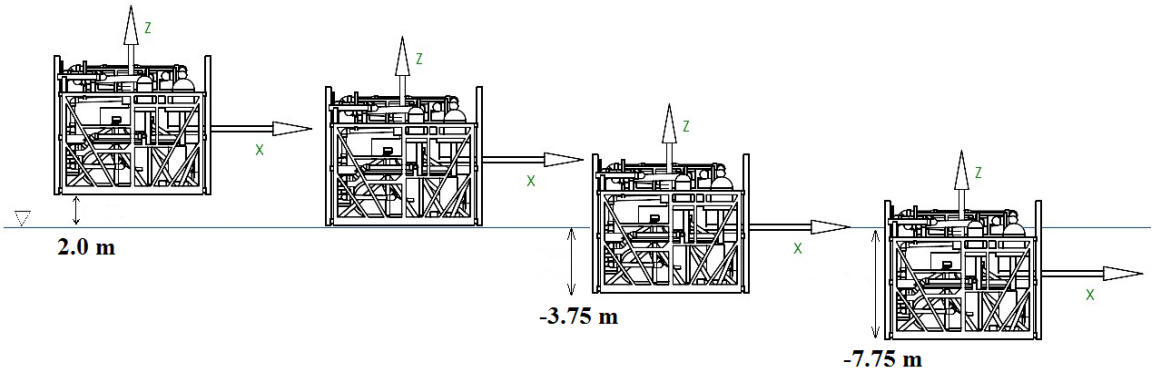

Figure 13 Illustration of elevations (Source: Anders Selvåg)

3.3 GENERAL TEST SETUP

The module is suspended in 4 different elevations with sufficient rigidly to ensure that no motions are involved. The module is oriented so the local X-direction is always pointing towards the incoming regular wave train, simulating head sea, when connected to the SHS, as shown in figure 14.

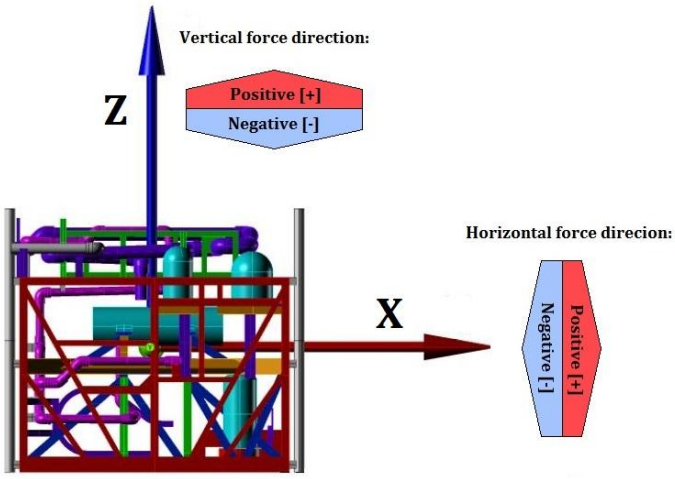

Figure 14 Illustration of force direction

All environmental inputs are based on the generated waves in the ocean basin. The wave elevation is measured in the test tank and will be given as input in the numerical analysis. Three environments will be generated.

The compressor module has been tested in 12 different conditions, three environments and four elevations.

The global horizontal and vertical forces are extracted from the model test and compared with results obtained from Orcaflex and SIMO.

CHAPTER 4

Experimental study

Technip is required by Statoil to validate their numerical models used for calculating the maximum allowable sea states at which the SHS can operate in. A model test focusing on the splash zone crossing phase was proposed and approved. The aim is to estimate the actual maximum forces in the splash zone and compare the maximum forces against results obtained from Orcaflex. The comparison is used by Technip AS to determine if the numerical model produces conservative results.

The compressor module is fixed to one of the two basin bridges. Using a 6D-load sensor forces in 6 degrees of freedom (DOF) is extracted. The module is subjected to 3 wave conditions in four different elevations.

In this thesis, the wave impact process on the compressor module is analyzed. The time history is studied and compared with results obtained from Orcaflex and SIMO. This chapter gives a detailed description of the experimental investigation and test setup.

Oceanide was contracted by Technip to perform the model tests. The testing was executed in the wave tank "BGO First" in La Seyne Sur Mer, France.

4.1 EXPERIMENTAL SET-UP

The offshore basin BGO First is used for the model testing. The basin is filled with freshwater and allows generation of waves, current and wind. The BGO First is 40 meter long 16 meter wide and has an adjustable water depth from 0 to 4.8 meters. A water depth of 4.8 meter is used in the current analysis.

The fabrication of the module is carried out by Oceanide using the simplified 3D model shown in figure 12. The scaled compressor module is built using wood and foam filled PVC piping to ensure sufficient rigidity. The weight, volume and submerged COG are not according to the weight report (AkerSolutions, 2012). For comparison purposes the static load has been subtracted in calm water at the beginning of each test. This action allows extraction of pure dynamic forces. The time varying buoyancy is not subtracted from the total hydrodynamic force.

The data presented in this report has been rescaled according to the Froude similarity law with a scale ratio of $\lambda = 10$:

$$Time: \quad t_f = \sqrt{\lambda} * t_m \tag{4.1}$$

$$Length: \quad L_f = \lambda * L_m \tag{4.2}$$

$$Force: \quad F_f = \rho_f/\rho_m \, \lambda^3 * F_m \tag{4.3}$$

$$Moments: \quad M_f = \rho_f/\rho_m \lambda^4 * M_m \tag{4.4}$$

The module is suspended in four different elevations at the center of the basin through a 6D-load sensor, according to section 3.2. The load sensor is connected to a vertical adjustable bridge to measure forces in every elevation. The module is connected to the load sensor using 3 vertical metal rods for sufficient stiffness. The module was oriented so that the modules X-direction is pointing towards the wave generator see figure 15.

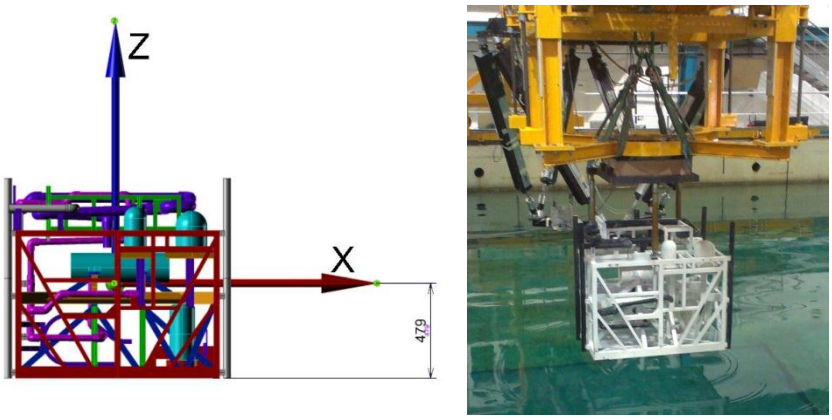

Figure 15 The compressor module axis system (left). The model connected to the basin bridge suspended in elevation 1 (right)

The wave generator is a horizontal plunger, powered by hydraulic jacks. This type of plunger has the ability to run current under the wave generator while generating waves. The shape is patented by Oceanide. All tests have been performed using waves that are ramped up from calm water conditions.

Figure 16 The wave generator at Oceanide

4.2 INSTRUMENTATION

Three instruments have been used in this campaign to record and collect data:

- Loads in 6-DOF using a MC12-transducer
- Wave elevation
- Video camera

4.2.1 Load measurement

The loads and moments are measured using a MC12 transducer, presented in figure 17. The MC12 transducer resolves the applied loads to force and moment components. The transducer consists of four Foil Strain Gauge Sensing Elements and four precision elements to insure low crosstalk and high accuracy. The crosstalk is measured to less than 2% on all channels (AMTI, 1995).

Figure 17 The MC12 transducer

The MC12 transducer is connected between a mechanical elevator and 3 steel rods. The steel rods provide distance from the free surface to prevent water on the transducer, as shown in figure 15. The steel rods are included in the static load, but subtracted from the final results.

4.2.2 Wave elevation

The wave elevation is measured by using two parallel conductive rods. A voltage is applied to the rods, and the total resistance of the rods is measured. As the wave elevates the resistance of the circuit is changed and the wave elevation can be measured

accordingly. The wave probe is located approximately 7 meters away from the module, in line with the center of the module.

The wave probe is calibrated by Oceanide and given in appendix 3.

4.2.3 Video camera

The video camera used is a standard camera at 25 Hz. All tests are recorded and synchronized with the final results.

4.3 ENVIRONMENTAL CALIBRATION

The transfer functions for generation of waves are made by Oceanide. The generated wave describes a regular wave similar to the Stokes 5^{th} wave theory. The environment calibration is carried out using 3 in-line wave gauges. The calibration plots are given in the report from Oceanide (Oceanide, 2013). The module was not present during the calibration process.

The wave reflection is computed using an irregular wave transformation called Goda's method. By using Fourier analysis on measurements of the wave elevation at two distinct points the amplitude of the incident and reflected waves for a given frequency can be estimated. Goda's method is used to provide an estimation of wave diffraction coefficients, C_r, for details see Appendix 4.

The calibration was carried out by Oceanide.

4.4 DATA ACQUISITION AND PROCESSING

The MC12 transducer provides analog output signals. The signal is amplified and processed to provide analog output suitable for an A/D converter. The digitalized signal is collected and processed on a data storage unit.

The data acquisition frequency is set to 2500 Hz (at model scale).

No filter on the digitalized or the analog signals was used during tests with the compressor module.

4.5 TEST PROGRAM

The Oceanide campaign included wave tests on all 7 modules in the ÅSC-project. Each module was tested in 3 different wave conditions and 4 elevations to simulate the submergence in the splash zone. A total of 82 regular wave tests were carried out between 11.02.2013 and 29.02.2013, including the wave calibration. The test program for the compressor module is presented below:

Table 10 Model test list (Source: Oceanide)

TESTS LIST									
Project:	**TECHNIP - ASGARD Subsea Compression Module - Wave tests**								
Ref.:	C12.2.073								
Test Number	**Acquisition file**	**Scope**	**Module**	**Test type**	**Heading (°)**	**Wave Height (m)**	**Period (s)**	**Elevation (m)**	**Current (m/s)**
Wave and current Calibration									
1		base		Wave calibration		8	7		
2		base		Wave calibration		8	10		
3		base		Wave calibration		5	7		
Test set-up mobilization - Compressor module mobilization									
8		Base	Compressor	Wave test	0°	8	7	Elevation 1	
9		Base	Compressor	Wave test	0°	5	10	Elevation 1	
10		Base	Compressor	Wave test	0°	5	7	Elevation 1	
14		Base	Compressor	Wave test	0°	8	7	Elevation 2	
15		Base	Compressor	Wave test	0°	5	10	Elevation 2	
16		Base	Compressor	Wave test	0°	5	7	Elevation 2	
20		Base	Compressor	Wave test	0°	8	7	Elevation 3	
21		Base	Compressor	Wave test	0°	5	10	Elevation 3	
22		Base	Compressor	Wave test	0°	5	7	Elevation 3	
26		Base	Compressor	Wave test	0°	8	7	Elevation 4	
27		Base	Compressor	Wave test	0°	5	10	Elevation 4	
28		Base	Compressor	Wave test	0°	5	7	Elevation 4	

4.6 ERROR SOURCES

Errors in the experimental values are present and originate from different error sources. This section will highlight sources that may impose errors in the measurements.

The ocean basin “BGO-First” is 40 meters long and its ability to damp out the generated wave may be questioned. By visual inspection of the free waves, no reflection was observed. Calculations using the Goda’s method are made to determine the magnitude of the reflected wave.

The wave generators are calibrated to produce a steady oscillating wave train. The calibration process and the wave measurements are based on the wave probe accuracy. The thickness of the wave probe rods will disturb the local fluid flow and possibly lead to inaccuracies in the wave train calibration. This effect will be dependent on the wave period and the wave height. In addition the wave probe can be influenced by spray and dirt on the rods which can reduce the surface tension effect, resulting in inaccurate measurements.

The wave train is produced in a gradually increasing manner until steady oscillating waves are achieved. This method leads to a significant disturbance of the free surfaces since the structure enters and exits the water. The free surface effect will affect the local wave kinematics and will be present in all measurements.

Oscillations in the force measurements were observed when the structure was suspended over the mean sea level. The eigenperiod of the force transducer where checked and rejected as a possible source. The way the module is connected to the basin bridge makes the measurements very sensitive to structural oscillations. It is assumed that the wave impact forces are causing structural oscillations in the bridge causing the force variation in the transducer. When the module is suspended in air, no damping of the structural

oscillations is present, making elevation 1 and 2 more exposed to inaccurate measurements.

The compressor module is believed to not generate any significant wave, hence the reflection of the waves from the tank wall is considered negligible.

4.7 RESULTS AND DATA ANALYSIS

4.7.1 Wave analysis

The wave generator is calibrated to produce three different regular wave conditions similar to the Stokes 5th theory. The calibration was carried out from free surface conditions to insure stable conditions throughout the tests. The wave train for environment 1, 2 and 3 is presented below.

Note: Due to limitations in SIMO, regular waves according to Airy's theory are used in the numerical analysis for both SIMO and Orcaflex.

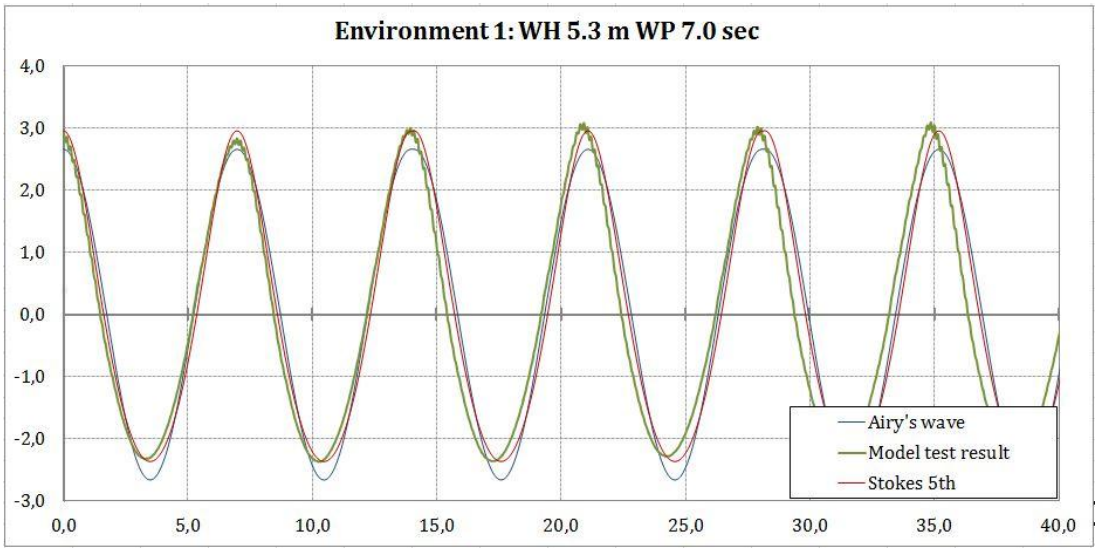

Figure 18 Comparison of waves in environment 1

Wave height 5.3 meters 7.0 second wave period: The wave measurements are taken from 199.2 sec to 256.1 sec into the test, the full wave series is given in Appendix 5. The generated wave represents the Stokes 5th theory in a good way. The wave crests are sharper and has flatter troughs compared to Airy's wave theory.

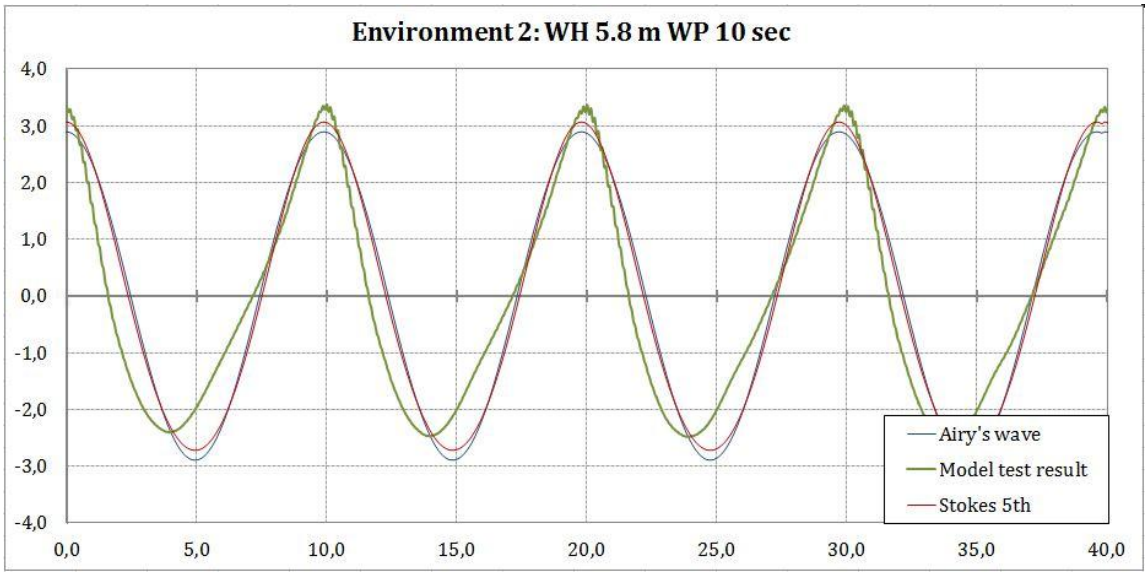

Figure 19 Comparison of waves in environment 2

Wave height 5.8 meters 10.0 second wave period: The generated wave has a significantly steeper wave crest compared to both the Stokes 5th and Airy's wave theory. The period of the wave crest is shorter compared to the wave troughs, indicating that the vertical elevation is decreasing more rapidly towards the wave trough. The reflected wave may contribute to the differences observed (Cinello, 2013). The wave elevation has been extracted between 237.2 sec and 322.6 sec.

At full scale, the Stokes 5th wave has a 0.4 meter deeper wave trough and a 0.12 meter lower wave crest compared to the model test.

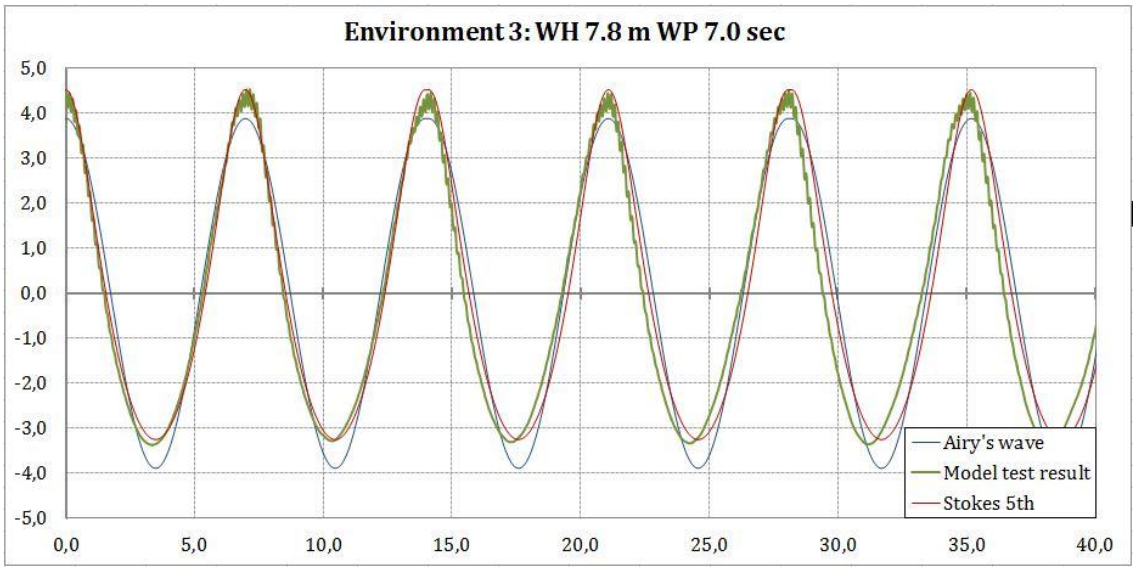

Figure 20 Comparison of waves in environment 3

Wave height 7.8 meters 7.0 second wave period: The generated wave represents the Stokes 5th theory in a sufficient way. The peaks may indicate splash on the wave probe or indicate that the local velocities in the surface is disturbed due to local wind.

The wave elevation has been extracted between 199.2 sec and 256.1 sec, see Appendix 5.

Table 11 Summary of wave statistics for all environments

Wave statistics									
	Heading	Wave Height [m]		Wave Period [m]		Wave crest [-]		Wave through [-]	
	[°]	Wanted	Measured	Wanted	Measured	Mean	σ [m]	Mean	σ [m]
Environment 1	0°	5	5,37	7	6,98	3,026	0,066	-2,320	0,048
Environment 2	0°	5	5,86	10	9,97	3,318	0,045	-2,480	0,043
Environment 3	0°	8	7,74	7	6,97	4,451	0,076	-3,336	0,031

The results indicate that the generated wave train is different than the input data given. This may originate from the limitations and uncertainties in the test facility. Goda's method is used to calculate the wave reflection. Based on calculations no wave reflection is present for environment number 1 and 3. For environment 2 the calculated reflection coefficient is 2 %. This will influence the wave particle kinematics and the wave elevation.

The full wave series is given in Appendix 5

The wave generator at the Oceanide First tank is able to generate a wave train with sufficient accuracy to replicate regular waves, according to Stokes 5th theory, for environment 1 and 3. The largest elevation differences appear in environment 2 using a wave period of 10 seconds.

To be able to determine the consistency of the wave train an uncertainty analysis has been performed on the maximum and minimum wave elevations.

The reported expanded uncertainty is based on a standard uncertainty including a covering factor, k=2, providing a level of confidence of approximately 95%. The elevation statistics is based on 8 measured waves. The wave crest and through is corrected for the estimated effect of incorrect measurements of the wave probe (Steen, 2012) p.129.

The wave elevation from the tests is checked versus regular wave theory, both Airy's and Stokes 5th. For comparison purposes, the wave height and period for the generated wave is used as input in the regular wave theory.

4.7.2 Force analysis

The forces are presented as time histories, both in X and Z direction, which are the governing forces for the SHS analysis. The force oscillation amplitudes are given according to the coordinate system given in figure 14. The results in this thesis are given for three passing waves during steady state conditions, i.e. for three steady oscillating waves. The full time series including the ramping and the time window of measurements is given in the model test report from Oceanide (Oceanide, 2013).

The static load, i.e. buoyancy force and the weight have been subtracted at the beginning of each test to obtain comparable results, with the numerical simulation.

The time history for the horizontal and vertical force is presented for all environments. General trends are discussed using results from all environmental conditions. Specific results for wave dependency of amplitude and period are given in separate sections.

A separate analysis has been carried out in Orcaflex to interpret the wave impact process. By separating the hydrodynamic force contributions a better understanding of the wave impact process can be obtained. This has been done to be able to interpret the results in a better way. An example of the analysis is given in Appendix 6.

4.7.2.1 Horizontal forces:

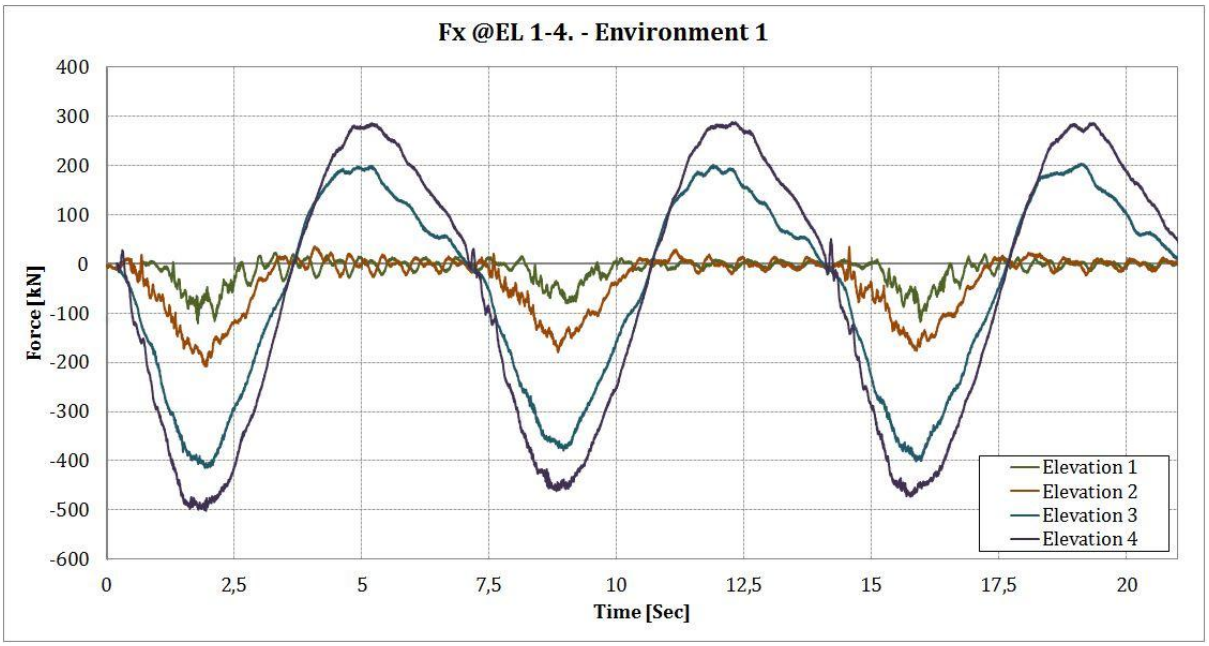

Figure 21 Total horizontal impact force on the module when subjected to Environment 1

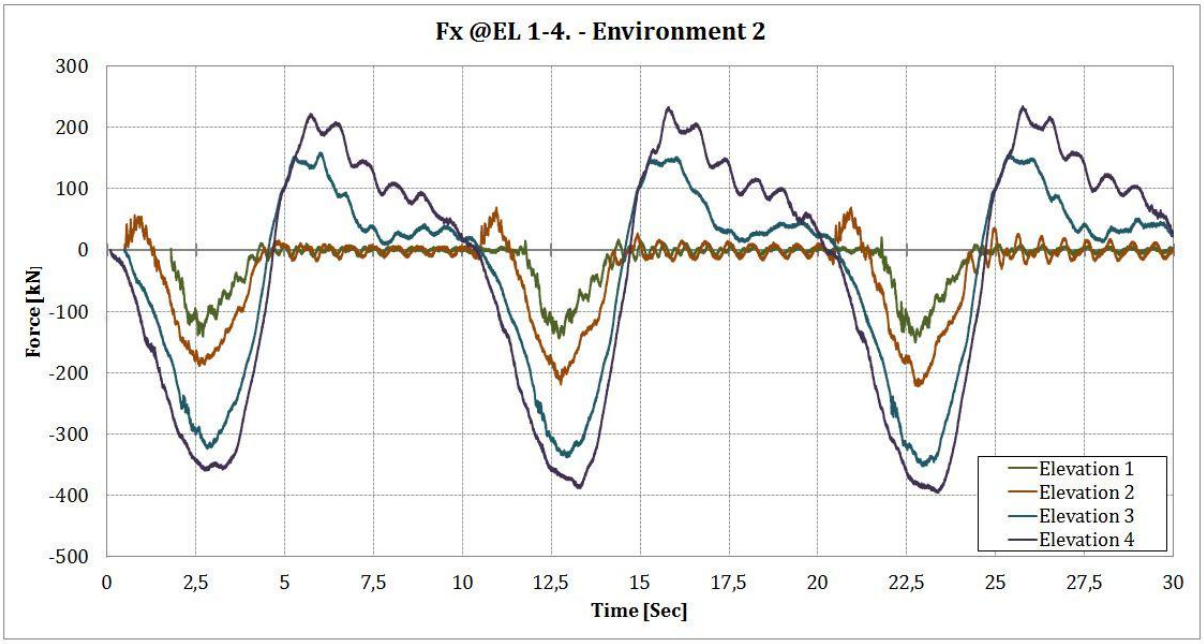

Figure 22 Total horizontal impact force on the module when subjected to Environment 2.

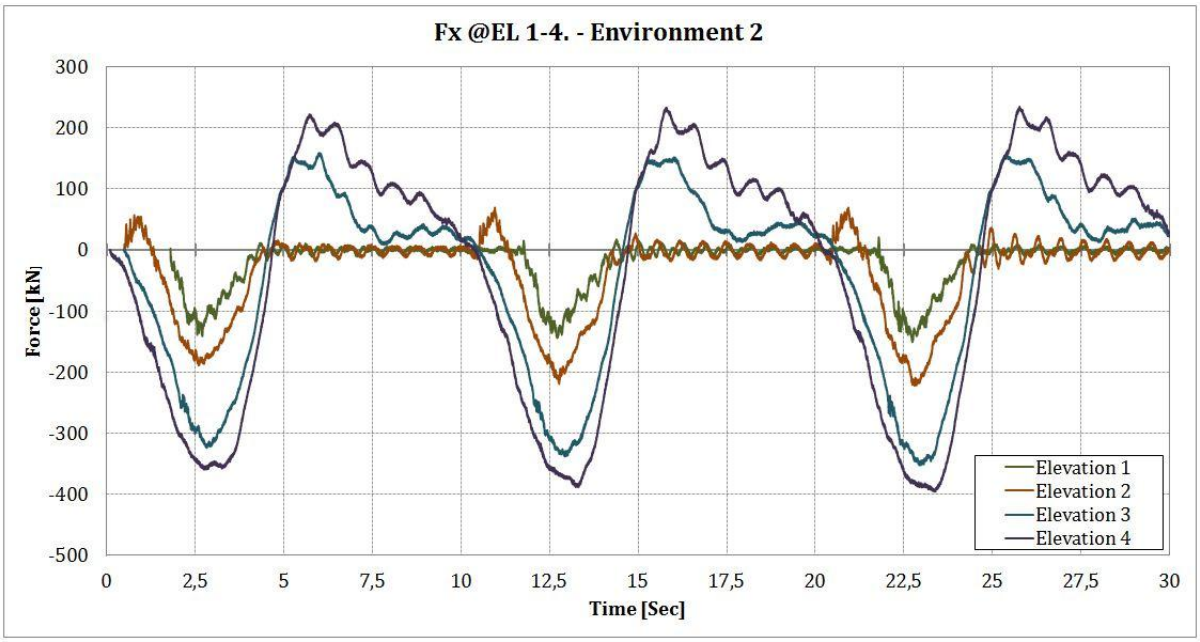

Figure 23 Total horizontal impact force on the module when subjected to Environment 3

Table 12 Summary of global horizontal forces

Global Horizontal forces					
Project:	Master thesis - ASGARD Subsea Compression Module - Model Wave tests				
Test number	Elevation	Environment		Model Test results	
		H [m]	T [s]	F_{Max}	F_{Min}
10	1	5,3	7,0	23,2	-120,6
16	2			49,7	-208,4
22	3			208,5	-414,6
28	4			294,1	-501,6
9	1	5,8	10,0	24,2	-150,6
15	2			72,0	-222,3
21	3			174,0	-355,5
27	4			235,1	-411,7
8	1	7,8	7,0	40,3	-365,3
14	2			88,3	-497,3
20	3			310,8	-792,4
26	4			462,9	-871,2

The time history of the horizontal forces are presented as the wave is propagating through the structure. Horizontal force trends are discussed for each elevation.

Elevation 1: The compressor is suspended 2 meters above the mean sea level (MSL). The compressor is subjected to the upper part of the wave crest, which implies that the module is only exposed to negative horizontal loads, see figure 14.

The governing horizontal forces in the first elevation are believed to originate from horizontal drag- and some horizontal slamming forces. This is caused by the horizontal velocity component in the upper part of the wave crest. The slam forces are believed to be the cause of some oscillations in the measured forces in the water entry phase. The horizontal accelerations are low, indicating low added mass forces.

Elevation 2: The compressor is subjected to the wave crest above MSL. The total horizontal load is governed by drag and horizontal slamming. In addition, added mass forces are present in the water entry and the water exit phase, due to the wave particle acceleration in the start and end of the wave crest.

During test number 15, elevation 2 environment 2, some irregularities in the horizontal force measurements were observed in the initial wave impact phase. This irregularity might originate from the reflected wave, which will disturb the wave particle kinematics in addition to the wave elevation.

Elevation 3: The structure is submerged by -3.45 meters below MSL. The governing forces at elevation 3 are drag and added mass forces. In addition, some horizontal slamming will be present.

As the wave propagates into the structure the combined drag and added mass force will lead to a minimum horizontal force before the wave crest has propagated into the center of the structure. This indicates that the horizontal forces at the water entry phase are larger compared to when the structure is fully wetted. This indicates a large contribution from the added mass and drag forces on the structure. The maximum positive forces are measured at the end of the water exit phase, where the fluid accelerations are large. This implies that the horizontal drag force is considerable lower than the added mass force during the water exit phase. This is caused by the structures wetted area. As the wave propagated out of the structure the wetted area reduces and the structure is less affected by horizontal velocity component in the wave through.

Elevation 4: At elevation 4 the structure is fully submerged. The wave impact process is dominated by drag and added mass forces. The maximum forces are measured before the wave crest has propagated into the center of the structure.

The maximum forces are measured at the end of the waver exit phase. At this stage the horizontal fluid acceleration are large indicating large added mass forces.

4.7.2.2 Vertical force:

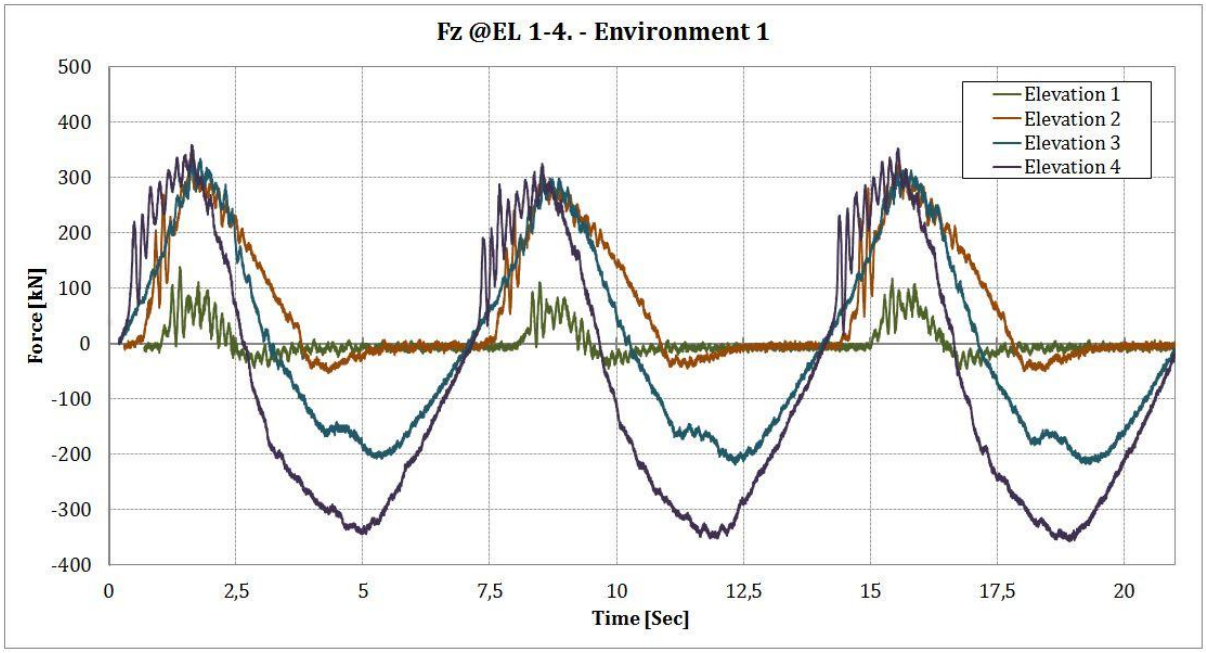

Figure 24 Total vertical impact force on the module when subjected to Environment 1.

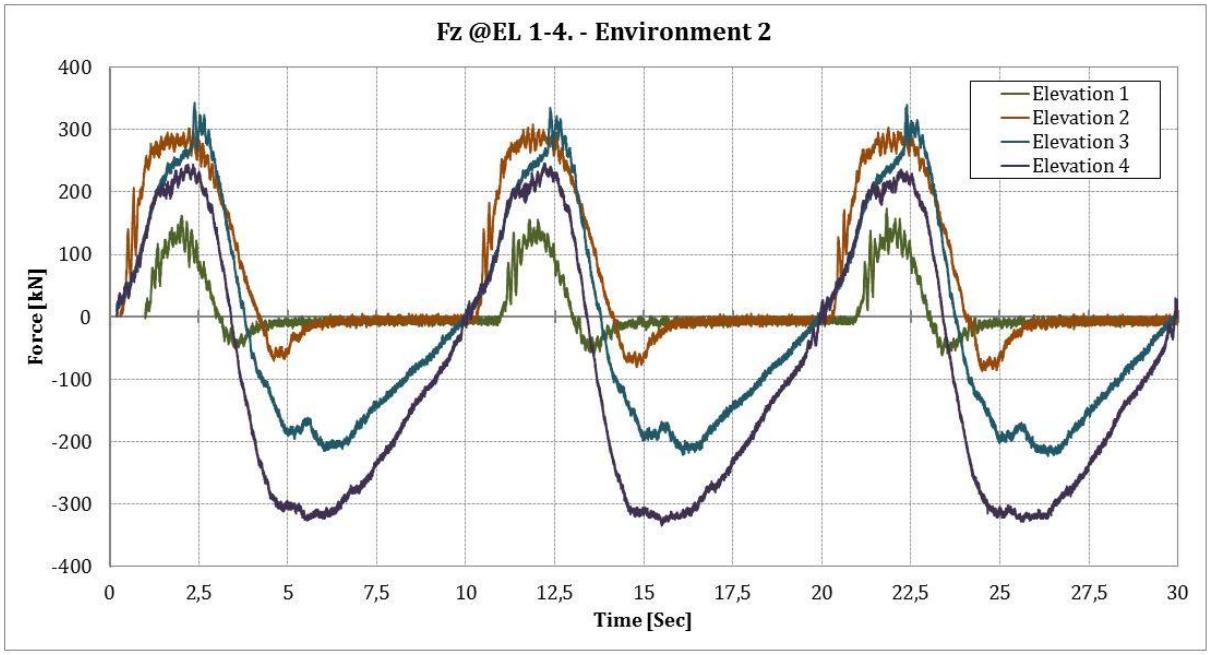

Figure 25 Total vertical impact force on the module when subjected to Environment 2

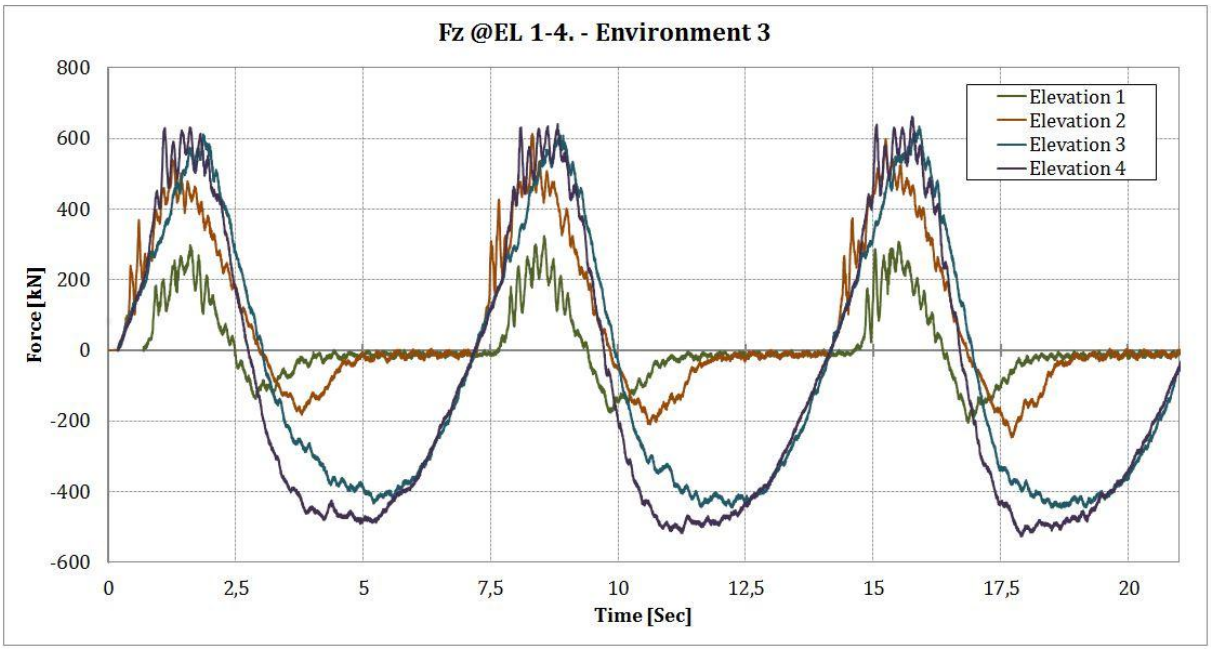

Figure 26 Total vertical impact force on the module when subjected to Environment 3.

Table 13 Summary of global horizontal forces

Global Vertical forces					
Project:	Master thesis - ASGARD Subsea Compression Module - Model Wave tests				
Test number	Elevation	Environment		Model Test results	
		H [m]	T [s]	F_{Max}	F_{Min}
10	1	5,3	7,0	138,60	-46,86
16	4			347,00	-54,55
22	7			335,88	-222,09
28	10			367,21	-360,09
9	2	5,8	10,0	173,73	-63,33
15	5			308,43	-94,74
21	8			343,26	-238,91
27	11			246,01	-342,61
8	3	7,8	7,0	323,89	-205,06
14	6			612,59	-246,95
20	9			653,35	-456,16
26	12			661,71	-526,81

The time history of horizontal force is presented as the wave is propagating through the structure. Vertical force trends are discussed for each elevation.

All vertical measurements show a force oscillation in the water entry phase. The force oscillation frequency was measured in 10 random time windows in elevation 1 and 2. These elevations are most effected by the oscillations. The results showed that all windows had similar frequencies ranging from 6.17 Hz to 7.75 Hz independent of elevation or environment. Oceanide has not measured the eigenfrequency of the system, hence the origin of the oscillations are hard to determine. It is assumed that the force oscillations originate from the impact of the wave, which again initiates a structural

oscillation in the bridge. The structural oscillations are damped when the structure is submerged, hence not as visible in elevation 4. The frequency analysis is given in Appendix 7.

Elevation 1: In the initial impact phase the module experiences a positive force peak. The positive peak force is dominated by buoyancy and slam forces. As the wave is propagating into the structure, all elements in the lower area are wetted. By hand calculations the buoyancy force is estimated to be in the range of 100kN to 150kN, depending on wave height and the wave period. Local slam forces on the wetted structural elements will be present, this is caused by the rapid increase of the added mass of each element. The magnitude and the duration of the slam force are strongly dependent on the environmental conditions. The negative forces in the latter phase of the impact are mainly added mass forces.

Elevation 2: The initial wave impact is dominated by buoyancy, drag and slam forces. The buoyancy is calculated to be in the range of 220kN to 260kN. The drag force is large in the initial phase due to the vertical fluid particle velocity. As the wave propagates into the structure the positive drag force decreases. The rapid increase of the wetted structural elements leads to a rapid increase in the added mass. As a result the slam forces are present.

As the wave propagates out of the structure the negative forces measures is a combination of added mass and drag forces.

Elevation 3: The maximum positive peak force is measured in the water entry phase. A combination of added mass, drag, slamming and buoyancy forces are present in the measured maxima as a result of the submerged volume and fluid particle velocity and accelerations.

The minimum force is measured in the water exit phase. This is a combination of added mass and drag forces.

Elevation 4: In the fully submerged condition the wave impact process is similar to elevation 3 but with less slamming forces due to fact that water will never fully escape the structure. For that reason the added mass forces will be larger compared to elevation 3.

4.7.3 Wave period dependency on the impact force

The water particle velocity for an undisturbed wave is decreasing with increasing wave period. This implies decreasing forces for a higher wave period. The horizontal measurements follow this trend, while the vertical measurements do not. Long period waves have low wave steepness, this will increase the speed of the wetted area indicating larger added mass and slamming forces. By comparing elevation 1 & 2 in figure 24 and 25, the rapid increase in vertical forces can be observed.

The horizontal negative forces follow the same trend where the forces are smaller for a higher wave period. The vertical forces are increased or similar.

Some of the force differences may originate from the increased wave amplitude differences of 0.25 m.

4.7.4 Wave amplitude dependency on the impact force

By increasing the wave amplitude the associated wave kinematics are increased, leading to increased F_{Max} and F_{Min}, both in the horizontal and vertical direction. The increased force is caused by additional slamming, added mass and drag forces. In addition the time varying buoyancy force is increased due to increased wave elevation.

4.7.5 Wave deformation

The waves are ramped up from free surface conditions. By visual inspection of the waves, the free surface is disturbed by the structure and water exiting the structure. The disturbance does not die out before the next wave hits the structure. This is believed to affect the local wave kinematics and in some cases reduce the forces on the structure. The disturbance can be seen in the figure below:

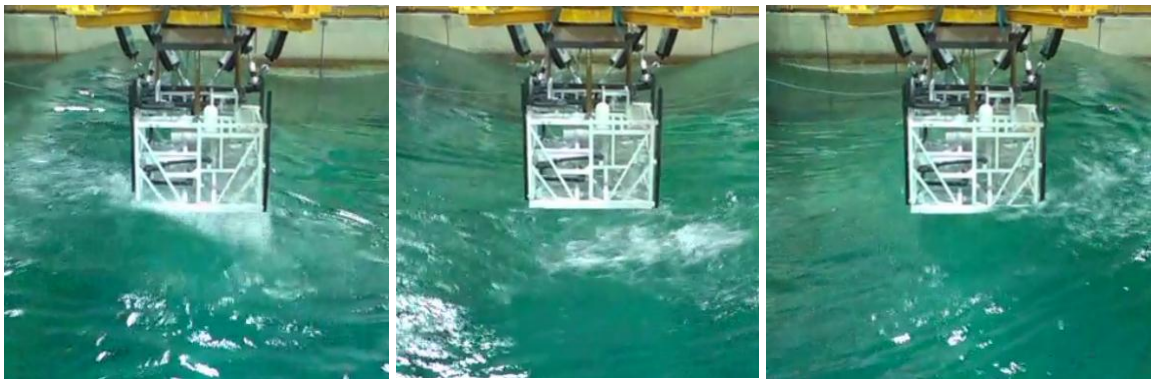

Figure 27 Wave disturbance

CHAPTER 5

Estimation of global hydrodynamic coefficients

In common marine operations, hydrodynamic coefficients are estimated based on documents for recommended practice in marine operations, such as DNV-RP-H103. The hydrodynamic coefficients are based on singular elements far from boundaries. When analyzing a structure consisting of several elements, the steady flow is disturbed by surrounding structural elements. In addition, when analyzing elements in regular waves the element will experience an oscillatory flow which will lead to a greater drag force and additional added mass compared to the steady flow coefficients. The recommended practice from DNV is considered to not be satisfactory when analyzing the modules in the ÅSC facility.

To ensure accurate numerical models Technip has carried out model testing to establish global hydrodynamic coefficients for each module. Two separate tests are performed to establish global coefficients for drag, added mass and slamming. The model testing was carried out at Oceanide's offshore basin "BGO First" in La Seyne Sue Mer, France. This chapter is written according to the "*Forced Oscillation and Slamming test*"-report from Oceanide and will only highlight results related to the compressor module.

The global coefficients from the model test are used to calibrate the global coefficients in the numerical model. To implement the global hydrodynamic coefficients into the numerical model a calibration of the local hydrodynamic coefficients for each element is carried out. The calibration process is described in detail in chapter 6.

5.1 TEST SET-UP

Two separate tests were carried out, one oscillation test to validate the drag and added mass coefficients, and one water entry test to validate the slamming coefficients. Both tests were conducted in calm water and connected to a rigid bridge suspended over the ocean basin. Motions were applied to the module using a hexapod frame. Between the frame and the module 3 1D load cells where used. An illustration of the setup is given in figure 27.

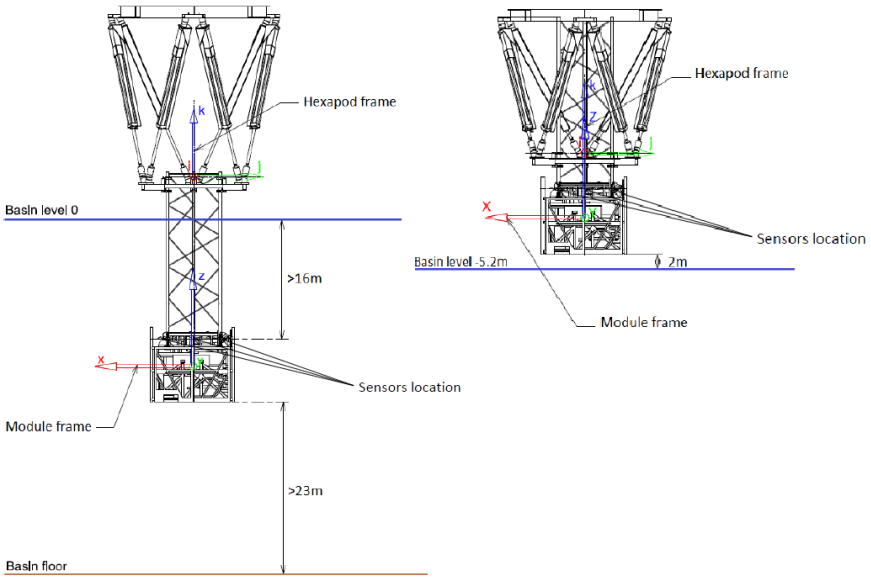

Figure 27 Illustration of test setup. Oscillation test (left), Slamming test (right)

5.1.1 Oscillation-test

The purpose of the oscillation test is to extract the added mass and drag coefficients for the compressor module when subjected to pure harmonic oscillations. The Oceanide software Alise is used to post process the data and allows extraction of the added mass and drag values. The coefficients are computed as follows:

$$C_a = \left(\frac{B}{\rho\omega}\right) * \frac{3\pi}{4 * S * A} \tag{5.1}$$

$$C_m = \left(\frac{M + M_a}{\rho} - \frac{M}{\rho}\right) * \frac{1}{V_{ref}} \tag{5.2}$$

Where:

C_a	-	Drag coefficient
$\left(\frac{B}{\rho\omega}\right)$ and $\left(\frac{M+M_a}{\rho} - \frac{M}{\rho}\right)$	-	Computed by the program ALISE, (Oceanide, 2013)
S	-	Drag surface
A	-	Amplitude of motion
C_m	-	Added mass coefficient
M	-	Model mass, in kg
V_{ref}	-	Reference volume

The hexapod frame has the ability to translate and rotate the module in 2 DOF, by rotating the module 90 degrees on the frame the coefficients in all 6 DOF is obtained. Only the translational oscillations tests have been presented in this thesis.

The drag and added mass coefficients are dependent on the oscillation amplitude. The amplitude will simulate the oscillating wave particle in a regular wave. Four different oscillation amplitudes were used.

Table 14 Oscillation test

Oscillation test		
	Amplitude [m]	Period [sec]
Translations - sensitivity to motion amplitude	1m, 2m, 3m and 4m	10 sec
Translations - sensitivity to motion period	4m	12 sec and 14 sec

5.1.2 Slamming-test

The purpose of the slamming test was to extract the slamming coefficient for the compressor module. The test was carried out at two different water entry velocities, 1,5m/s and 3 m/s.

The module were suspended above the surface and forced at a constant velocity through still water. The slamming coefficient is only estimated for the lower part of the module.

The model test results were re-scaled after the Froude similarity law, and calculated as described in DNV-RP-H130 (Det Norske Veritas, 2011).

$$F_s = \frac{1}{2}\,\rho\, C_s\, S_s\, V_s^2 \tag{5.3}$$

Where:

F_s	-	Slam force
C_s	-	Slamming coefficient
S_s	-	Slam Area
V_s	-	Water entry speed

The slamming coefficient where computed by considering the maximum load in the initial impact. Using this method implies that the measured total measured force in the initial impact will include the buoyancy force and drag force. It is believed that in the initial phase the slamming force will dominate.

The results from the slamming test are based on an area of 29.6 m^2, equivalent to the projected area of beams, pipes and plates in the lower part of the module, as shown in the figure below.

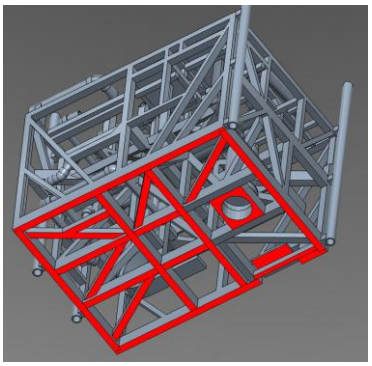

Figure 28 Illustration of slamming area (Source: Inventor 3D)

5.2 SCALE EFFECTS

Some factors will contribute to inaccuracy in the measured forces. Boundary effects, measurement accuracy and modeling accuracy are believed to account for around 1-2 % uncertainty in the final results, according to the "Dynamic analysis review" conference held at Sola Airport Hotel 23.01.2013 (Technip, 2013).

The module consists of several components which can be classed into two categories: smooth components (piping, cylinders…) and components with sharp edges (plates, beams…). The hydrodynamic coefficients for components with sharp edges only depend on the KC-number (Keulegan-Carpenter). This number is kept for each model test, as the same scale ratio is applied to module dimensions and motion amplitude. This implies that there are no scale effects on the sharp edged objects.

The scale effects on the smooth components are caused by differences in the vortex shedding between small and large components. This effect has to be accounted for in cases where the model shall give results for a real full scale module. Programs such as Orcaflex and SIMO do not take into account vortex shedding in lifting analysis, hence will generate comparable results with no scale effects.

5.3 RESULTS AND DATA ANALYSIS

5.3.1 Oscillation test

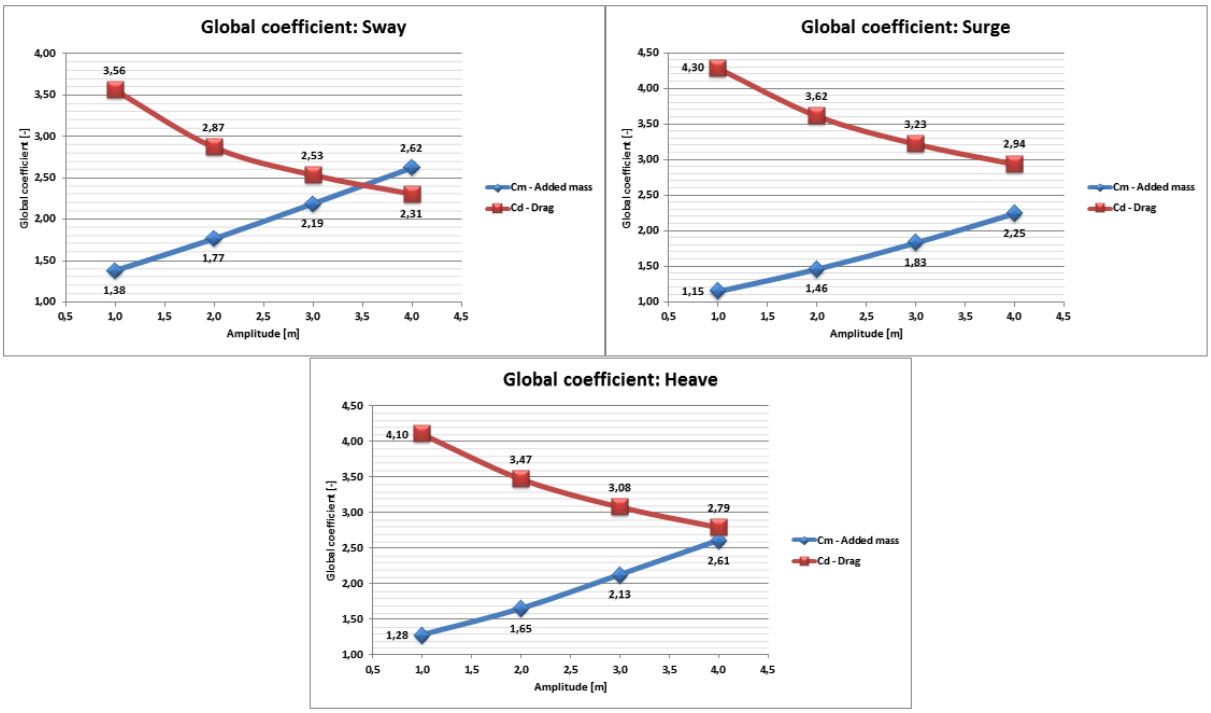

Figure 29 Global coefficients in Sway (top left), Surge (top right) and Heave (center)

As the motion amplitude is increased the added mass coefficient will increase and the drag decrease. This behavior is to be expected for porous structures in infinite water conditions.

The global hydrodynamic coefficient's dependency of oscillation period was, according to theory, not significant.

The hydrodynamic coefficients extracted from the oscillation tests depend on the wave amplitude used in the numerical analysis. The regular wave tests are carried out in wave heights of 5.0 and 8.0 meters. This corresponds to oscillation amplitude of 2.5 and 4.0 meters. The oscillation amplitude of 3.0 meters has been chosen in order to obtain valid results for both tests. The coefficients are presented below:

Table 15 Results from the oscillation test

Global Coefficients from model tests:			
	X (Surge)	Y (Sway)	Z (Heave)
Drag Coefficient [-]	3,23	2,53	3,08
Added Mass Coefficients [-]	1,83	2,19	2,13

5.3.2 Slamming test

The slamming coefficient is based on the maximum load value after water impact. The water impact is shown in red in the graphs below for 1.5 m/s and 3.0 m/s. The slamming test was carried out one time for each velocity.

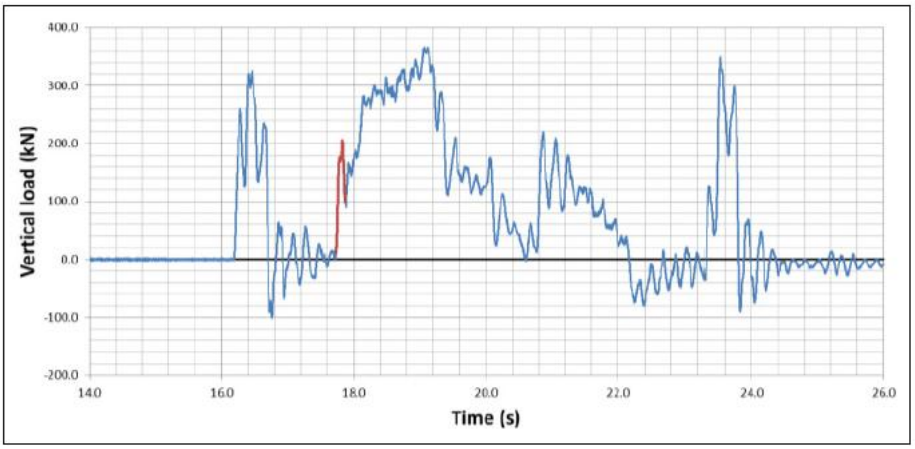

Figure 30 Compressor module slamming test at 1.5 m/s

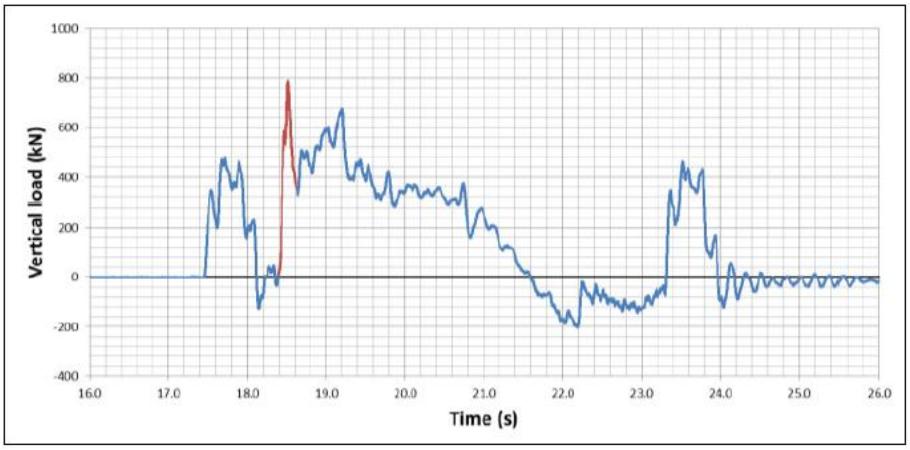

Figure 31 Compressor module slamming test at 3.0 m/s

Note: Measurements taken before the initial impact is acceleration of the compressor module in air.

Table 16 Results from the slamming test

Slamming results		
Velocity [m/s]	**Load [kN]**	**Corresponding Cs**
1,5	205,5	6,0
3,0	787,5	5,8

The slamming coefficient is close to constant for both tests. The slamming coefficient used in the numerical model is 6.0 to prevent the slamming force to be underestimated.

By using the maximum load obtained from the experiments the calculated slamming coefficient is initially over-predicted. The maximum load is a sum of forces and not only slamming force. This problem has been investigated by Campell & Weynberg (1980) and Sarpkaya (1978). Both investigations show that the experimental value on C_s varies greatly depending on test setup and the calculation theory used.

CHAPTER 6

Numerical analysis

The theoretical background of SIMO and Orcaflex has been presented in chapter 2. In this chapter the setup of the module is presented for both programs and the extreme maximum and minimum results from the analysis are compared and discussed. In addition to the extreme value comparison, a study of the wave impact process for some relevant cases has been presented and compared.

6.1 BASIC ASSUMPTIONS

Assumptions for the fluid flow in SIMO and Orcaflex:

- Hydroelasticity is neglected.
- Inviscid and incompressible flow.
- The wave particle kinetics is not affected by the structure.
- No air cushion below the structural elements.
- Long wave approximation, the body dimension is small compared to the wavelength.
- VIV is neglected.

6.2 CALIBRATION OF GLOBAL COEFFICIENTS

The global coefficients from the oscillation test are used to calibrate the local hydrodynamic coefficients for the pipes and beams in the numerical model. This process is not a part of DNV's recommended practice, but is carried out in order to obtain results that are as close as possible to the actual loads and moments on the real module. The calibration process is presented below:

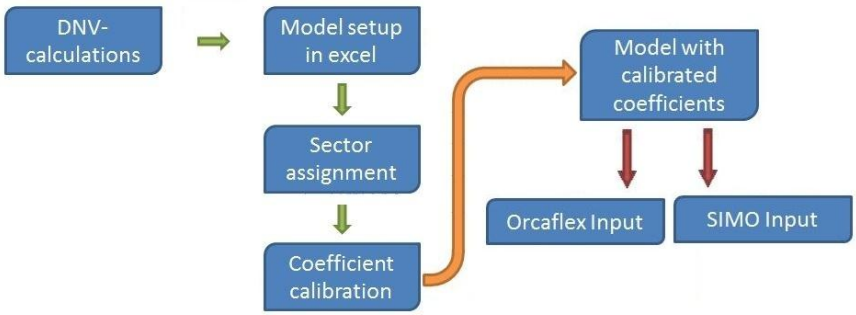

Figure 30 The calibration process when implementing the global coefficients from the oscillation test to the numerical analysis

The calibration process for the hydrodynamic coefficients consists of 5 steps. The calibrated model is used to calculate the input parameters for Orcaflex and SIMA. A summary of the process is described in the sections below, a detailed description of the process is given in the attached Excel file.

6.2.1 DNV-calculations

The first step in the calibration process is to establish the global coefficients based on DNV's recommendations.

The simplified 3D model has been used to retrieve details for the structural elements. The compressor module consists of 239 structural elements with 15 different properties. The recommended practice from DNV has been followed and properties for each beam and pipe have been assessed depending on dimension and direction of flow. Some general assumptions are listed below:

- The drag coefficients have been estimated based on DNV-RP-H103 appendix B1. To account for nonlinear oscillations the steady flow drag should be increased to 2-3 times the steady flow coefficient. The steady flow drag coefficient has been multiplied with 2.5, according to DNV-RP-H103 section 4.6.2.4.

- The analytical added mass for the beams and pipes are calculated for two dimensional bodies far from boundaries, according to table A-1 in DNV-RP-H103 appendix A.

- The analytical added mass for the plates is calculated based on three dimensional bodies. The added mass for motion in the vertical plane is found and distributed, given in table A-2 in DNV-RP-H103 appendix A. The distribution depends on program input data (See section 6.2.5).

6.2.2 Model setup

The 3D-drawings received from Oceanide have been used to set up the model in Excel. Coordinates and orientation for each structural component have been plotted in order to calculate the total added mass and drag for the compressor module.

Based on the DNV recommended practice the global hydrodynamic coefficients are calculated in surge, sway and heave. The surge global coefficients calculations are presented below:

6.2.2.1 Global added mass coefficient

$$C_{m,Surge,Global} = \frac{V_M * \rho}{\sum AM_x} \quad (6.1)$$

Where:

$C_{m,Surge,Global}$ - Global added mass coefficient in x-direction
V_M - Volume of displaced fluid
AM_x - Added mass in x-direction for each structural element (incl. plates)

6.2.2.2 Global drag coefficient

$$C_{a,Surge,Global} = \frac{\sum(A_x * C_a)}{A_{Box-X}} \quad (6.2)$$

Where:

$C_{a,Surge,Global}$ - Global drag coefficient in x-direction
A_x - Projected area in x-direction for each structural element
C_a - Local drag coefficient
A_{Box-X} - Total area of module in x-direction

The global hydrodynamic coefficients in each translational direction, based on the DNV-recommendations, are presented below. See (Det Norske Veritas, 2011) for more details.

Table 17 Comparison of global hydrodynamic coefficients between DNV and model test estimations

Global Coefficients for analysed model:			
	X	Y	Z
Drag Area [m^2]	81,1	115,0	81,5
Drag Coefficient [-]	**8,33**	**7,37**	**6,93**
Added Mass [te]	78,9	95,5	94,7
Added Mass Coefficients [-]	**0,79**	**0,95**	**0,95**
Global Coefficients from model tests:			
	X (Surge)	Y (Sway)	Z (Heave)
Drag Coefficient [-]	3,23	2,53	3,08
Added Mass Coefficients [-]	1,83	2,19	2,13
Difference in Global Coefficients			
	X	Y	Z
Drag Coefficient [-]	61,3 %	65,6 %	55,6 %
Added Mass Coefficients [-]	-132,9 %	-129,9 %	-124,9 %

When comparing the DNV recommendations to the global coefficients obtained from the model test the difference is large. Using the DNV recommended practice is believed to overestimate the drag coefficient and underestimate the added mass. To account for the differences in the global coefficient, the local coefficients for the structural elements are calibrated based on the location of the element inside the module.

6.2.3 Sector assignment

The DNV recommended practice is based on calculations for individual components far form boundaries and not for complex structures. By applying this method, the analysis will not account for any interaction, such as the wake fields generated by the structural components or trapped water between components. The wake field will reduce the drag force on the upstream parts of the structure, and the trapped water will increase the total added mass. This needs to be accounted for to obtain results as close as possible to the real wave impact process.

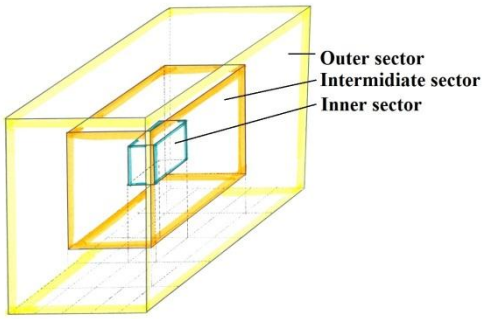

Figure 31 Illustration of the sectors inside the compressor module (Source: Silje N. Torgersen)

To simulate interaction effects the numerical model has been divided into 3 main sectors, outer-, intermediate- and inner sector as illustrated in the figure above.

Each main sector will have a different factor for added mass and drag. Due to wake fields, partially trapped water and other flow restrictions the center of the structure, i.e. the inner sector, shall have a larger factor for C_a and C_m. The inner sector is more affected by the flow disturbance compared to the outer sector. The outer sector shall have coefficients closer to what was originally estimated.

Each structural element are assigned to one sector based on its center of COG using macros in excel.

6.2.4 Calibration

The numerical input in excel have been calibrated in order to achieve the same global coefficients as obtained in the model test. This is done by factoring the local coefficients in X and Y direction for each structural element depending on the sector-location. The calibration is done manually.

Table 18 Calibration of local elements in different sectors

Drag Calibration:		
	LocalX	LocalY
Outer sector:	37 %	50 %
Middle sector:	30 %	47 %
Inner sector:	23 %	10 %

100% means no reduction, 0% means no drag.

Added Mass Calibration:		
	LocalX	LocalY
Outer sector:	230 %	220 %
Middle sector:	320 %	320 %
Inner sector:	450 %	310 %

100% means no increase, 200% means original 2X.

Additional drag/added mass to match global coefficients:			
	X	Y	Z
Additional Drag Area [m^2]	0,3	0,0	7,2
Additional Added Mass [te]	2,7	0,0	26,3

Difference in Global Coefficients			
	X	Y	Z
Drag Coefficient [-]	0,0 %	16,2 %	0,0 %
Added Mass Coefficients [-]	0,0 %	6,4 %	0,0 %

The local drag coefficient for every structural element located in the "Outer Sector" is reduced 37% of the original value in local X direction and 50% of the original value in the local Y direction. The added mass coefficient are increased with 230% (X) and 220% (Y)

By only calibrating the local coefficients some differences are still present. Additional drag area and added mass are inserted into the numerical model to match the global coefficients.

Note: The drag and added mass coefficient in Y-direction has a significant offset. This is believed not to affect the final results due to the module's rotation relative to the incoming wave.

6.2.5 Model setup with calibrated coefficients

All structural elements have been set up in the spreadsheet with new local coefficients, to match the global coefficients from the model tests. The input for SIMO and Orcaflex are different, but based on the same properties. The full overview of the element input is given in the attached excel document.

6.2.5.1 Orcaflex input

Line setup

Using the start and end coordinates, each structural element are plotted into Orcaflex. To orient the elements "Azimuth", "Declination" and "Gamma" is used to assign the local orientation relative to the global axes. This way, non-symmetric and declined elements can be modeled.

Buoyancy setup

Orcaflex calculates the wetted volume using the outer diameter of the pipe, OD_{Pipe}. The wetted volume is used to calculate the buoyancy force, see sec 2.1.2.2.

The same input, OD_{Beam}, is used for beam elements. The beam elements outer diameter has to be recalculated to obtain the correct buoyancy force. This is accomplished by using the inner- and cross section area of the beam, as illustrated in figure 32.

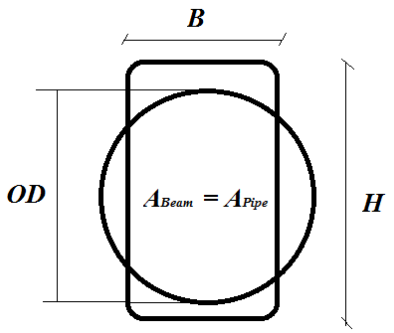

Figure 32 Correction for rectangular elements in Orcaflex

$$ID_{Beam} = \sqrt{\frac{4 * A_I}{\pi}} \tag{6.3}$$

$$OD_{Beam} = \sqrt{\frac{ID_{Pipe}^2 + 4 * A_{CS}}{\pi}} \tag{6.4}$$

Where:

ID_{Beam}	-	Beam equivalent inner diameter
A_I	-	Inner beam area
OD_{Beam}	-	Beam equivalent outer diameter
A_{CS}	-	Beam cross section area

The new OD_{Beam} is used as input for beam elements. To obtain correct added mass and drag force on beam elements the local coefficients has to be changed according to the new outer diameter.

Added mass setup

The added mass calculations are based on the elements outer diameter and the added mass coefficient, see section 2.1.2.3 for details. For circular elements the calibrated local added mass coefficient is used directly.

To obtain the correct added mass for beams using the recalculated outer diameter, OD_{Beam}, a scaling of the added mass coefficient has to be performed on the input data. The scaling is performed using the following formula:

$$C_{m,X-beam} = C_{m,X} * \left(\frac{H}{OD_{Pipe}}\right)^2 \tag{6.5}$$

$$C_{m,Y-beam} = C_{m,Y} * \left(\frac{B}{OD_{Pipe}}\right)^2 \tag{6.6}$$

Where:

$C_{m,X-beam}$	-	Scaled added mass coefficient in local X-dir
$C_{m,X}$	-	Added mass coefficient in local X-dir
H	-	Height of beam
$C_{m,Y-beam}$	-	Scaled added mass coefficient in local Y-dir

$C_{m,Y}$	-	Added mass coefficient in local Y-dir
B	-	With of beam

Drag Setup

The drag calculations are based on the cross flow principle using the outer diameter and the drag coefficient, see section 2.1.2.3 for details. For circular elements the calibrated local drag coefficient is used directly.

To obtain equivalent drag for beam elements, the drag coefficient is rescaled according to the recalculated outer diameter.

$$C_{A,X-beam} = \frac{H * C_{A,X}}{OD_{Pipe}} \tag{6.7}$$

$$C_{A,Y-beam} = \frac{B * C_{A,Y}}{OD_{Pipe}} \tag{6.8}$$

Where:

$C_{A,X-beam}$	-	Scaled drag coefficient in local X-dir
$C_{A,X}$	-	Drag coefficient in local X-dir
$C_{A,Y-beam}$	-	Scaled drag coefficient in local Y-dir
$C_{A,Y}$	-	Drag coefficient in local Y-dir

Slamming Setup

The slam force and the water exit force are accounted for by using 76 lumped 6D-buoys. Each buoy is assigned a slamming coefficient and a projected area. The buoys are attached to the horizontal lines/beam in Orcaflex and will represent the respective projected area of each line/beam, in the global Z-direction.

The main horizontal supporting structure is divided in three layers, lower middle and upper layer. Making the buoys distributed in three layers vertically as shown in figure 33.

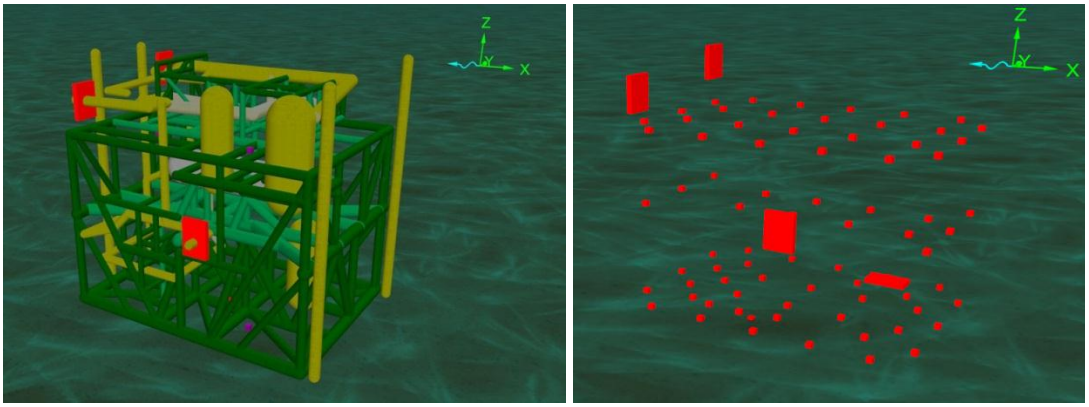

Figure 33 The compressor module setup in Orcaflex (left) Slam buoy setup (right) (Source: Orcaflex)

6.2.5.2 SIMA input:

Line setup:

Start and end coordinates is used to define each structural element in SIMA. The orientation for the local XY-plane is given by assigning a reference point.

Buoyancy setup:

The buoyancy force is calculated using the specific volume (m^3/m). The specific volume for each structural element is calculated according to the following formulas:

$$V_{Pipe} = \frac{\pi}{4} * OD_{Pipe}^2 \tag{6.9}$$

$$V_{Beam} = H * B \tag{6.10}$$

Added mass setup:

The added mass for the structural elements are calculated per unit length, according to table A-1 in DNV-RP-H103 appendix A.

$$A_{ij} = \rho * C_{m,ij} * (\pi * a^2) \tag{6.11}$$

Where:

A_{ij}	-	Added mass in local X or Y, per unit length
$C_{m,ij}$	-	Scaled added mass coefficient in local X or Y
a	-	Width of element in flow direction

The analytical added mass is calculated and assigned to each structural element depending on the local orientation.

Drag Setup

The quadratic drag force on each element is calculated per unit length, according to table B-1 in DNV-RP-H103 appendix B.

$$\frac{f}{u^2}_{ij} = ½\rho C_{A,ij} D \tag{6.12}$$

Where:

$\frac{f}{u^2}_{ij}$	-	Quadratic drag force in local X or Y, per unit length
$C_{A,ij}$	-	Scaled drag coefficient in local X or Y
D	-	Width of element in flow direction

Slamming Setup

The slamming force is proportional change in the added mass. The slamming force is based on the input off the added mass properties and the depth dependent hydrodynamic coefficients, see section 2.2.3 for details.

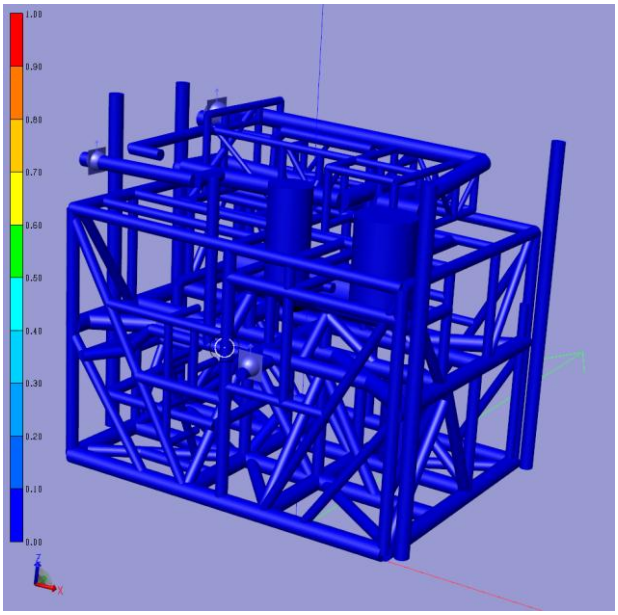

Figure 34 The compressor module setup in SIMA (Source: SIMA)

6.3 TEST SETUP

The numerical module is suspended in four elevations, according to section 3.2. Regular waves, according to Airy's theory, are subjected to the model in a time period of 50 seconds. The model is analyzed in three different environmental conditions, all wave heights are according to conditions measured in the ocean basin. In total, the model is analyzed in 12 different cases.

A time step of 0.01 sec is used to ensure all impact loads are captured.

Table 19 Test list for the numerical simulations

Test list						
Project:	**Master thesis - ASGARD Subsea Compression Module - Numerical Wave tests**					
Test Number	**Module**	**Wave type**	**Heading (°)**	**Wave Height (m)**	**Period (s)**	**Elevation (m)**
1	Compressor	Airy's	0°	5.325	7	2
2	Compressor	Airy's	0°	5.798	10	2
3	Compressor	Airy's	0°	7.782	7	2
4	Compressor	Airy's	0°	5.351	7	0
5	Compressor	Airy's	0°	5.829	10	0
6	Compressor	Airy's	0°	7.782	7	0
7	Compressor	Airy's	0°	5.370	7	-3,75
8	Compressor	Airy's	0°	5.866	10	-3,75
9	Compressor	Airy's	0°	7.742	7	-3,75
10	Compressor	Airy's	0°	5.302	7	-7,45
11	Compressor	Airy's	0°	5.831	10	-7,45
12	Compressor	Airy's	0°	7.740	7	-7,45

6.4 RESULTS AND DATA ANALYSIS

The global maximum and minimum forces for SIMO and Orcaflex has been extracted in horizontal and vertical direction. They are given only for dynamic forces; hence the static load is not included in the final results.

The difference between the results obtained from SIMO and Orcaflex is compared and analyzed.

6.4.1 Static loads

The static force measurements have been removed at the beginning of each analysis. By analyzing the static load differences, the time varying buoyancy force difference can be established. The buoyancy force differences will only affect the vertical force calculations.

Table 20 Summary of static loads in SIMO and Orcaflex

Global Static Loads				
Project:	Master thesis - ASGARD Subsea Compression Module - Numerical Wave tests			
Elevation	Test number	SIMA-Static load [kN]	Orcaflex-Static load [kN]	Comparison [kN]
1	1	-1095,0	-1100,5	5,5
2	4	-1021,0	-1024,5	3,5
3	7	-689,1	-707,8	18,7
4	10	-261,1	-294,7	33,6

Differences in the static load calculations are present in all elevations. In air, a total difference of 5.5 kN is present; this is caused by weight difference.

In elevation 2, 3 and 4 the module is in contact with water, indicating that buoyancy forces are included. The difference may originate from the recalculations of the outer diameter in Orcaflex or the input for depth dependent hydrodynamic coefficients in SIMO. In fully submerged condition the differences caused by time varying buoyancy force should not exceed 33.6 kN in the vertical force calculations.

6.4.2 Dynamic forces

Table 21 Global horizontal force comparison between Orcaflex and SIMO

Global Horizontal forces									
Project:	Master thesis - ASGARD Subsea Compression Module - Numerical Wave tests								
Test number	Elevation	Environment		SIMA-calculation		Orcaflex-calculation		Comparison	
		H [m]	T [s]	F_{Max}	F_{Min}	F_{Max}	F_{Min}	F_{Max}	F_{Min}
1	1	5,3	7,0	0,00	-182,38	0,22	-146,08	-	19,9 %
4	2			41,26	-302,82	37,20	-295,38	9,8 %	2,5 %
7	3			226,64	-561,74	211,26	-545,51	6,8 %	2,9 %
10	4			380,30	-616,43	352,98	-618,46	7,2 %	-0,3 %
2	1	5,8	10,0	0,00	-120,98	1,10	-99,67	-	17,6 %
5	2			30,36	-175,69	34,47	-190,19	-13,5 %	-8,3 %
8	3			132,57	-344,63	136,18	-365,99	-2,7 %	-6,2 %
11	4			249,76	-418,64	249,49	-452,91	0,1 %	-8,2 %
3	1	7,8	7,0	0,00	-483,98	1,30	-462,59	-	4,4 %
6	2			51,32	-911,05	48,89	-811,29	4,7 %	11,0 %
9	3			315,14	-1289,55	295,33	-1245,65	6,3 %	3,4 %
12	4			566,52	-1140,56	518,57	-1177,00	8,5 %	-3,2 %

The horizontal force calculations in SIMO and Orcaflex follow the same trend as observed in the model tests; maximum negative forces are measured in the water entry phase while the positive maximum forces are obtained from the water exit phase. For elevation 1 the maximum positive force is close to non-existing, and is for that reason not presented in the final comparison.

The horizontal force calculations are similar in both programs. The force difference varies from 19.9% to -13.5%, where SIMO is generally more conservative compared to Orcaflex calculations. This depends on the module elevation and the analyzed environment. The largest differences appears in elevation 1 & 2; the splash zone.

Table 22 Global vertical force comparison between Orcaflex and SIMO

Global Vertical forces									
Project:	Master thesis - ASGARD Subsea Compression Module - Numerical Wave tests								
Elevation	Test number	Environment		SIMA-calculation		Orcaflex-calculation		Comparison	
		H [m]	T [s]	F_{Max}	F_{Min}	F_{Max}	F_{Min}	F_{Max}	F_{Min}
1	1	5,3	7,0	128,12	-2,20	237,25	-82,96	-85,2 %	-
2	4			355,53	-34,05	454,66	-118,91	-27,9 %	-249,2 %
3	7			438,16	-278,08	304,66	-311,47	30,5 %	-12,0 %
4	10			475,78	-485,92	396,87	-521,19	16,6 %	-7,3 %
1	2	5,8	10,0	170,68	0,00	257,95	-61,43	-51,1 %	-
2	5			289,31	-0,28	393,36	-79,48	-36,0 %	-
3	8			349,97	-182,02	273,53	-186,54	21,8 %	-2,5 %
4	11			378,18	-282,69	331,82	-319,74	12,3 %	-13,1 %
1	3	7,8	7,0	317,05	-142,01	543,45	-325,90	-71,4 %	-129,5 %
2	6			591,06	-254,65	678,26	-362,01	-14,8 %	-42,2 %
3	9			890,88	-619,88	719,20	-619,84	19,3 %	0,0 %
4	12			977,78	-1034,17	789,36	-1062,73	19,3 %	-2,8 %

The vertical force calculation is a combination of drag, inertia, buoyancy and slamming forces. All maximum positive forces are obtained in the water entry phase.

In the initial elevations 1 & 2, Orcaflex is more conservative compared to SIMO. The largest force difference in the water entry phase is -85.2% and can be observed in elevation 1, test 1, see appendix 8. Orcaflex calculates the initial wave impact 109kN larger than SIMO.

In elevation 1 & 2, Orcaflex calculates water exit slam forces in the water exit phase. SIMO calculations does not account for this, hence the force differences are very large in the maximum negative forces. The maximum difference between Orcaflex and SIMO is -129.5 % and is obtained in elevation 1 environment 3. The comparison with the model test will reveal if the water exit slam force should be included in the analysis.

In elevation 3 & 4, half submerged and fully submerged, SIMO predicts larger positive forces in the water entry phase.

The differences in the maximum negative forces are decreasing as the model is submerged through the splash zone. In all cases Orcaflex is conservative.

6.4.3 Separated force components

To analyze the data more closely, all simulations are re-analyzed in Orcaflex and SIMO using only one input data, e.g. only drag input. The results are compared to better understand the wave impact process. Only a few cases are presented in the final results, the selected cases are representing trends appearing in several cases. The separation of force components is presented for case 4 and case 11.

Due to multiple connections between input data and the forces analyzed a complete picture of the separated force components is not possible. For example in SIMO where the input added mass forces results in both inertia and slam forces.

6.4.3.1 Case 4

In case 4, the module is subjected to waves, 5.3 meters tall with a wave period of 7 seconds. The module is suspended 0 meters above the mean sea level. The total force history is presented in appendix 8. The total horizontal force calculations in SIMO and

Orcaflex showed a difference of 9.8% and 2.5%. In both cases SIMO was conservative. The vertical force calculations had a difference of -27.9% and -249.2% where Orcaflex predicted larger forces both positive and negative forces.

Drag

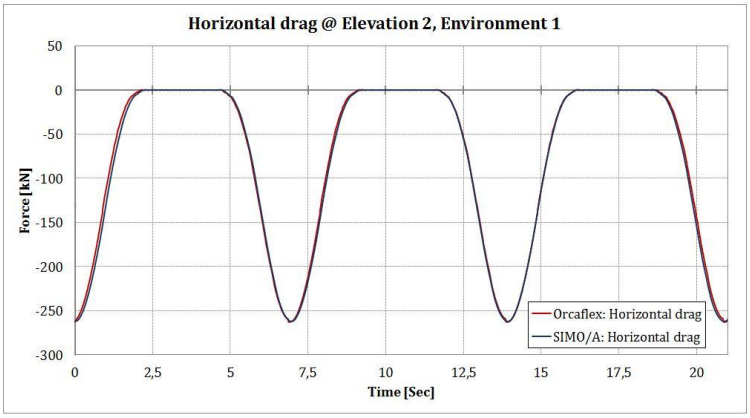

Figure 35 Horizontal drag forces on the compressor module in environment 1

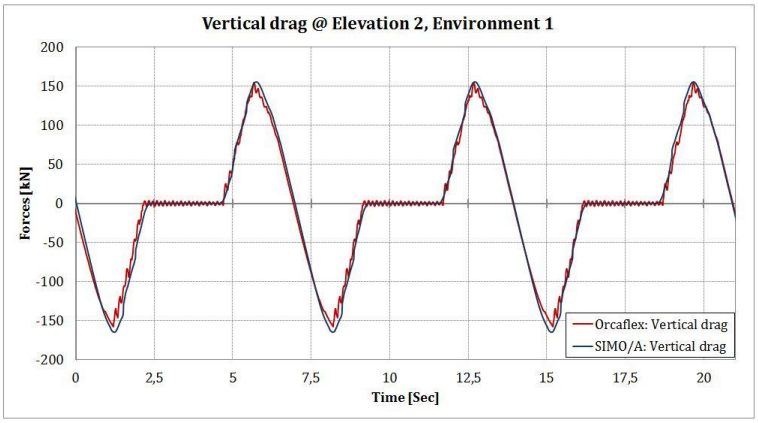

Figure 36 Vertical drag forces on the compressor module in environment 1

The drag forces have been extracted from both analysis and compared.

The results in figure 35 indicate that there is not a significant difference in the predicted drag force in the horizontal direction. The maximum negative force calculated by Orcaflex is –262.8 kN while SIMO calculated –262.06 kN. In practical matters the calculations are alike.

The vertical drag calculation in figure 36 is similar. The two programs is only separated by 0.97 kN maximum positive force and 7 kN for the maximum negative force. In both directions SIMO are more conservative.

Inertia, Slam and Buoyancy

The horizontal and vertical contributions from slamming buoyancy and added mass are combined to obtain comparable results.

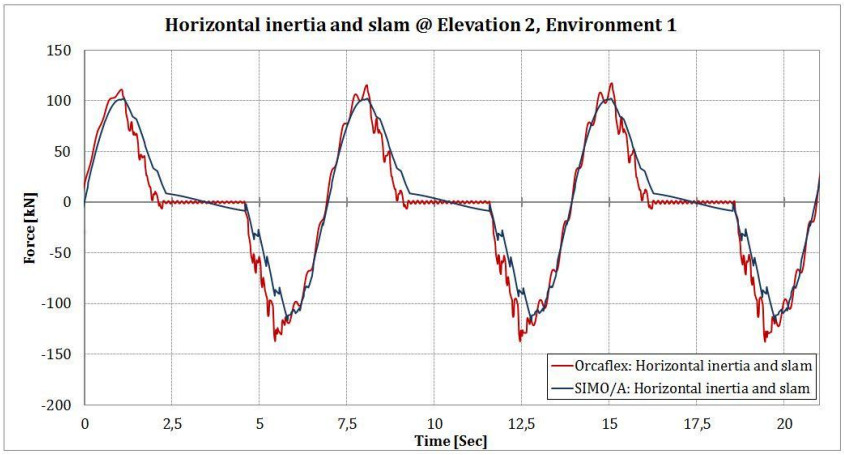

Figure 37 Horizontal inertia and slam forces on the compressor module in environment 2

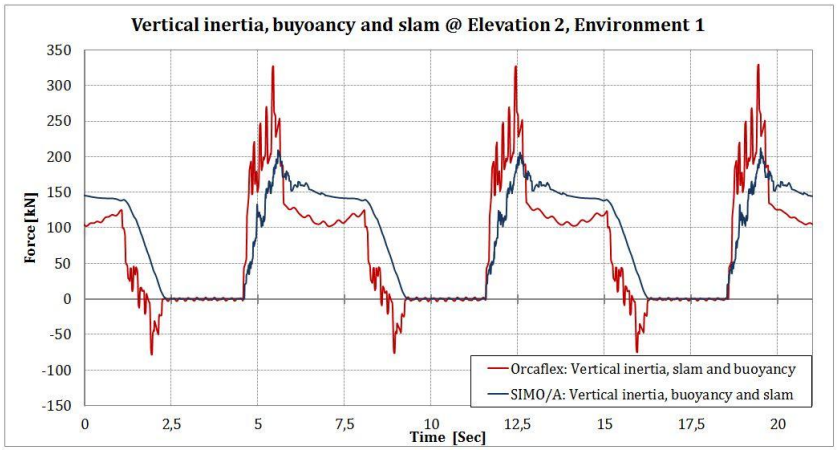

Figure 38 Vertical inertia, buoyancy and slam forces on the compressor module in environment 2

The difference in the negative force calculation in the horizontal direction is 21.5 kN, while the maximum force are separated by 16.61 kN, as seen in figure 37. The time history of the Orcaflex calculations shows that the horizontal force has a number of local peaks. The peaks appear as the wave propagates into the structure and contributes to most of the measured differences.

By comparing the vertical Orcaflex and the SIMO forces in figure 38, a significant difference is observed. Orcaflex predicts forces 117.9 kN higher than SIMO. Based on the impact profile, the sudden increase in forces indicates slam forces. In addition Orcaflex predicts a rapid decrease in the vertical force, after the initial impact, while SIMO does not. In this phase the module is partly submerged, some buoyancy differences may contributing to a lower force in Orcaflex calculations, see static load section 6.4.1.

SIMO calculations indicate no negative forces in the water exit phase, while Orcaflex predicts -78.4 kN.

6.4.3.2 Discussion: Case 4

The total force analysis contained differences in the measured maxima and minima for both horizontal and vertical forces. The total horizontal force comparison showed differences up to 9.8%, the total force separating the calculations was only 4.06 kN.

The horizontal drag force from SIMO and Orcaflex are practically alike, and would not contribute to any significant difference in the total force calculations. Small differences in the added mass and slamming calculation will influence the final comparison. The slam force formulation in Orcaflex allows the projected area of the lumped buoy to act normal to the water surface, causing some horizontal forces differences. In practical matters the force differences are very small and would not inflict any limitations to a marine operation connected to the lifts of the compressor module.

The total vertical force comparison showed differences up to -249.2%, where Orcaflex predicted the largest forces. The vertical drag force calculations in SIMO and Orcaflex are not a large contributing factor to the differences observed in the total force calculations.

The largest differences can be found in the comparison of added mass, buoyancy and slam forces. The maximum buoyance difference can only account for 33.6 kN of the total measurements, according to the static load comparison in 6.4.1.

The formulation of the slam force in Orcaflex is different compared to SIMO calculations. Further investigation of the slam forces was initiated. By removing the slam force contribution from the Orcaflex measurements we can see from figure 39, that slam forces are the main contributing factor to the differences observed in the vertical force results. In the water exit phase Orcaflex's lumped buoy formulation calculates water exit slam forces over 100 kN.

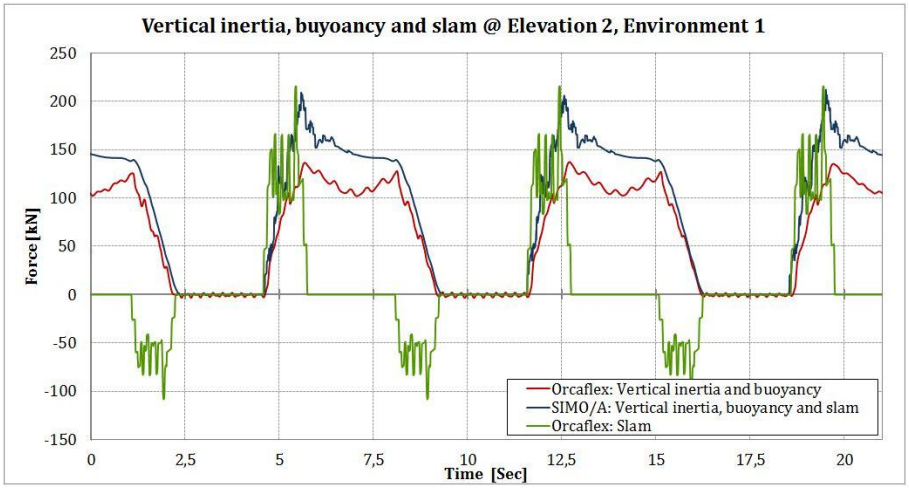

Figure 39 Illustration of the slam force significance in Orcaflex calculations

6.4.3.3 Case 11

In case 11, the module is fully submerged and subjected to waves with a wave height of 5.8 m and a wave period of 10 seconds. The module will be fully submerged and partly submerged due to the wave elevation. The total horizontal forces calculated by Orcaflex was conservative compared to SIMO. The results had a difference of -0.1% for maximum positive forces and -8.2% for the maximum negative forces.

The vertical force measurements had a difference of 19.7% and -15.9%. SIMO was conservative for positive forces, while Orcaflex for the negative forces.

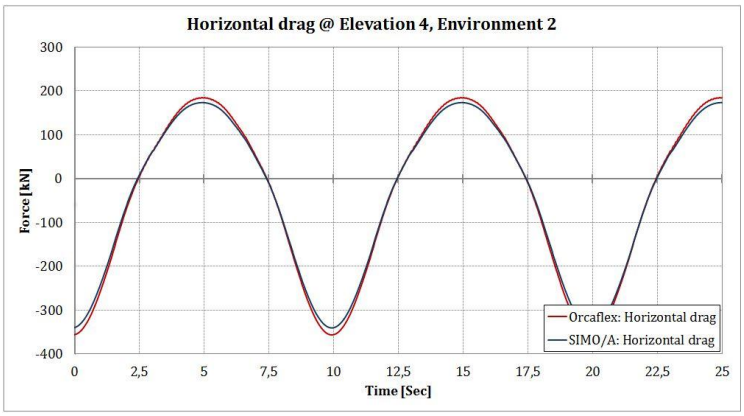

Figure 40 Horizontal drag forces on the compressor module in environment 2

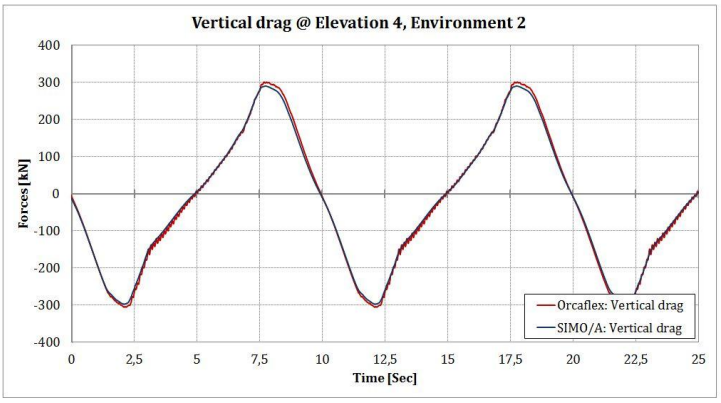

Figure 41 Vertical drag forces on the compressor module in environment 2

By comparing the horizontal drag a small difference between the maximum and minimum values can be observed. Orcaflex predicts 11.4 kN larger horizontal drag forces compared to SIMO. The maximum negative drag forces are obtained as the module is fully submerged by the wave, the calculation differences are 15.93kN.

Inertia, Slam and Buoyancy

The horizontal and vertical contributions from slamming buoyancy and added mass are combined to obtain comparable results.

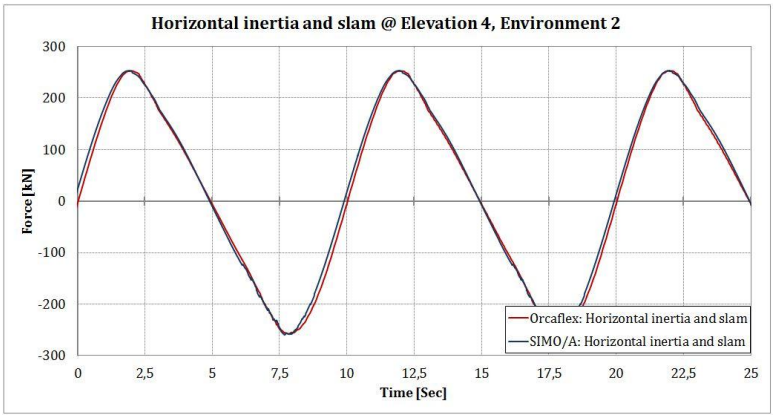

Figure 42 Horizontal inertia and slam forces on the compressor module in environment 2

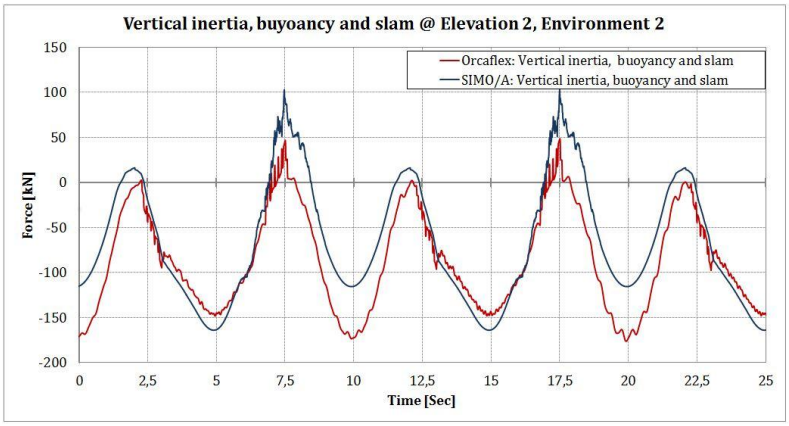

Figure 43 Vertical inertia, buoyancy and slam forces on the compressor module in environment 2

By comparing the inertia forces and the slamming in the horizontal direction the calculation results are alike. The calculation difference of the inertia and slam force will not influence the total force differences measured.

The vertical force calculations are different in the water entry phase. As the structure is being submerged slamming forces are present in both calculations. SIMO estimates the combined slamming, buoyancy and inertia to be 54.07 kN larger than Orcaflex. From partly submerged to fully submerged, approximately 7.5~10.0 seconds and 17.5~20.0 seconds, Orcaflex calculates a rapid drop in the vertical force more significant compared to SIMO. The drop may originate from the buoyancy force calculation or inertia differences in the two programs.

6.4.3.4 Discussion: Case 11

The estimation of the drag forces is very similar in the two programs. The differences between the calculations are believed not to influence the final results in a significant way.

The main difference in vertical forces originates from the calculation of Inertia, buoyancy and slam. By separating inertia and buoyancy from Orcaflex's calculation a better understanding of the wave process is obtained, see figure 44. Fully submerged, the structure is not affected by the slam force calculation and will for that reason not affect the comparison in any significant degree. The other possible source of error is the difference in buoyancy. When the structure is fully wetted (10 sec and 20 sec) the SIMO calculations are more conservative. As described, in section 6.4.1, the buoyancy forces in SIMO is 33.6 kN larger and will for that reason give more conservative results. This would indicate a higher negative value when the structure has its lowest wetted area (5 sec and 15 sec and 25 sec). This matches the results given in figure 43. In addition to the buoyancy extra inertia forces in the Orcaflex calculation seems likely, due to the steeper force curve as the structure is submerged. The source of the extra inertia has not been found.

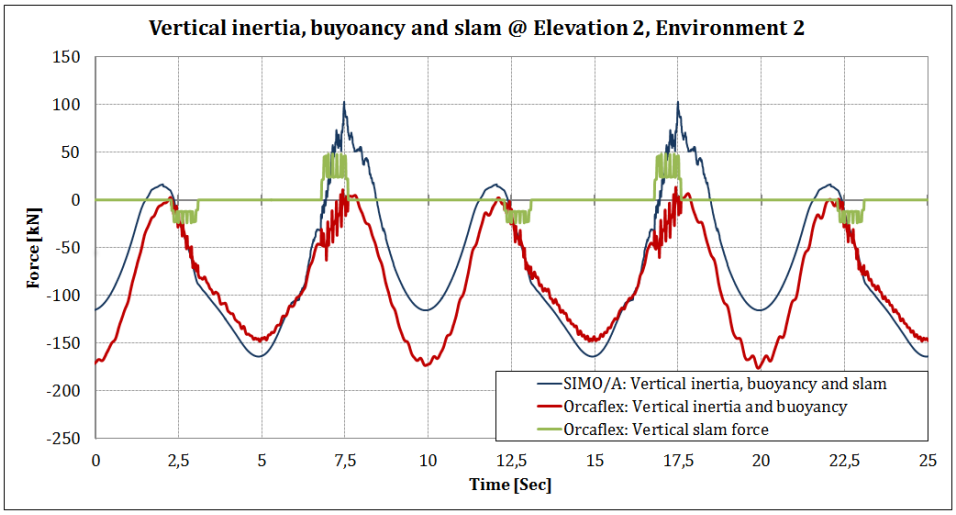

Figure 44 Investigation of force calculation differences.

6.5 DISCUSSION

The horizontal forces in SIMO and Orcaflex have largest differences in the splash zone. By analyzing the time history in the splash zone, see appendix 8, local peaks appears to be the main cause of the differences observed in the horizontal direction. These peaks are assumed to originate from slamming, drag and inertia from elements, as the wave propagates into the module. SIMO's and Orcaflex's calculation of slamming will in most cases calculate a horizontal force component, see section 2.1.2.4 for details. This component appears to have different magnitude and is not in phase.

The environmental impact on the horizontal force calculations shows that Orcaflex is more conservative when subjected to a wave with a 10 second period compared to lower period waves. The horizontal velocity component is increasing as the wave period increases. Small differences in the calculated drag force are causing the difference for longer period waves. Further investigation of horizontal drag differences is presented in section 6.4.4.

The magnitude of the dynamic load difference in the horizontal direction is not very large. In practical matters, the load difference will affect any limitations to a marine operation.

The vertical force comparison shows a significant difference between SIMO and Orcaflex. In the initial elevations 1 & 2 Orcaflex is more conservative compared to SIMO. This trend is present for all environmental conditions. By analyzing the time history, see appendix 8, the slam forces appears to be the main contributor to the calculated differences. The slam forces are calculated in Orcaflex using "lumped 6D-buoys", these buoys are assigned an area and a slamming coefficient, while SIMO calculates the slam force based on the rate of change in the added mass. The slamming coefficient used in Orcaflex is estimated based on model tests. The accuracy of the model test can be questioned since the calculation of the slamming coefficient is based on the maximum forces at water entry. The maximum force measurements will contain force contributions from drag, inertia and buoyancy, hence the slamming coefficient might be

over predicted. In addition the research carried out by (Sarpkaya, 1978) indicates a large scatter of the slamming coefficient.

For elevation 1 some large differences were discovered as water was exiting the structure. These differences occurred for all environmental conditions. Orcaflex will calculate "water exit"-forces using "lumped 6D-buoys". For many types of problems the water exit force contribution can be neglected, according to DNV-RP-H103. In the analysis of the SHS this force is included to capture all hydrodynamic effects that may affect the structure. SIMO does not include this force, see section 2.3.5. A comparison of the calculations versus the model tests will indicate if this force should be included.

In addition to the water exit force, investigation showed that some difference may originate from the beam input in SIMO and Orcaflex. In elevation 1 the model was suspended over the mean sea level so that the wave crest only hit the lower SHS 600x300x10 beams, i.e. 0.6 meter tall beams. The beams were not completely submerged by the wave. In SIMO the beams depth dependent hydrodynamic coefficients calculated that the negative forces was very small during the water exit phase. In Orcaflex the outer diameter of each structural element is rescaled to match the buoyancy forces, see section 6.2.5.1. The rescaled beam measured 0.48 m in diameter making the beam more submerged as the wave is propagating by. The drag force calculations are based on the PW area making the wetted area larger compared to the SIMO calculations, see section 2.1.3. This problem will occur in other simulations but will not be as visible.

In fully submerged condition buoyancy differences are present. Based on the static load analysis the vertical force differences caused by the buoyancy calculations are 33.6 kN.

The force calculations show a trend as the module is lowered through the splash zone; the differences between Orcaflex and SIMO reduces. This may indicate that one of the programs is less equipped to handle vertical forces in the splash zone.

Comparing the vertical force time history of inertia, buoyancy and slamming in case 4 and case 11, similar trends after the initial impact are present. SIMO calculates the negative forces less rapid and not as dominant as Orcaflex. The buoyancy force calculations will account for maximum 33.6kN difference is the compared results. The vertical force differences may indicate more inertia forces in the Orcaflex calculations. This is believed to originate from small differences in the input data for beams close to the surface. The exact source has not been found.

CHAPTER 7

Comparison

Marine operations related to the ÅSC-project have several challenges regarding hydrodynamic forces in the splash zone. A correct estimation of these forces is vital to ensure safe working conditions and to avoid economic losses. Based on recommendations from O. Faltinsen, Technip carried out model tests in waves, to insure that Orcaflex's calculations were conservative in all phases of the lift (Technip, 2013).

Numerical results obtained from SIMO and Orcaflex, in chapter 6, are compared against results from the model tests in chapter 4. The maximum and minimum values for all environmental conditions and all elevations are compared.

The time histories of some cases showing general trends are presented for a better understanding of the wave impact process.

7.1 INPUT DATA

The modules are suspended in four different elevations and subjected to regular waves, according to chapter 3. Due to limitations in SIMO, Airy's wave theory has been used in the numerical simulations for both Orcaflex and SIMO. The Oceanide model is subjected to regular waves similar to the Stokes 5th wave theory.

All environmental data used in the analysis are based on wave measurements in the ocean basin. The environments are given in the table below:

Table 23 Environmental input

Environmental conditions			
	Heading [°]	Wave Height [m]	Period [s]
Environment 1	0	5,3	7
Environment 2	0	5,8	10
Environment 3	0	7,8	7

The test program for the numerical analysis and the model tests is given in chapter 6 and chapter 4 respectively.

7.2 RESULTS

The global forces in the vertical and horizontal direction are extracted from all analysis. The results from the model test are scaled up, according to the Froude similarity law (Oceanide, 2013).

7.2.1 Static loads

The static load has been removed from all analysis in the beginning of each test to obtain comparable results.

The volume is compared to account for static load and time varying buoyancy differences. The model constructed by Oceanide had a total volume of 84.7 m^3. The numerical model in Orcaflex and SIMO had a volume of 97.06 m^3 and 98.05m^3 respectively. The buoyancy difference will affect the final vertical measurements. Hand calculations show that in a worst case scenario the maximum positive force difference due to buoyancy is 124.28 kN higher in the model tests than what the results in Orcaflex shows. For SIMO the value can be up to 134.23 kN. For the maximum negative forces the model test will measure less force. The effect of different buoyancy is more present in elevation 3 & 4.

The horizontal forces are not affected by difference in volume.

7.2.2 Dynamic loads

The dynamic results from all analysis are compared. A complete overview of the measured positive and negative forces is given in appendix 9.

The dynamic forces are presented for each environment, both horizontal and vertical. The results show the maximum positive and negative force measurements during steady state conditions, i.e. during steady oscillatory waves.

7.2.2.1 Environment 1:

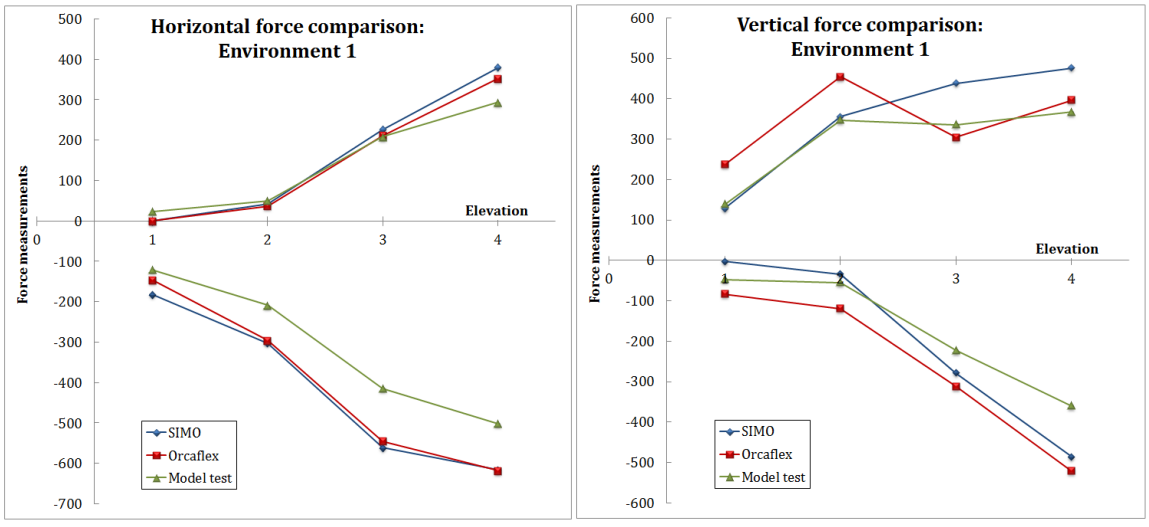

Figure 45 Comparison of maximum forces from numerical and experimental analysis using environment 1 in all elevations

In environment 1, the module is subjected to wave with a wave height of 5.3 meters and a wave period of 7 seconds.

The horizontal forces are compared and analyzed. SIMO and Orcaflex calculate the water entry phase (negative forces) conservatively. The largest differences between the model test and the numerical simulation is measured in elevation 3. SIMO estimates a horizontal force 147.1 kN larger compared to the model test. Orcaflex estimates 130.9 kN. The water exit phase (positive forces) the numerical simulations and the model test are very similar. The largest difference is measured in elevation 4, were SIMO predicts 86.2 kN larger forces than the model test. Orcaflex are closer to the mode tests with a 58.9 kN difference.

The horizontal force comparison shows that the Orcaflex calculation of the wave impact process is closer to the model tests compared to SIMO.

The vertical force comparison indicates that the water entry phase (positive forces) is well predicted by SIMO. In elevation 1 & 2 the positive force calculation in SIMO are very close to the measured forces obtained from the model test. Orcaflex calculations indicate that the initial wave impact is over predicted. This is mainly caused by Orcaflex's calculation of slam forces. The slam force calculation will be discussed in section 7.3.

In elevation 3 & 4 SIMO calculations are conservative. In elevation 3, Orcaflex underestimates the vertical forces. Reasons for this will be discussed in section 7.3.

SIMO calculations are not conservative in the water exit phase for elevation 1 & 2. SIMO considers the water exit forces to be negligible. By comparing with the model tests this may not be optimal.

Orcaflex are conservative in the water exit phase, mainly due to the calculation of "water exit slam forces".

7.2.2.2 Environment 2:

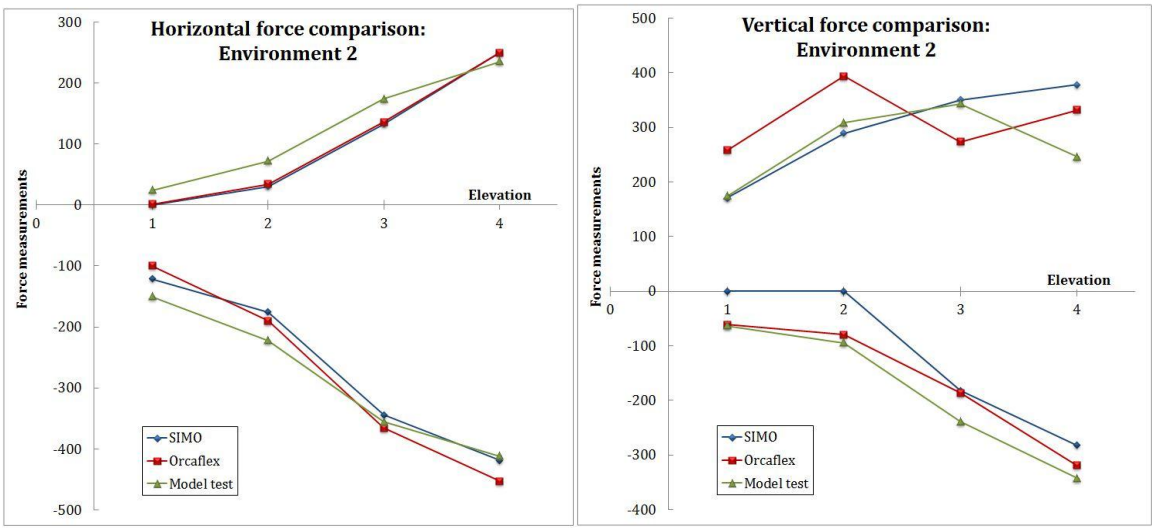

Figure 46 Comparison of maximum forces from numerical and experimental analysis using environment 2 in all elevations

In environment 2, the module is subjected to waves 5.8 meters tall with a wave period of 10 seconds.

The horizontal force comparison show that the numerical simulations are not conservative compared to the model test. Only in elevation 4 for both positive and negative maxima the forces obtained from the numerical simulation is on the conservative side.

The vertical forces follow a similar trend as environment 1. The water entry forces in SIMO are close to the model test results, while Orcaflex's predictions are conservative. In elevation 3, the Orcaflex calculations are not conservative. The same trend can be observed in environment 1. This trend is discussed with Orcina Ltd, in appendix 10.

The vertical forces in the water exit phase (negative forces) are not conservative for the numerical simulations. This may some degree be influenced by the lack of buoyancy but other error sources will be discussed. In all elevations Orcaflex are closer to the model test data compared to SIMO. In elevation 2 the largest difference appears. SIMO calculated 94.5 kN less forces than measured in the model test.

The comparison in environment 2 shows that the numerical simulations are generally not conservative. The differences and possible error sources is discussed in section 7.3.

7.2.2.3 Environment 3:

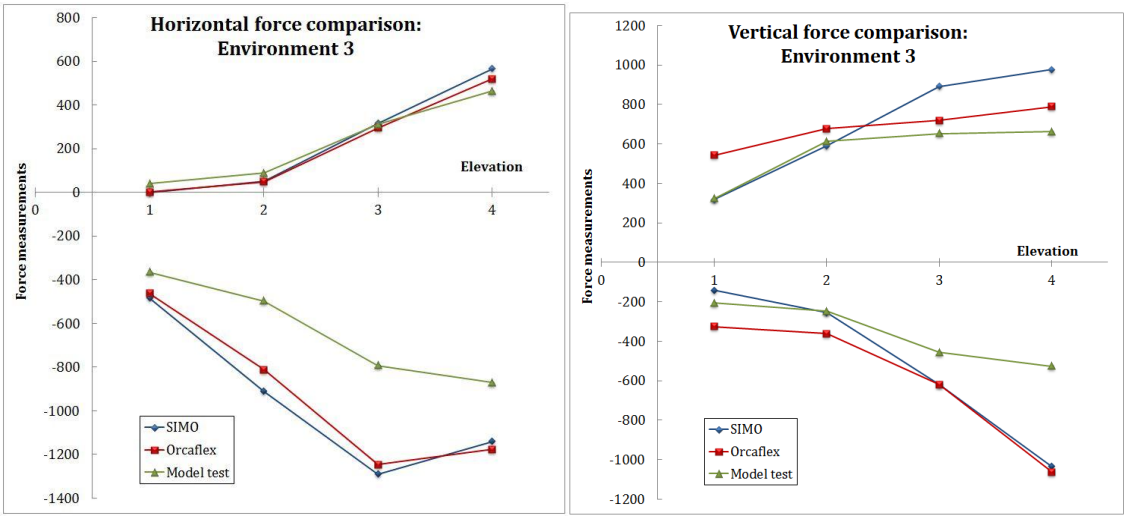

Figure 47 Comparison of maximum forces from numerical and experimental analysis using environment 3 in all elevations

In environment 3 the module is tested in waves 8 meters tall with a wave period of 7 seconds.

The horizontal forces are well predicted in the water entry phase by the numerical simulations for all elevations. I the water exit phase the numerical simulations are very conservative compared to the model tests. The largest appears in elevation 3, where SIMO calculated 497.1 kN more forces in the water exit phase compared to the model tests, while Orcaflex predicts 453.2 kN. Some of the conservatism may originate form wave deformation in the model tests.

Orcaflex's calculation of the vertical forces in elevation 1 & 2 are conservative compared to the model test. SIMO calculates forces that are closer to the model test, but is not conservative in the water exit phase in elevation 1.

In elevation 3 & 4 the numerical simulations are conservative for both water entry and water exit forces. SIMO are more conservative in the water entry phase compared to Orcaflex and predicts forces that are 316.1 kN larger than the model tests.

The water exit phase is very conservative in the numerical simulations. SIMO and Orcaflex predicts twice the force measured in the model test for elevation 4. This may originate from several sources and will be discussed in section 7.3.

The forces are compared while the module is subjected to "environment 3". The comparison shows that results from the numerical simulation are generally conservative. Orcaflex predicts forces that are closer to the mode test, especially in elevations where forces are large.

7.2.3 Wave impact process comparison:

The time history is compared to obtain a better understanding of the wave impact process. The two cases, 4 & 11, are reflecting general trends in their respective submergence.

In case 4 the module is fixed in elevation 2, the bottom of the module is in line with the mean sea level. The module is subjected to waves with a wave height of 5.3 meters and 7 second wave period. In this elevation the slam forces are the governing forces, according to the numerical study in section 6.4.4.2.

In case 11 the module is fully submerged, i.e. in elevation 4. The module is subjected to waves with a wave height of 5.8 meters and 10 second period. According to the numerical study the drag forces were found to be the governing force in elevation 4.

7.2.3.1 Case 4: Time History comparison

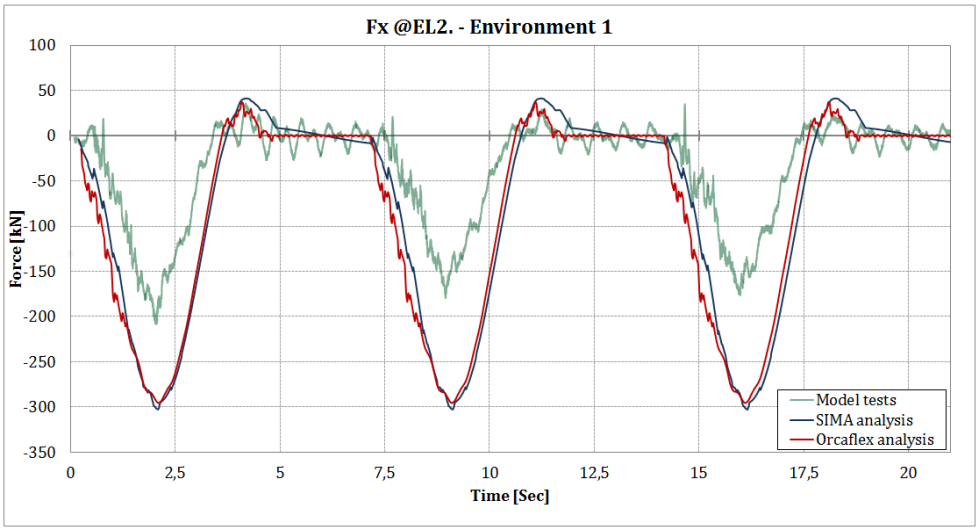

Figure 48 Time history of horizontal forces in elevation 2 subjected to environment 1

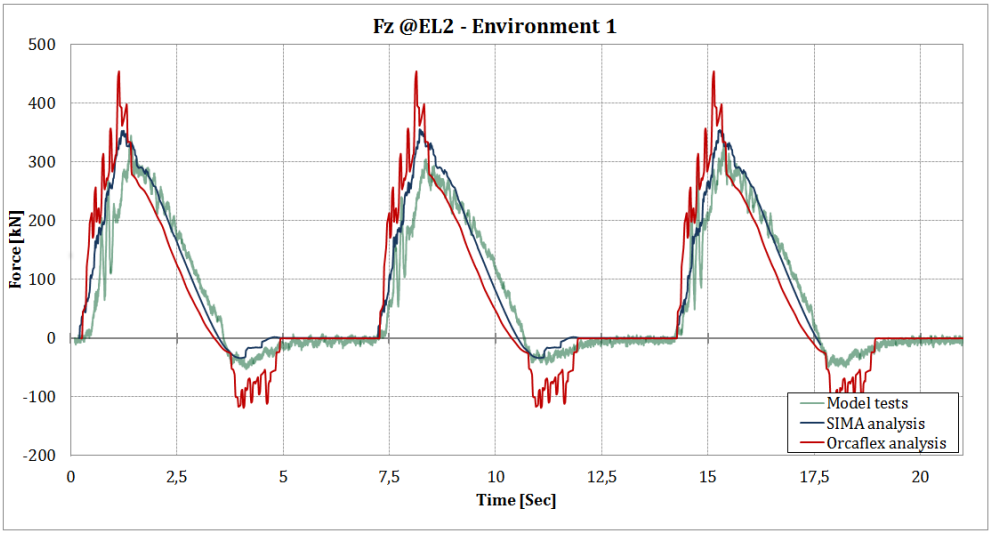

Figure 49 Time history of vertical forces in elevation 2 subjected to environment 1

The horizontal forces in SIMO and Orcaflex are very similar. Both simulations overestimate the forces compared to the model tests. This over estimation is believed to

be caused by disturbances in the model test waves. When gradually ramping up waves the wave kinematics is disturbed, causing reduced drag due to deformation of the free surface. The added mass forces are in this case very low due to the low horizontal acceleration in the wave crest. In the numerical analysis the wave kinematics are not affected by the structure (SIMO Project team, 2010) & (Orcina, 2013).

The vertical force calculations in the numerical simulations in case 4 are conservative compared to the measurements in the model test. As seen in figure 49, Orcaflex calculations are more conservative than results in SIMO and the model test. The numerical separation of forces show that the overestimation of forces is caused by slamming calculations in Orcaflex, see section 6.4.4.2 for details.

The water exit phase in Orcaflex is conservative and overestimated compared to the model test and SIMO calculations. By separating the forces in the numerical simulation in Orcaflex the calculation of "water exit slam forces" are causing the overestimation.

7.2.3.2 Case 11: Time History comparison

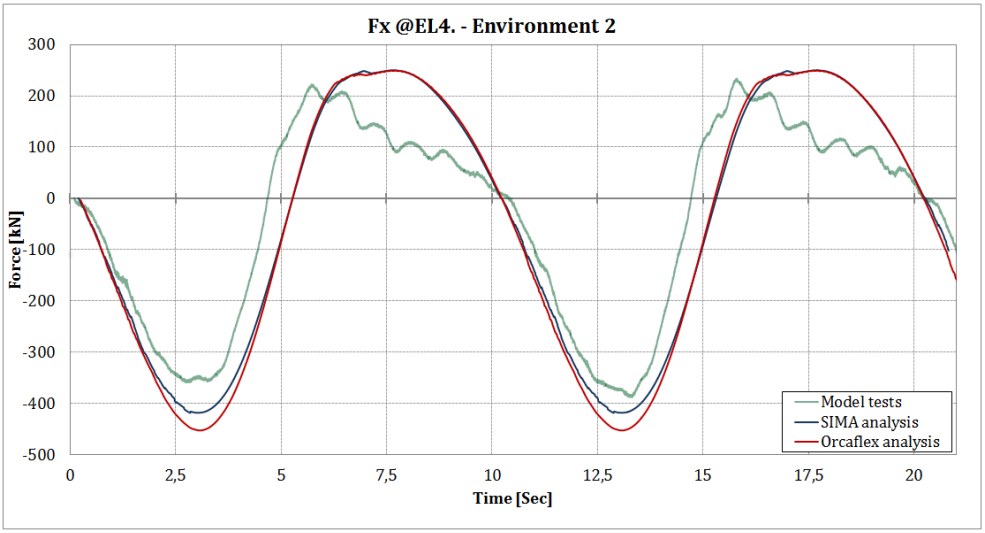

Figure 50 Time history of horizontal forces in elevation 4 subjected to environment 2

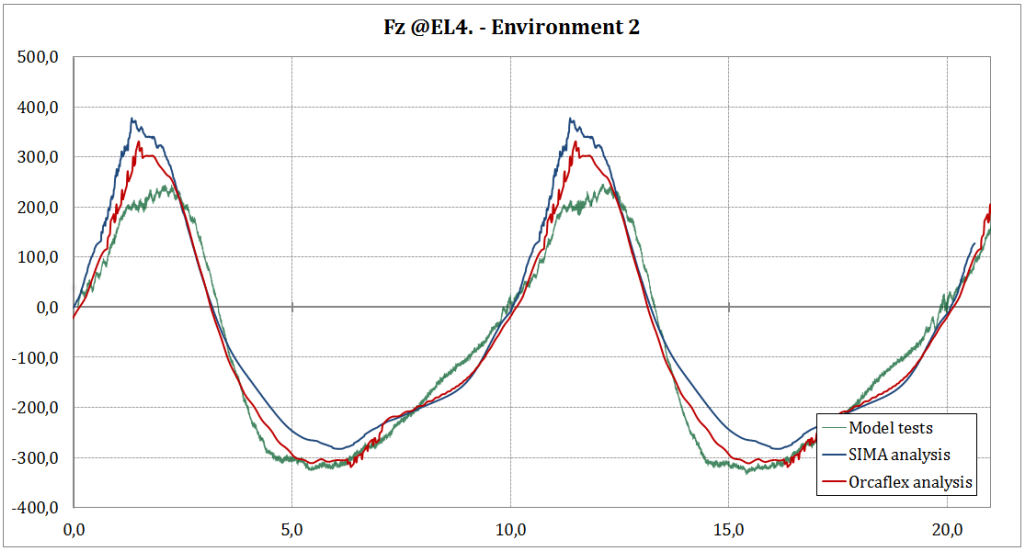

Figure 51 Time history of vertical forces in elevation 4 subjected to environment 2

The horizontal forces on the module are well predicted by the numerical simulations. In fully submerged condition both simulations are conservative but not in a significant manner. The main contributor to differences between the numerical results and the model test are believed to be the horizontal drag forces, see section 7.3.

The vertical forces calculated by SIMO and Orcaflex are overestimated in the water entry phase for environment 2. The overestimation is linked to two possible sources; the disturbance for wave particle kinematics and the generated wave in the Oceanide. By comparing environment 2 in the ocean basin to the Airy's wave theory, in section 4.7.1, the wave have a less steep wave elevation and does not represent a regular wave in a good way. This may result in less added mass and drag forces.

The vertical forces in the water exit phase are not conservative in SIMO or in the Orcaflex calculations. Orcaflex is closer to the model test measurements.

7.3 DISCUSSION

This section will highlight aspects of calculation and model test differences that will influence the final comparison.

The global hydrodynamic coefficients used in the numerical simulations are obtained from a forced oscillation test, see section 5.3. The global coefficients will change depending on the amplitude of oscillation, where the oscillation amplitude is similar to the wave amplitude of a regular wave. The global hydrodynamic coefficients were extracted using oscillation amplitude of 3 meters, in order to obtain valid global hydrodynamic coefficients for a 2.5 and 4.0 meters amplitude wave. This will indicate that the numerical simulation running 5 meter tall regular waves, environment 1 and 2, will in reality have a larger drag coefficient and a smaller added mass coefficient, according to the results from the forced oscillation test. For a regular wave 8 meter tall the drag will be smaller and the added mass larger compared to what is used in the current numerical analysis.

The global hydrodynamic coefficients are implemented to the model by calibrating all beams and pipes according to their position inside the model. The calibration process are based on completely submerged structures where the inner sector are assumed to have more added mass and less drag compared to the outer sector, see section 6.2 for details. When a structure is partly submerged this assumption may be questioned. The current analysis does not take into account the compressor modules vicinity of the free surface and the global effect this may have on the added mass and drag coefficients. (Det Norske Veritas, 2010) sec. 6.9.3.

The sector assignment scaling factor may be questioned for a propagating wave. "*Due to wake fields, partially trapped water and other flow restrictions the center of the structure, i.e. the inner sector, has a larger factor for C_a and C_m. The inner sector is more affected by the flow disturbance compared to the outer sector"*. When a wave propagates through the structure the elements on the downstream parts of the structure is most affected by the disturbance of wave particle kinematics. In the current analysis the outer sector goes around the compressor. As the wave exits the structure the scaling factor applied to the local elements indicates that the flow is less disturbed, when in a real case this will not be the case.

The numerical simulations have been carried out using regular waves according to Airy's theory. The input properties, wave height and wave period, are based on measurements in the wave tank. The waves generated in the ocean basin are waves similar to the Stokes 5th theory, which is higher than the corresponding Airy's wave. The result is that the wave in the numerical model is larger than the wave in the model tank. This will result in larger forces on the numerical model.

The wave particle kinematics in the Airy's wave is higher than the corresponding Stokes 5th wave, except for the vertical acceleration component, according to section 2.4.5. In general terms this will result in larger forces on the module when using Airy's wave theory compared to Stokes 5th.

By comparing forces using "Environment 2", see section 4.7.1, the forces in the numerical simulation are generally not conservative. Figure 19 show that the generated wave is not an accurate representation of the Stokes 5th wave train. By using Goda's method, given in appendix 4, the reflected wave has been calculated and shows that there is a 2% wave reflection. This reflection will disturb the wave particle kinematics and the wave elevation, and possibly lead to the observed force difference.

Comparing the volume between the numerical and the model, some differences were found. Several sources for additional volume in the numerical models have been discovered. 1. The 3D model may not accurately represent the final model as built by Oceanide. 2. In the numerical simulation beams that overlap, i.e. in corners, will be accounted for twice. 3. All beam and pipe coordinates are based on a coordinate-file from Aker Solutions and all dimensions are based on the Oceanide 3D-model. In the top section of the compressor module slanted elements had been removed in the simplified 3D.model, but implemented in the numerical simulation. This mistake was not discovered until a later stage of the project. The added beams account for $\sim 1 m^3$ extra volume, and will not affect elevation 1 & 2. 4. All pipe dimensions in the numerical model are based on the joint diameter, see figure in appendix 11. This will increase the difference further.

The sum of these mistakes is believed to account for the increased volume in the numerical simulations. The main effect of the buoyancy difference will occur in elevation 4.

Based on research by (Sarpkaya, 1978) and (Faltinsen, 1998) the slamming coefficient is very dependent on how the structure hits the water surface and the natural frequency of the analyzed object. Experimental research showed that there is a considerable degree of scatter in the estimated slamming coefficient during tests in similar conditions. The slamming coefficient used in the Orcaflex calculations is based on two tests, with different lowering velocities. By running more slamming tests a mean value of the slamming coefficient could be obtained to ensure a more accurate estimation of the slamming coefficient.

In elevation 1 & 2 for all tests Orcaflex's calculation of the vertical forces proved to be conservative. This is believed to be caused by the conservative approach in the estimation of the slamming coefficient. The slamming coefficient used in Orcaflex is based on the forced model test, see section 5.3.2, where the maximum value after the initial impact is used to calculate the slamming coefficient. This value will contain contributions from drag, inertia and buoyancy, and will therefore give a conservative estimation of the slamming coefficient.

The water exit force is caused by the increased added mass in heave as an object approaches the free surface (DNV-RP-H103 3.2.11.3). The water exit force is accounted for in Orcaflex's calculation of vertical force by using the "water exit slam coefficient". The water exit slam coefficient, C_e, is calculated according to DNV's recommended practice. The necessity of the water exit force calculation can be questioned. For partly submerged objects this force can be neglected when no large horizontal surfaces is below the free surface. The water exit force is neglected in the SIMO calculations. The comparison of vertical negative forces showed that in some cases the water exit force was necessary to predict forces close to the model tests. SIMO was generally not conservative in the elevation 1 & 2, while Orcaflex's calculations where conservative. The water exit force can be necessary to estimate forces in the water exit phase, but the comparison show that the "water exit slam coefficient" might be over predicted using recommended practice form DNV-RP-H103. This is observed in several cases and presented in appendix 8, case 3, 1 and 6.

CHAPTER 8

Conclusions and recommendations for further work

8.1 CONCLUTIONS

The main objective of this thesis is to reduce the uncertainties related to numerical analysis of the wave impact process. The wave impact on complex structures is in reality a very complicated process considering the wave kinematics and the involved forces. Two programs, SIMO and Orcaflex, have been used to give an estimation of forces involved in the wave impact process on a complex structure.

To validate the numerical solutions experiments have been carried out in Oceanide's ocean basin "BGO First". Here the model structure has been subjected to 3 regular wave conditions in four elevations.

The numerical comparison shows that the main differences between SIMO and Orcaflex occur when the structure is suspended above the mean sea level. In these elevations the slamming forces are large which is believed to be the root cause of the observed differences. Orcaflex's and SIMO's calculation of slam forces are different and will give different results. The calculation of vertical forces show a trend as the module is lowered through the splash zone; the difference between Orcaflex and SIMO reduces. Analysis has shown that Orcaflex's calculation of slam forces are the main contributor and gives high impact forces compared to SIMO. Fully submerged the structure is less affected by the slamming forces and the results are more alike. The main differences observed in fully submerged condition is believed to originate from lack of buoyancy in the Orcaflex model.

The comparison between the model test and the numerical analysis in SIMO and Orcaflex indicates that the numerical prediction of forces is conservative in most cases. The largest over prediction of forces is in elevation 3 & 4.

In a few cases, 2 5 and 8, the model test horizontal forces where higher compared to the numerical simulation. In these cases, the involved forces are not very large and that the model test wave was not representing the regular wave theory in a sufficient way. In

addition to this, the numerical model is produced with global coefficients close to the wave height the module was analyzed in. No safety factor is included in the global coefficients. Technip includes a safety factor on all the analysis connected to marine operations with the SHS system. This is believed to increase the conservatism additionally.

The comparison of forces in elevation 1 & 2 proved that Orcaflex's estimation of slam forces are conservative, when the slamming coefficient is based on slamming tests. The slamming forces in SIMO gives a good estimation of the forces compared to the model test results. As the modules are submerged the slam forces are less governing. Orcaflex estimation is in many cases closer to the forces obtained in the model tests compared to SIMO.

8.2 SUGGESTIONS FOR FURTHER WORK

In this thesis the compressor module has been fixed in space. When the module is connected to the SHS tower and suspended on the outside of North Sea Giant additional forces from motions and hydrodynamics phenomenons will be present. The effect of shielding and growing waves, as the wave propagated downstream of the vessel are some of them. A model test focusing on the forces on the module while suspended on the outside of the vessel is ongoing and expected to be finished in July 2013. A comparison of forces between the vessel model test and a numerical simulation with a vessel would reduce the uncertainty in the marine operations related to the SHS.

As described in section 2.1.2 the slam force formulation in Orcaflex allows the projected area of the lumped buoy to act normal to the water surface. The compressor module's structural elements are mainly pipes and beams. For pipes and beams this is considered a good approach for estimating the direction of slam forces. The same approach is used when analyzing structures with horizontal plates or large flat objects, such as manifolds and templates with large mudmats. This implies that the projected area will act normal to the wave surface. Even if the plate is divide into a large number of lumped buoys this calculation will lead to an overestimation of the horizontal forces for steep waves, a force which in reality is not present. An investigation on the slam force calculation would be of interest to see if the formulation could be improved.

Important aspects regarding the calculation of wave impact forces have been highlighted during this thesis. Forces on the compressor module have been compared. This structure consists mainly of pipes and beams. An investigation of more challenging structures such as the inlet cooler or the scrubber would be of interest. The inlet cooler's cooling system and the air cushion under the scrubber is having hydrodynamic aspects which are not replicated by Orcaflex and SIMO.

Computational fluid dynamics is a method used to solve and analyze problems involving fluid flows using numerical methods. This technique for solving complex fluid flows has in recent years grown rapidly in the oil industry, due to high speed computers and better accuracy. The objective is to be able to predict forces acting on the body through the dimensionless drag and lift coefficients. Comparing CFD testing versus the numerical model and the model test would be of interest.

BIBLIOGRAPHY

Airy, G. B., 1841. *Tides and Waves.* Encyclopaedia Metropolitana : Mixed Sciences, Vol. 3, ed. HJ Rose, et al. Also Trigonometry.

AkerSolutions, 2012. *Weight & CoG and Buoyancy & CoB.* D11-AKS-W-RB-0001_081 ed. -: Aker Solutions.

AMTI, 1995. *MC12 Series, Force/Torque sensors,* Watertown: Advances Mechanical Technology INC. (AMTI).

Angvik, I., 2012. *Comparison SIMO – Orcaflex, Internal technical note.,* Stavanger: Technip A/S.

Baarholm, R. J., 2001. *Theoretical and Experimental studies of wave impact underneath decks of offshore platforms.* ISBN 82-7984-199-7 ed. NTNU, Trondheim: Dr. Ing. Thesis.

Campbell, I. M. C. &. W. P. A., 1980. *Measurement of parameters affecting slamming.* Technology Reports Centre No. OT-R-8042 ed. s.l.:Southampton University: Wolfson Unit for Marine Technology.

Cinello, A., 2013. *Environment calibration* [Interview] (26 03 2013).

Dahle, M., 2012. *Handling of heavy loads in rough seas.* Sildajazz conference 09.08.2012., s.n.

Det Norske Veritas, 2010. *Environmental conditions and environmental loads.* DNV-RP-C205 ed. -: Det Norske Veritas.

Det Norske Veritas, 2011. *Modeling and analysis of marine operations.* DNV-RP-H103 ed. -: Det Norske Veritas.

Faltinsen, O. M., 1998. *Sea Loads on ships and offshore structures.* ISBN: 0-521-45870-6 ed. UK: Cambridge University.

Fenton, J., 1985. *A Fifth-Order Stokes Theory for Steady Waves.* Vol. 111, No. 2 ed. s.l.:Journal of Waterway, Port, Coastal and Ocean Engineering.

Greco, M., 2012. *Exercise 2, Cource: Sea Loads,* Trondheim: NTNU.

Hauteclocque, G. d., 2009. *Installation de corlis lourd en grande profondeur.* Neuilly Sur Seine, France.: Bureau Veritas Research Depaartment.

Hulbert, C. a., 1993. *A time integration algorithm for structural dynamics with improved numerical dissipation: The generalized-α method..* page 371-375 ed. s.l.:Journal of Applied Mechanics.

Kaplan, P., 1992. *Wave impact forces on offshore structures: Re-Examination and New interpretations.* Houston, Texas, Offshore Technology Conference.

Knott, T., 2011. *MAN to put pressure on Asgard.* [Online] Available at: http://oedigital.com/subsea/equipment/item/265-man-to-put-pressure-on-

asgard
[Accessed 21 05 2013].

Knott, T., 2013. Upstream Technology. *Subsea gas feels the pressure*, Q2, pp. 14-25.

Oceanide, 2013. *MODEL TESTS REPORT IN WAVES - SPLASH ZONE CROSSING PHASE.* 2nd ed. La Seyne Sur Mer, France: Oceanide.

Orcina, L., 2013. *OrcaFlex manual: Version 9.6b.* 9.6b ed. Cumbria: Orcina Ltd..

Sandvik, P., 2012. *Depthe dependent hydrodynamic coefficients* [Interview] 2012.

Sarpkaya, T., 1978. *Wave impact loads on cylinders.* ISBN 978-1-55563-555-8. 1978 ed. Houston, Texas: Offshore Technology Conference.

Selvåg, A., 2012. *Wave impact loads on horizontal plates.* NTNU, Trondheim, s.n.

SIMO Project team, 2004. *SIMO – User's Manual Version 3.7.* Referance no: 2001-516412-01131560 ed. Trondheim: Marintek, Norwegian Marine Technology Research Institute.

SIMO Project team, 2010. *SIMO – Theory Manual Version 3.7.* Referance no: 516412/MT51 F93-0184 ed. Trondheim: Marintek, Norwegian Marine Technology Research Institute.

Statoil, 2012. *Havbunnsfabrikken.* [Online] Available at: http://www.statoil.com/no/technologyinnovation/fielddevelopment/aboutsubsea/Pages/Lengre%20dypere%20kaldere.aspx
[Accessed 21 5 2013].

Statoil, 2013. *Fakta om Åsgard.* [Online] Available at: http://www.statoil.com/no/ouroperations/explorationprod/ncs/aasgard/Pages/default.aspx
[Accessed 21 5 2013].

Statoil, 2013. *Åsgard havbunns gasskompresjon.* [Online] Available at: http://www.statoil.com/no/technologyinnovation/fielddevelopment/aboutsubsea/Pages/The%C3%85sgardComplex.aspx
[Accessed 21 5 2013].

Steen, S., 2012. *Experimental Methods in Marine Hydrodynamics.* Trondheim: Institute for Marin Technology.

Technip, 2013. *Module Splash-Zone analysis Report*, D110-TEP-J-CA-00002: Technip Norge.

Technip, M., 2013. *ÅSC SHS - Dynamic Analysis and Model Test Design Review meeting.* Stavanger, Sola airport hotel, Mikal, Dahle.

Tecnip_Aagard_B_Final. 2012. [Film] Directed by Visco. -: Visco.

APPENDIX 1: THE COMPRESSION PROCESS

The Åsgard subsea compression facility consists of two identical compressor trains that boosts the gas from several production templates to the floating gas production platform "Åsgard B". One compressor train is capable of boosting gas pressure by up to 50 bar and together deliver over 21 million SCM gas per day [2]. The compression train consists of 6 process modules and a number of support modules for power and control-distribution.

Production from several templates are combined and routed to the ÅSC-station. The compression process is described in figure 52. The inlet gas is hot and needs to be cooled down. The Inlet cooler module cools the incoming gas down to 10-16℃ using seawater. The cooled gas will pass through the vertical scrubber module to remove condensate liquids from the production. The condensate liquids are directly pumped into the export line to Åsgard B using the condensate pump module. The gas will exit the scrubber at the top and be compressed to required pressure in the compressor module. The gas compression process generates heat, requiring the gas to be cooled before it can enter the export line. This is achieved using the discharge cooler module. [8]

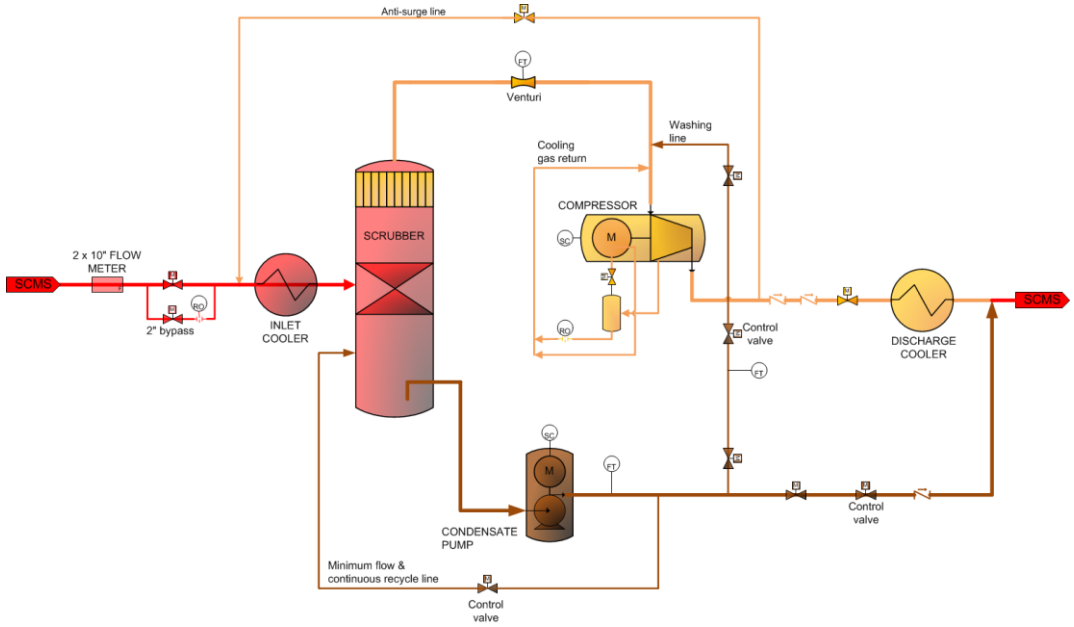

Figure 52 Process and instrumentation diagram over the compression process

The compression process is a normal procedure on platforms for gas fields, but Statoil ASA will be the world's first oil and gas company to develop a full scale all electric subsea compression station. Statoil has ordered three separate compression trains, two are going to be located subsea and a third standby onshore. If maintenance is required on one of the modules, Technip deploys the respective standby module using the SHS-system.

APPENDIX 2: THE TOWER STRUCTURE

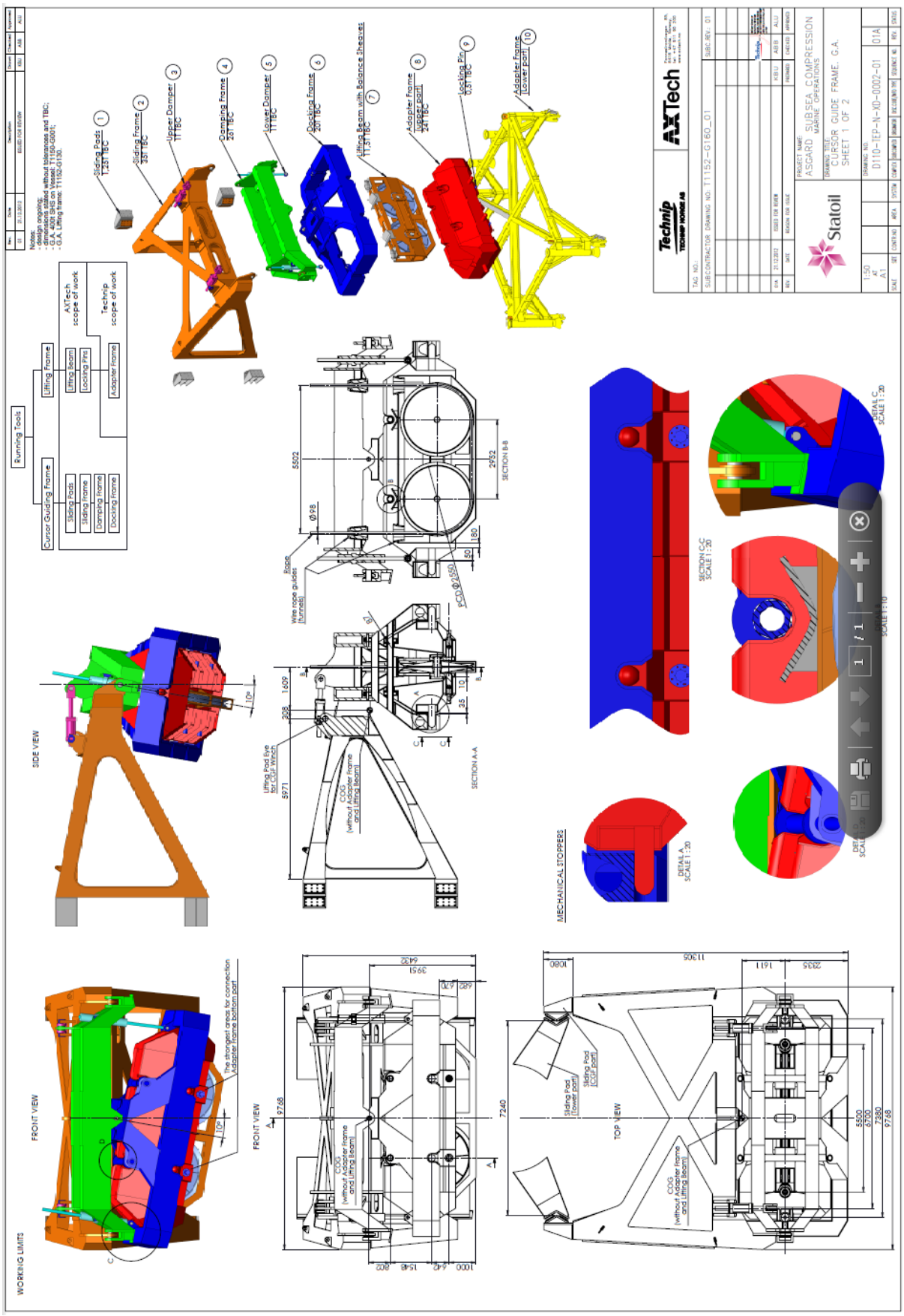

APPENDIX 3: WAVE PROBE CALIBRATION

océanide

Wave probes calibration

Acqisition files 08021025.a13

wg1	493.4	1.00
wg2	495.4	1.00
wg3	471.5	1.00
wg4	469.2	1.00

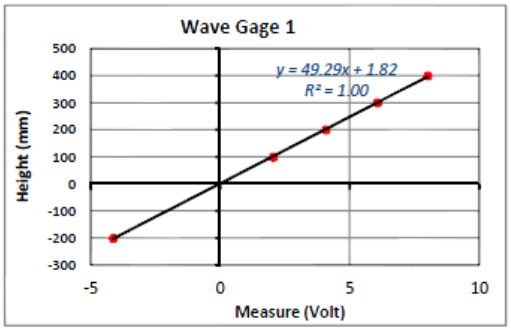

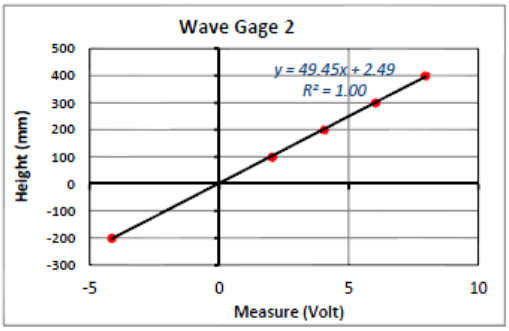

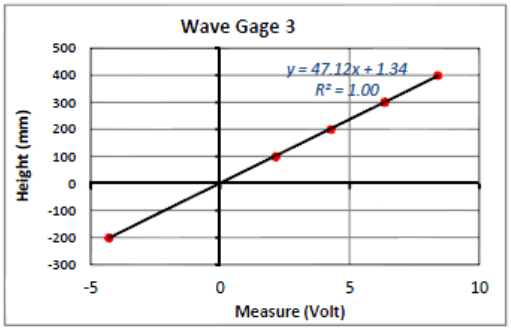

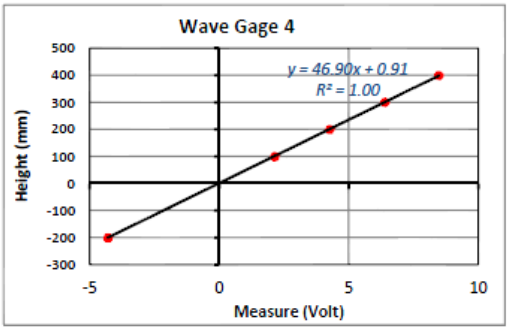

APPENDIX 4: ENVIRONMENT CALIBRATION

GODA'S METHOD FOR INCIDENT AND REFLECTED WAVES SEPARATION

Waves separation in regular waves

The method used is the GODA's one.

let $y_{i,p}$ be the water elevation measured at time t_i on waves located at abscissa x_p

the water elevation n at abscissa 0 is considered as the superposition of an progressive incident wave and a regressive reflected wave. We can write the water elevation in a complex notation :

$$H(f,t,x) = \left[A(f)\exp(-ik_1x) + B(f)\exp(ik_2x)\right]\exp(2\pi ift)$$

k_1 and k_2 are respectively wave number of the incident wave and of the reflected wave, solutions of the Airy propagation equation, eventually combined with a current U :

$$\sqrt{gk\ th(kd)} + kU = 2\pi f$$ progressive wave

$$\sqrt{gk\ th(kd)} - kU = 2\pi f$$ regressive wave

where d is the water depth, U is the current velocity and f is the wave frequency.

For a group of n waves, we calculate the n^{th} Fourier complex coefficient of the water elevation, that is to say the coefficient corresponding to the wave frequency.

Let Y_p be this coefficient. A and B are constants determined with a smallest square method on the whole wave probes, that is to say minimizing the following expression :

$$\sum_p \left| A\exp(-ik_1x_p) + B\exp(ik_2x_p) - Y_p \right|^2$$

That amounts to solving the following equations:

$$\begin{bmatrix} \sum_p w_p \exp(-ik_1x_p)\exp(-ik_1x_p) & \sum_p w_p \exp(ik_2x_p)\exp(-ik_1x_p) \\ \sum_p w_p \exp(ik_2x_p)\exp(-ik_1x_p) & \sum_p w_p \exp(ik_2x_p)\exp(ik_2x_p) \end{bmatrix} \begin{bmatrix} A \\ B \end{bmatrix} = \begin{bmatrix} \sum_p w_p \exp(-ik_1x_p)Y_p \\ \sum_p w_p \exp(ik_2x_p)Y_p \end{bmatrix}$$

Here w_p are weighting coefficients using the distance between each of the probes pair and complying with the GODA criteria :

$$0.05 \leq \frac{|x_i - x_j|}{L} \leq 0.45$$

Using the wave number of the progressive wave, we can write those inequalities :

$$0.305 \leq |x_i - x_j| k_1 \leq \pi - 0.305$$

Consequently, we can write the weighting coefficients for each wave probe :

$$w_p = \sum_{q \neq p} \varepsilon_q \qquad \text{with} \quad \varepsilon_q = 1 \quad \text{if} \qquad 0.305 \leq |x_p - x_q| k_1 \leq \pi - 0.305$$

$\varepsilon_q = 0$ in any other case

The reflection coefficient for the wave frequency f is given by : $Cr = \left|\frac{B}{A}\right|$

Waves separation in irregular waves

The calculation method consist of the following steps :

- Interpolation of the wave probe signal on N points, N is the second power immediately lower than the points number of the signal
- Calculation of the Fourier transformation of the interpolated signals
- Waves separation for each of the N/2 waves frequencies by the method described in the previous paragraph, that amounts to have the Fourier transformation of the incident and reflected waves at the point with zero abscissa

Reconstitution of the water elevation (incident and reflected waves) in calculating the inverse Fourier transformation

APPENDIX 5: WAVE SERIES

Environment 1

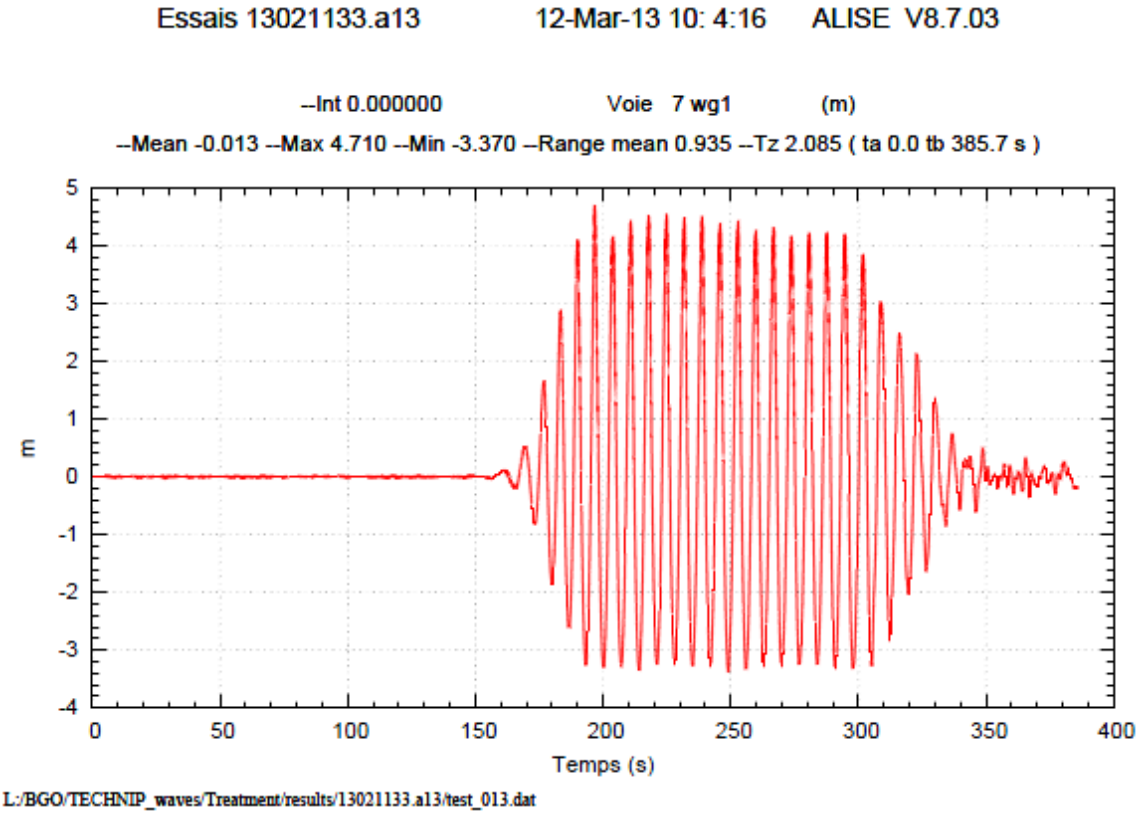

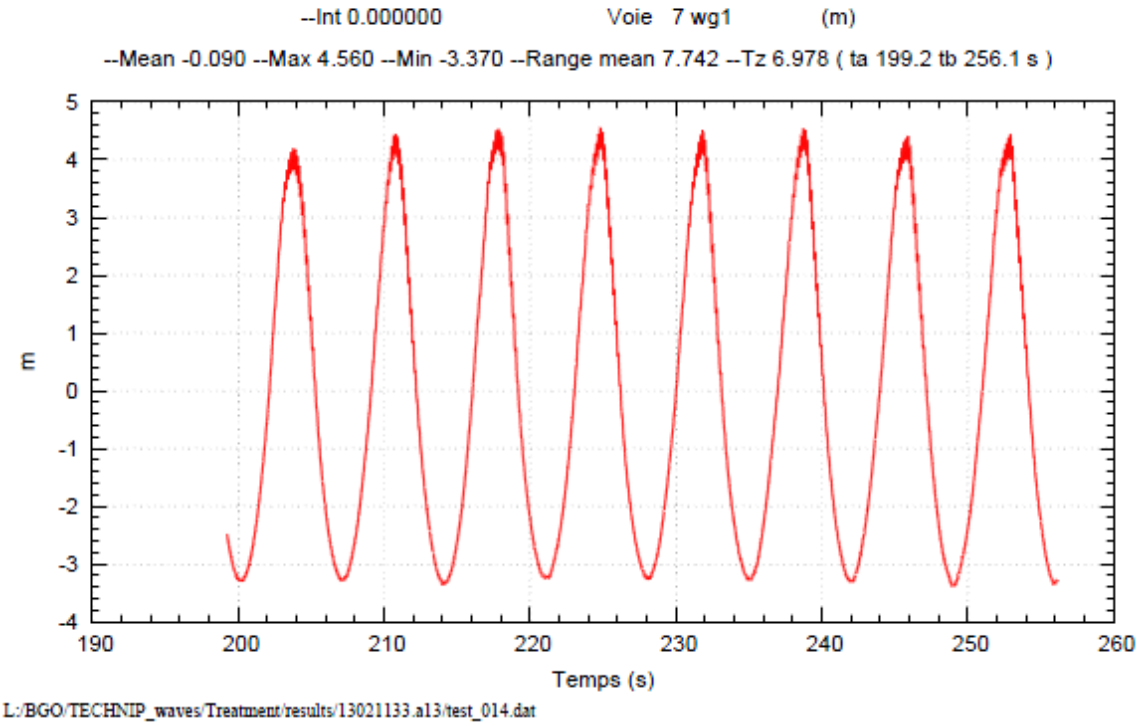

Environment 2

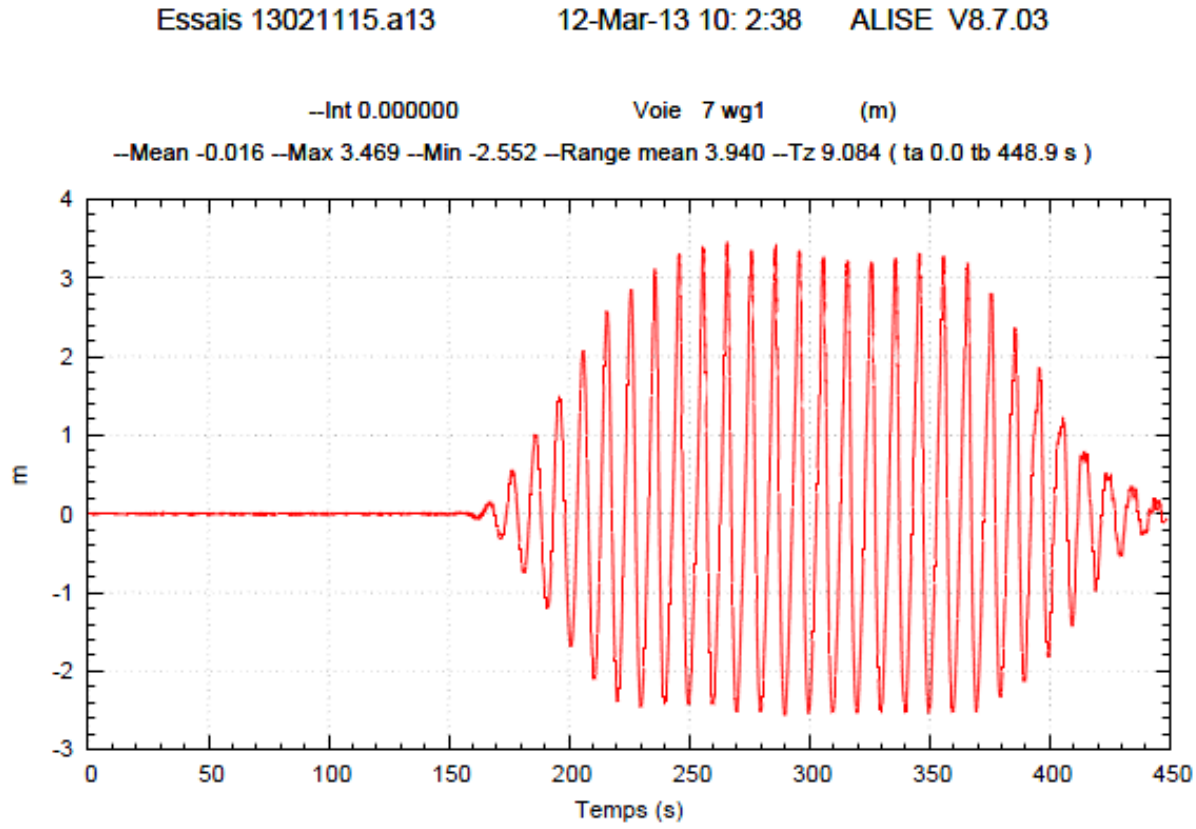

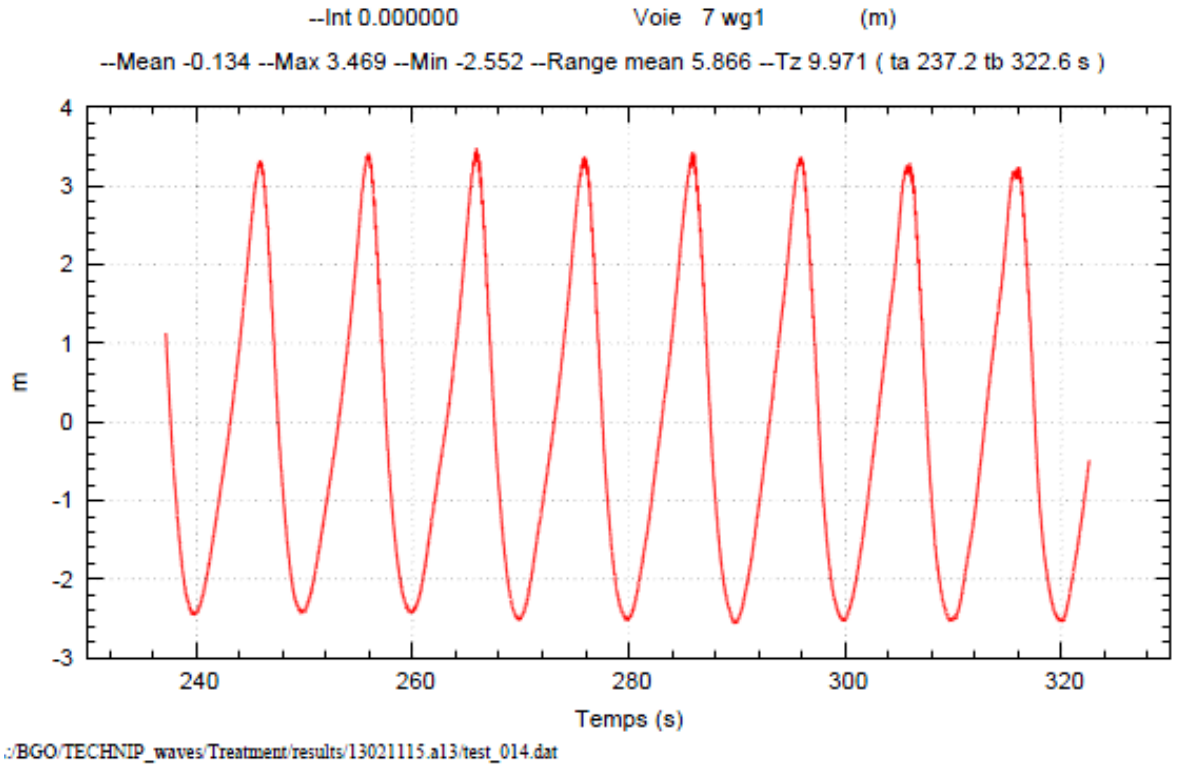

Environment 3

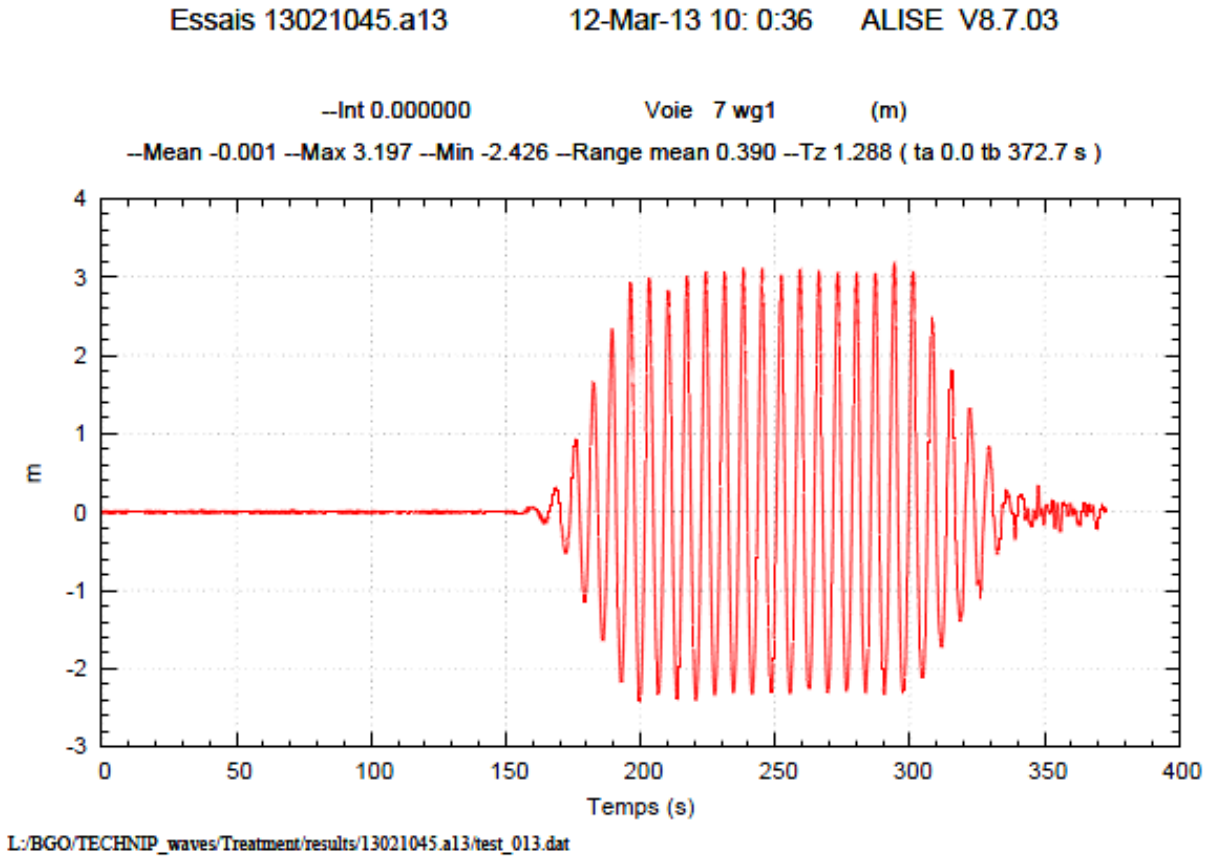

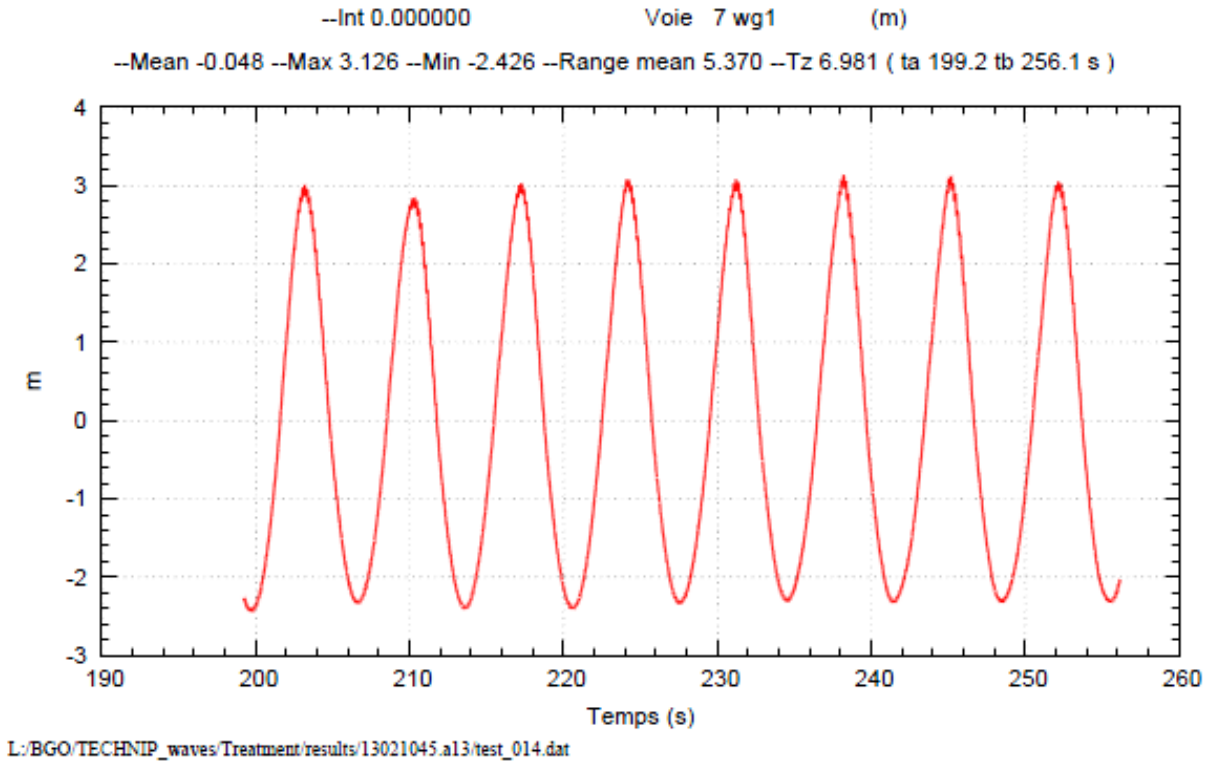

APPENDIX 6: EXAMPLE OF SEPERATION OF FORCE ANALYSIS

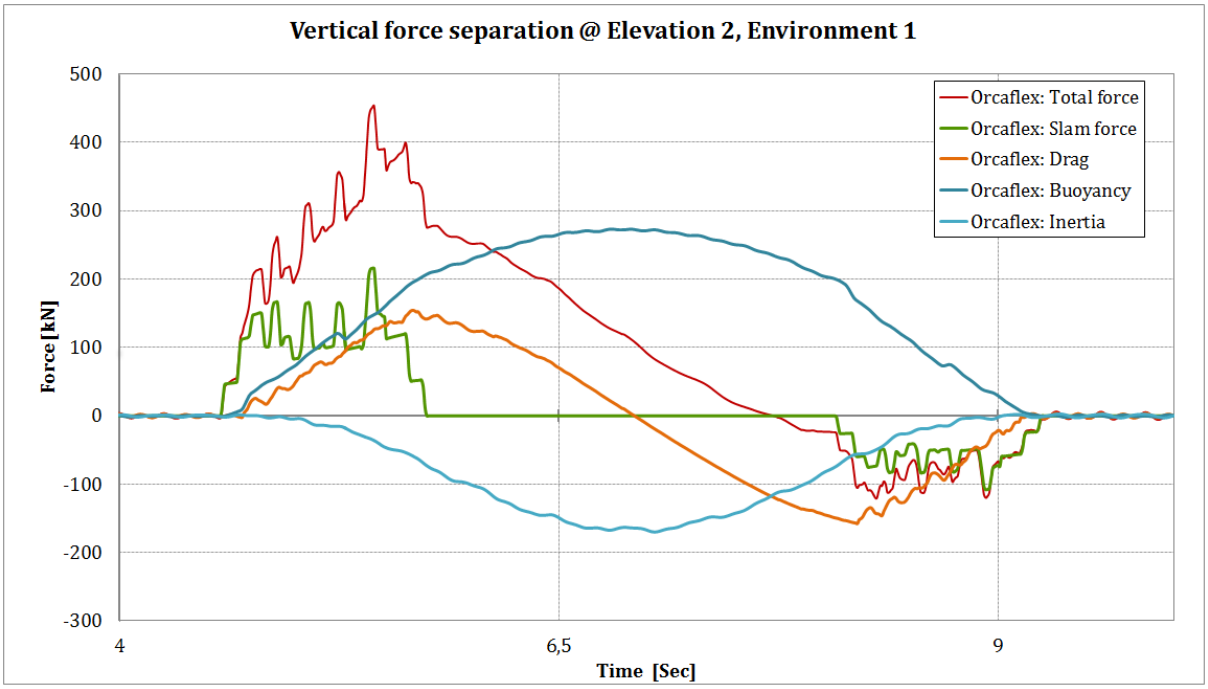

APPENDIX 7: FREQUENCY ANALYSIS ON FORCE PEAKS

Frequency analysis					
Test 1	Environment [-]	Elevation [-]	Local peak		Frequency [Hz]
			1st	2nd	
1	1	1	203,205	203,364	6,289308176
2	1	1	204,04	204,188	6,756756757
3	2	2	242,438	242,567	7,751937984
4	2	2	242,934	243,069	7,407407407
5	3	3	203,219	203,369	6,666666667
6	3	3	204,068	204,224	6,41025641
7	1	1	203,281	203,433	6,578947368
8	1	1	204,512	204,656	6,944444444
9	2	2	239,725	239,88	6,451612903
10	3	2	202,892	203,054	6,172839506

APPENDIX 8: TIME HISTORY FORCE COMPARISON

Note: Some of the comparison results have a phase shift which has not been corrected for. This originates from the numerical integration in SIMO.

Case 1:

Fx

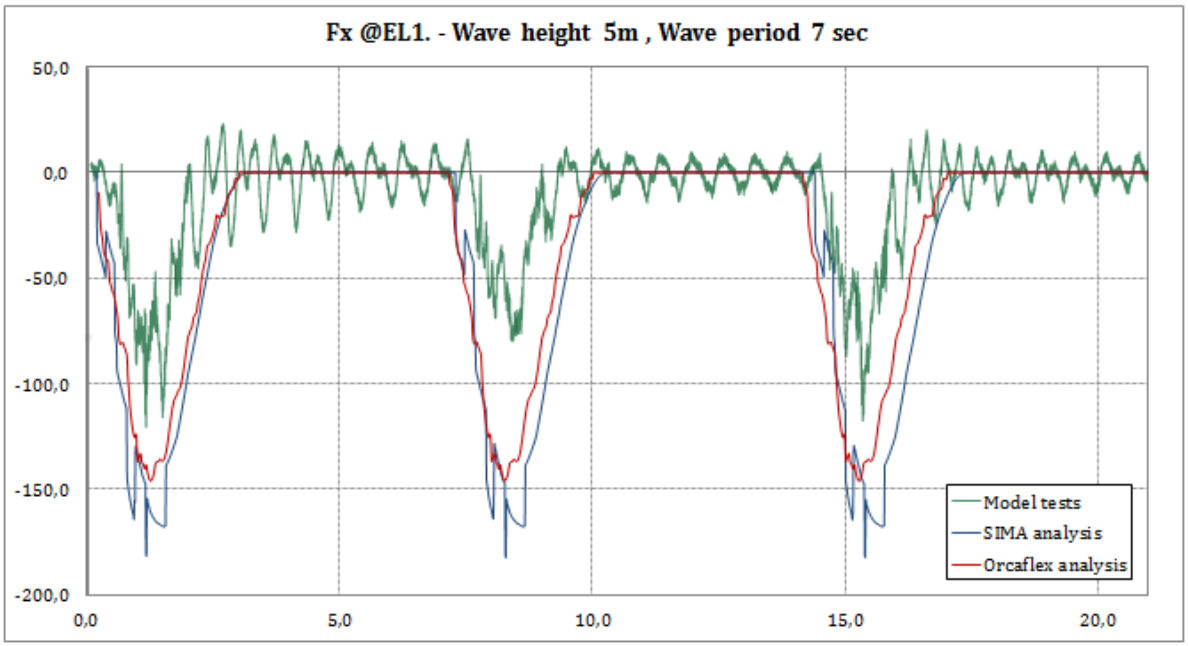

Fz

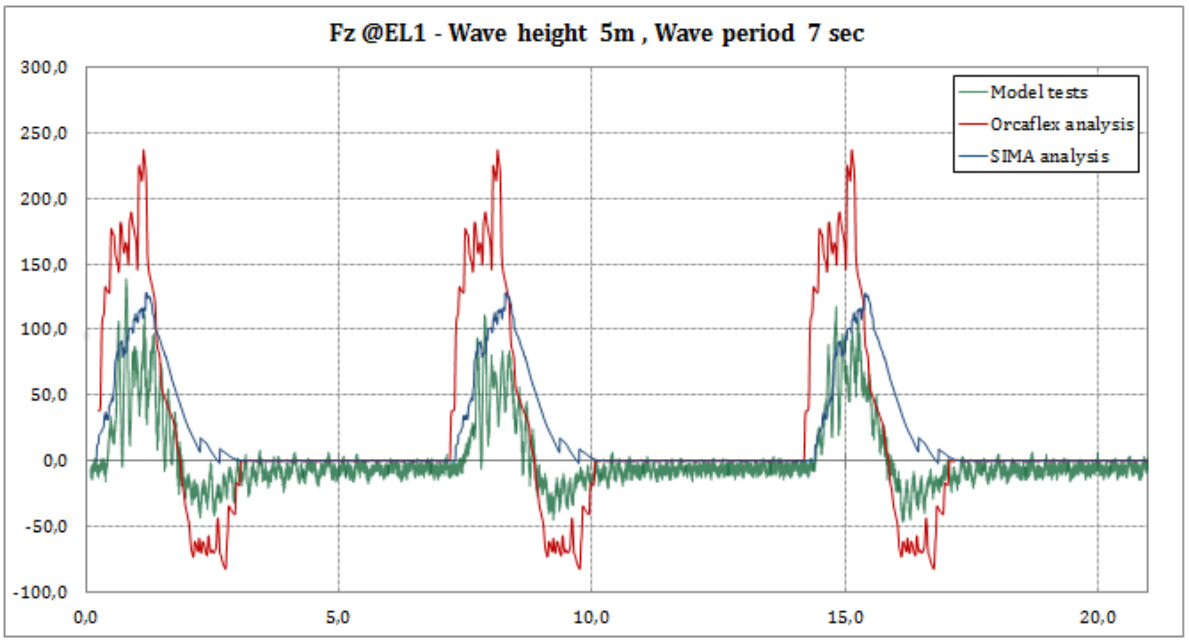

Case 2:

Fx

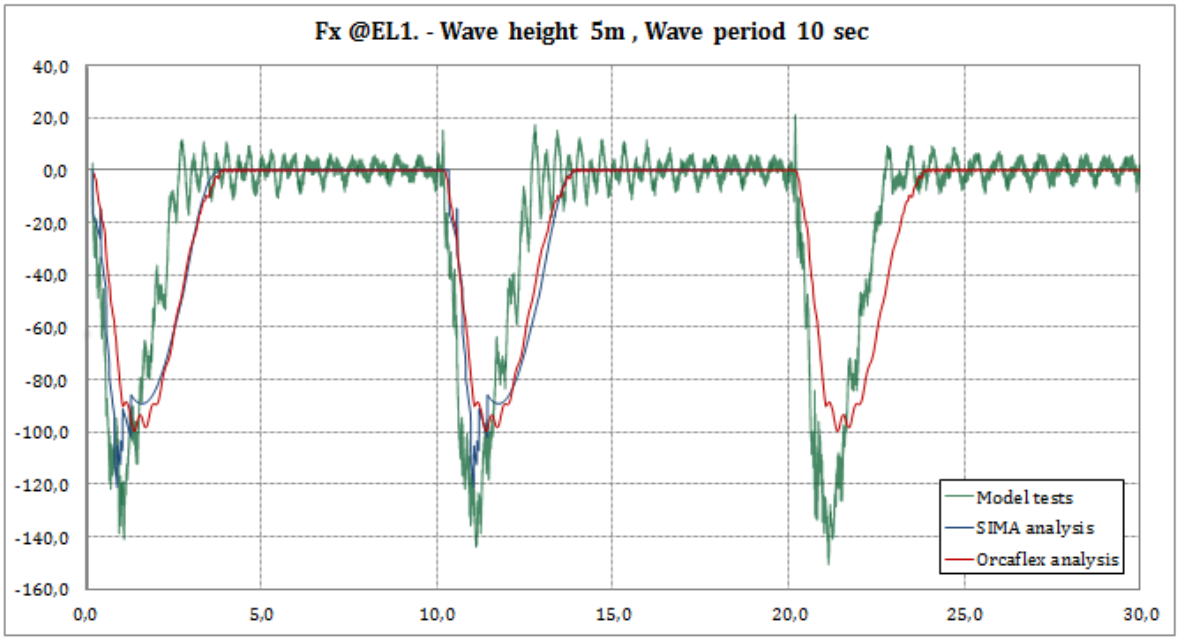
Fx @EL1. - Wave height 5m , Wave period 10 sec
40,0
20,0
0,0
-20,0
-40,0
-60,0
-80,0
-100,0
-120,0
-140,0
-160,0
0,0
5,0
10,0
15,0
20,0
25,0
30,0
Model tests
SIMA analysis
Orcaflex analysis

Fz

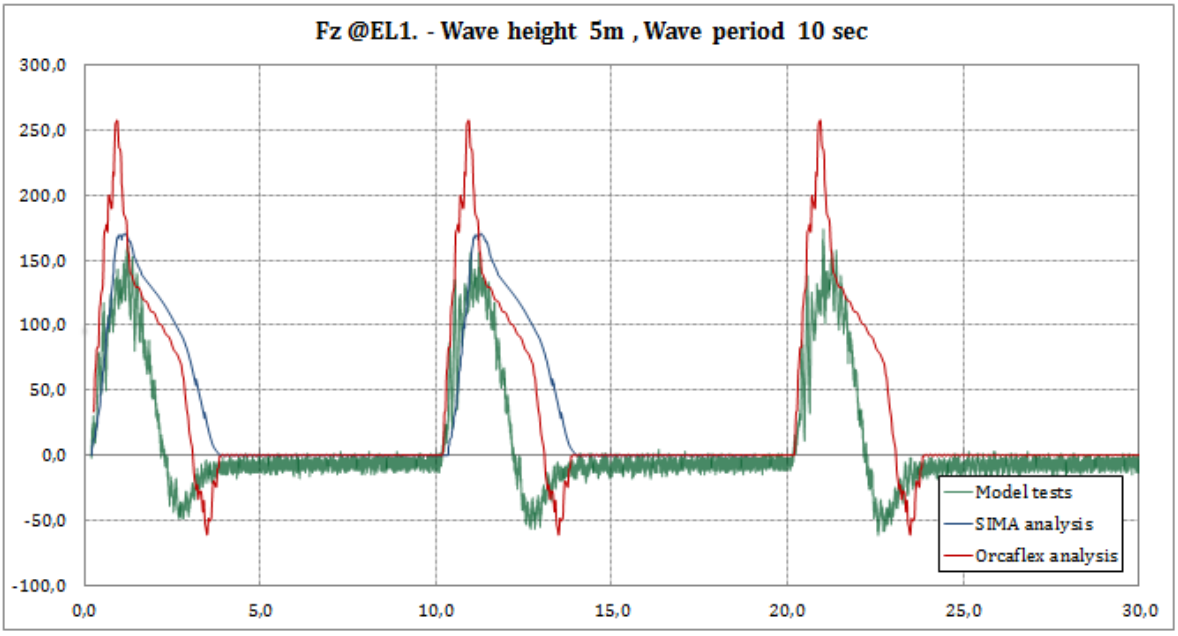
Fz @EL1. - Wave height 5m , Wave period 10 sec
300,0
250,0
200,0
150,0
100,0
50,0
0,0
-50,0
-100,0
0,0
5,0
10,0
15,0
20,0
25,0
30,0
Model tests
SIMA analysis
Orcaflex analysis

Case 3:

Fx

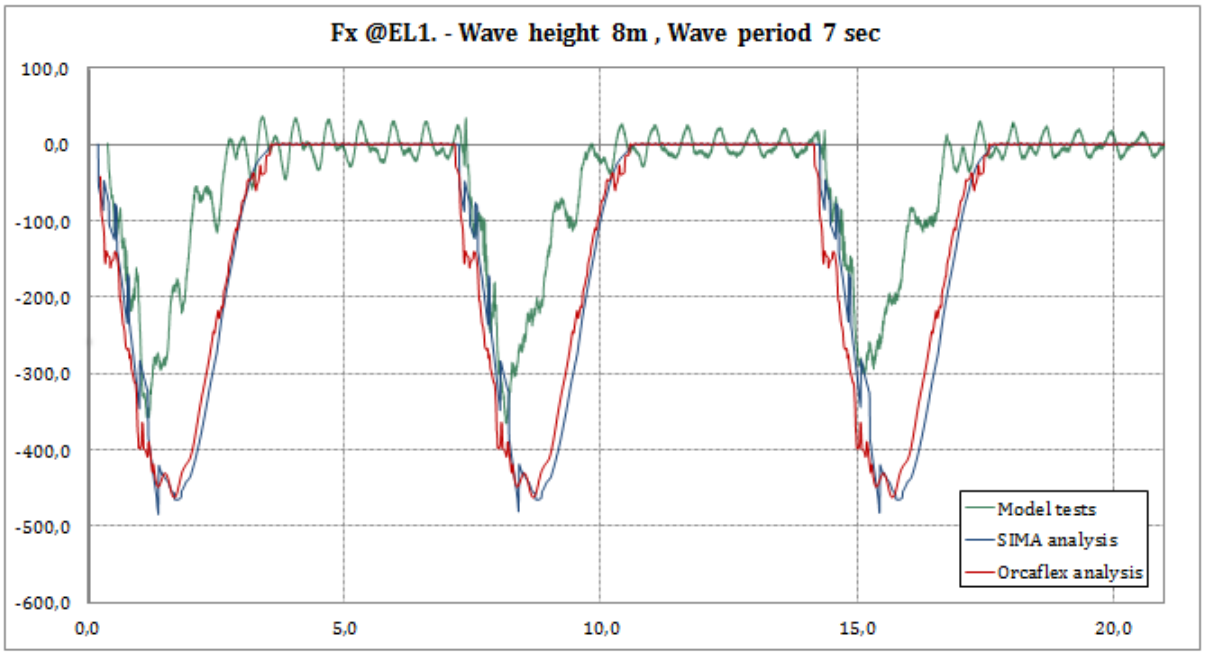
Fx @EL1. - Wave height 8m , Wave period 7 sec
100,0
0,0
-100,0
-200,0
-300,0
-400,0
-500,0
-600,0
0,0
5,0
10,0
15,0
20,0
Model tests
SIMA analysis
Orcaflex analysis

Fz

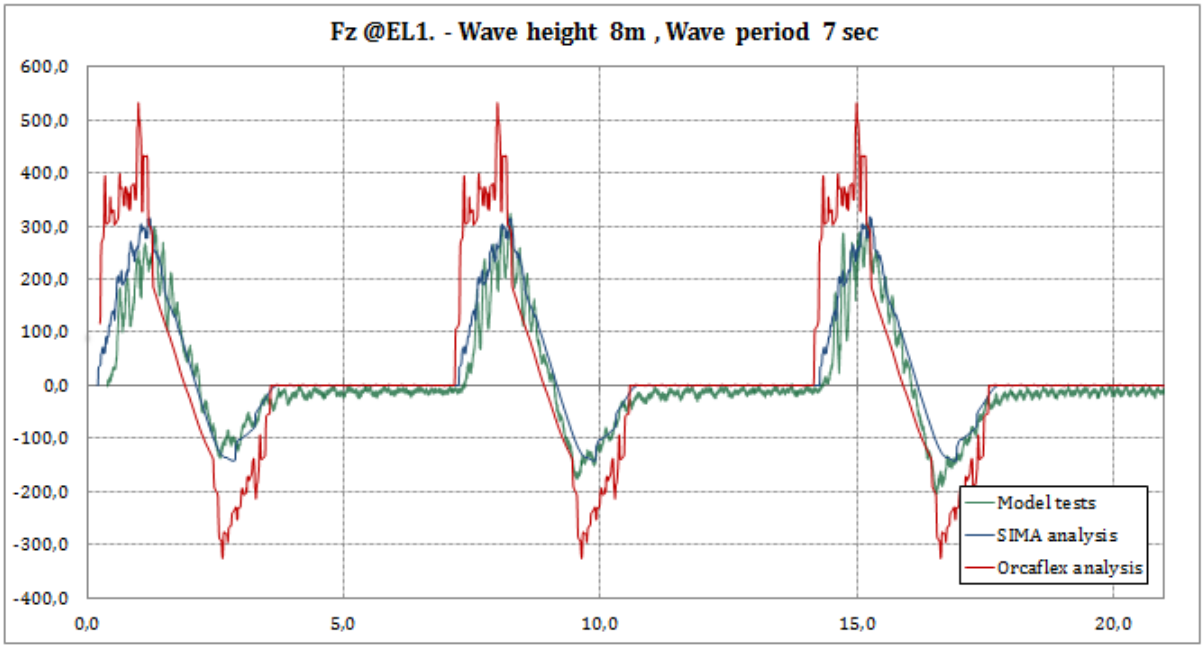
Fz @EL1. - Wave height 8m , Wave period 7 sec
600,0
500,0
400,0
300,0
200,0
100,0
0,0
-100,0
-200,0
-300,0
-400,0
0,0
5,0
10,0
15,0
20,0
Model tests
SIMA analysis
Orcaflex analysis

Case 4:

Fx

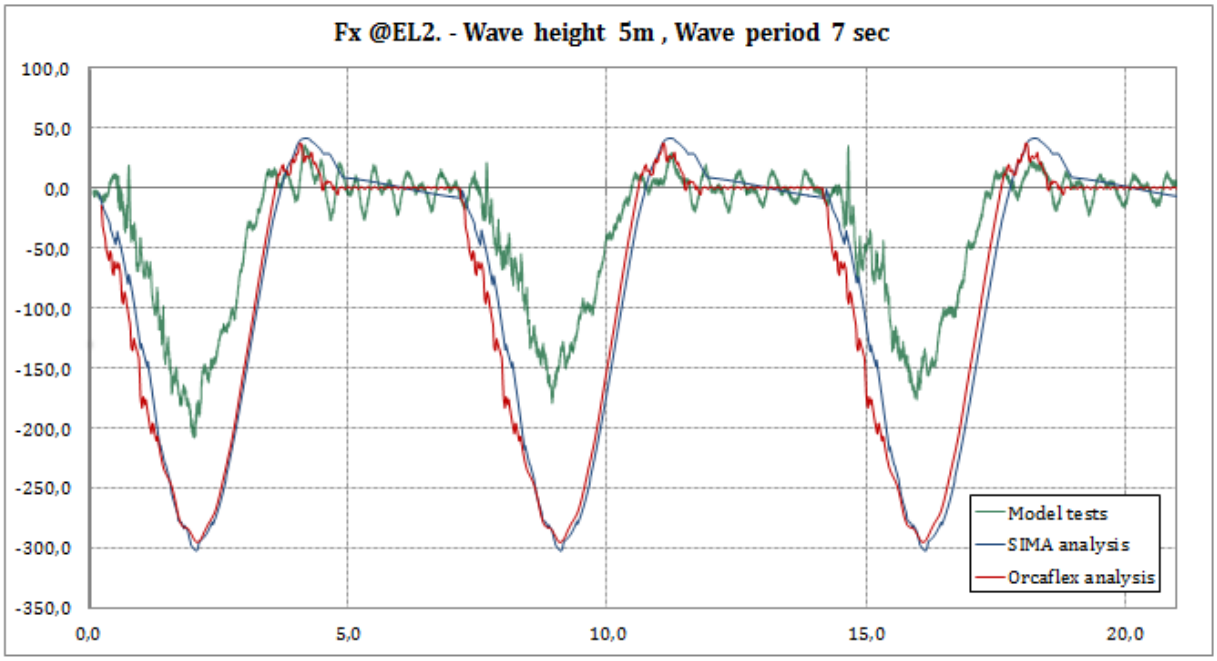
Fx @EL2. - Wave height 5m , Wave period 7 sec
100,0
50,0
0,0
-50,0
-100,0
-150,0
-200,0
-250,0
-300,0
-350,0
0,0
5,0
10,0
15,0
20,0
Model tests
SIMA analysis
Orcaflex analysis

Fz

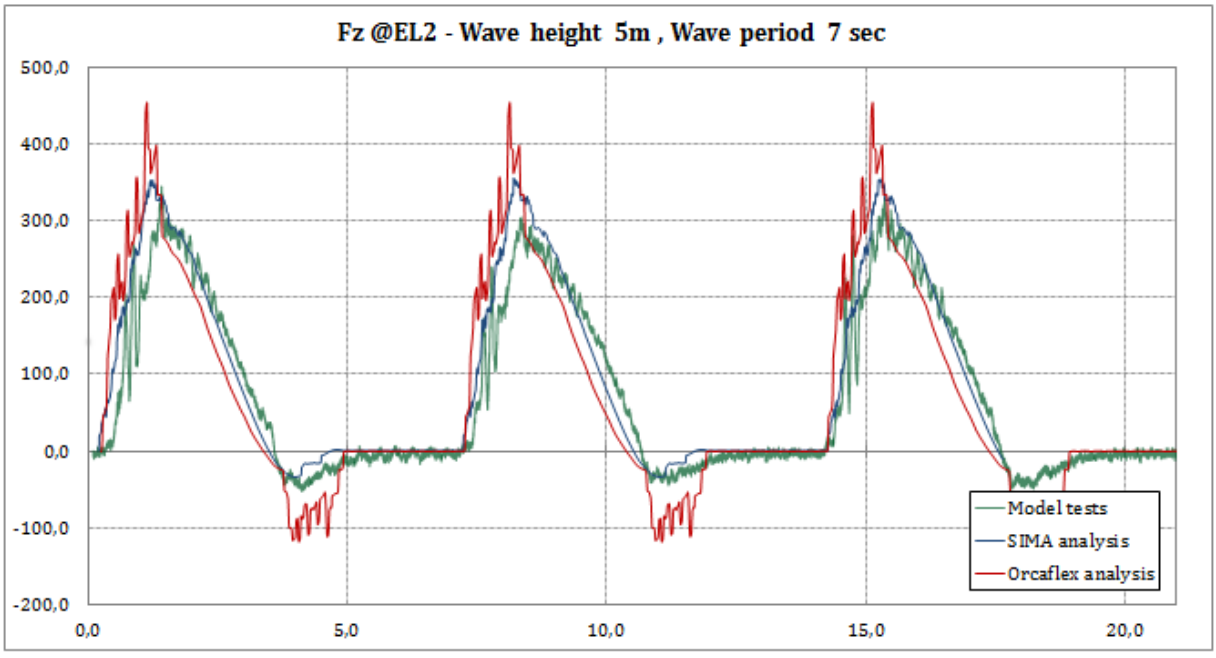
Fz @EL2 - Wave height 5m , Wave period 7 sec
500,0
400,0
300,0
200,0
100,0
0,0
-100,0
-200,0
0,0
5,0
10,0
15,0
20,0
Model tests
SIMA analysis
Orcaflex analysis

Case 5:

Fx

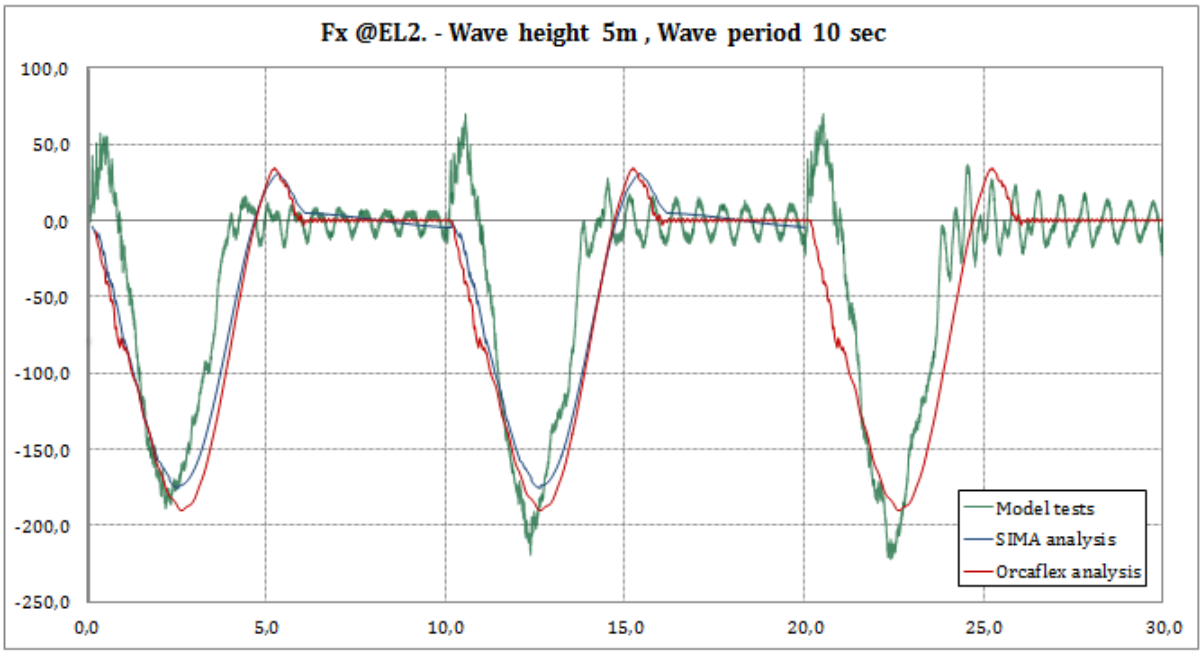
Fx @EL2. - Wave height 5m , Wave period 10 sec
100,0
50,0
0,0
-50,0
-100,0
-150,0
-200,0
-250,0
0,0
5,0
10,0
15,0
20,0
25,0
30,0
Model tests
SIMA analysis
Orcaflex analysis

Fz

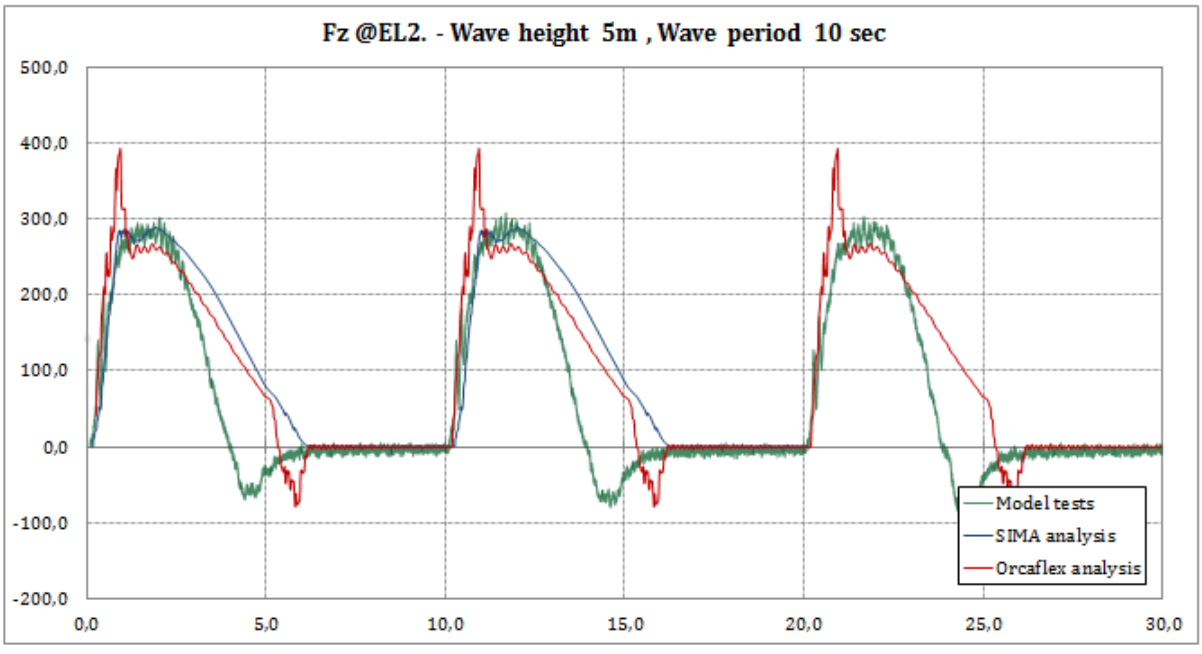
Fz @EL2. - Wave height 5m , Wave period 10 sec
500,0
400,0
300,0
200,0
100,0
0,0
-100,0
-200,0
0,0
5,0
10,0
15,0
20,0
25,0
30,0
Model tests
SIMA analysis
Orcaflex analysis

Case 6:

Fx

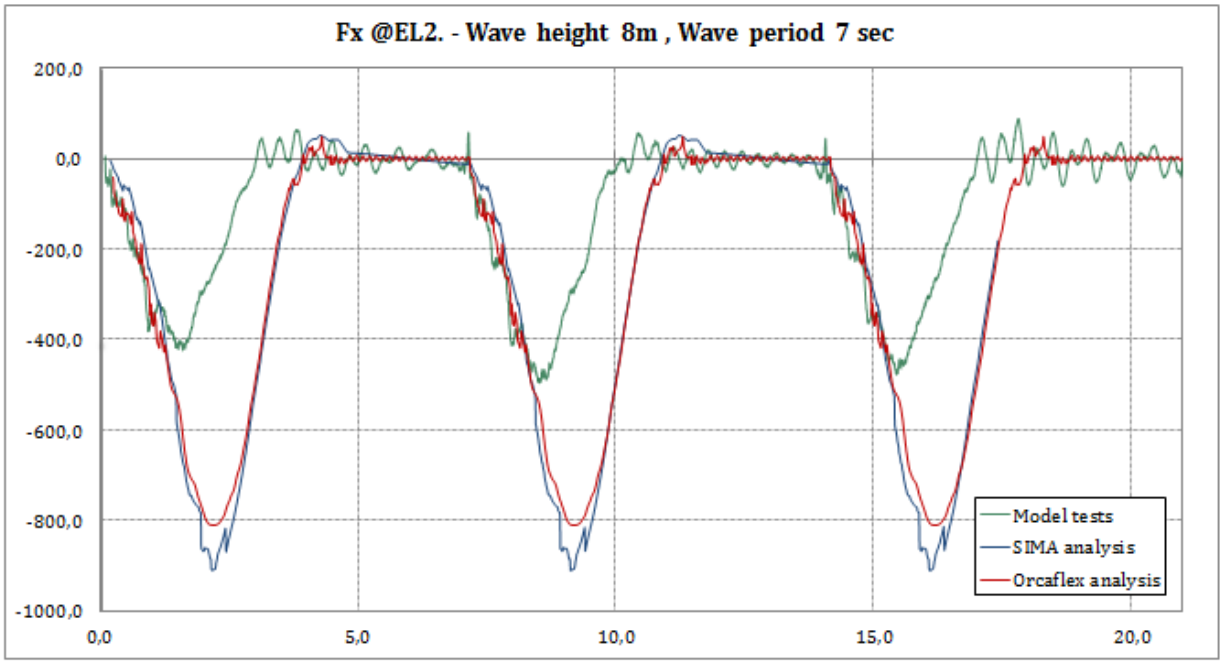
Fx @EL2. - Wave height 8m , Wave period 7 sec
200,0
0,0
-200,0
-400,0
-600,0
-800,0
-1000,0
0,0
5,0
10,0
15,0
20,0
Model tests
SIMA analysis
Orcaflex analysis

Fz

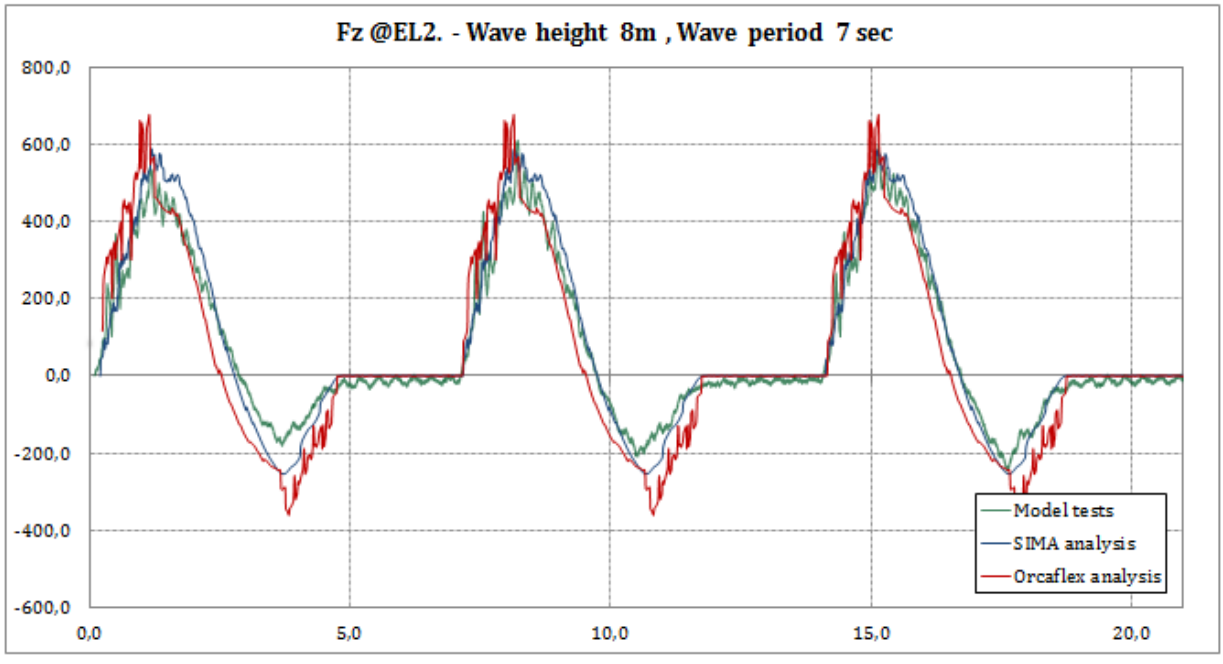
Fz @EL2. - Wave height 8m , Wave period 7 sec
800,0
600,0
400,0
200,0
0,0
-200,0
-400,0
-600,0
0,0
5,0
10,0
15,0
20,0
Model tests
SIMA analysis
Orcaflex analysis

Case 7:

Fx

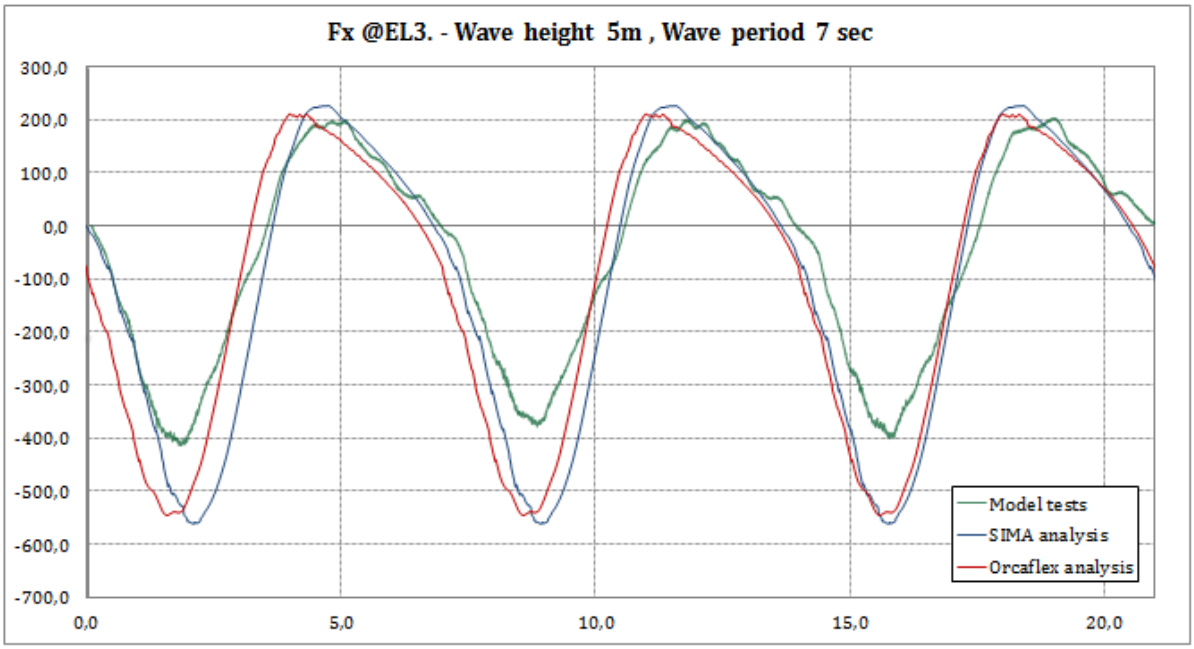
Fx @EL3. - Wave height 5m , Wave period 7 sec
300,0
200,0
100,0
0,0
-100,0
-200,0
-300,0
-400,0
-500,0
-600,0
-700,0
0,0
5,0
10,0
15,0
20,0
Model tests
SIMA analysis
Orcaflex analysis

Fz

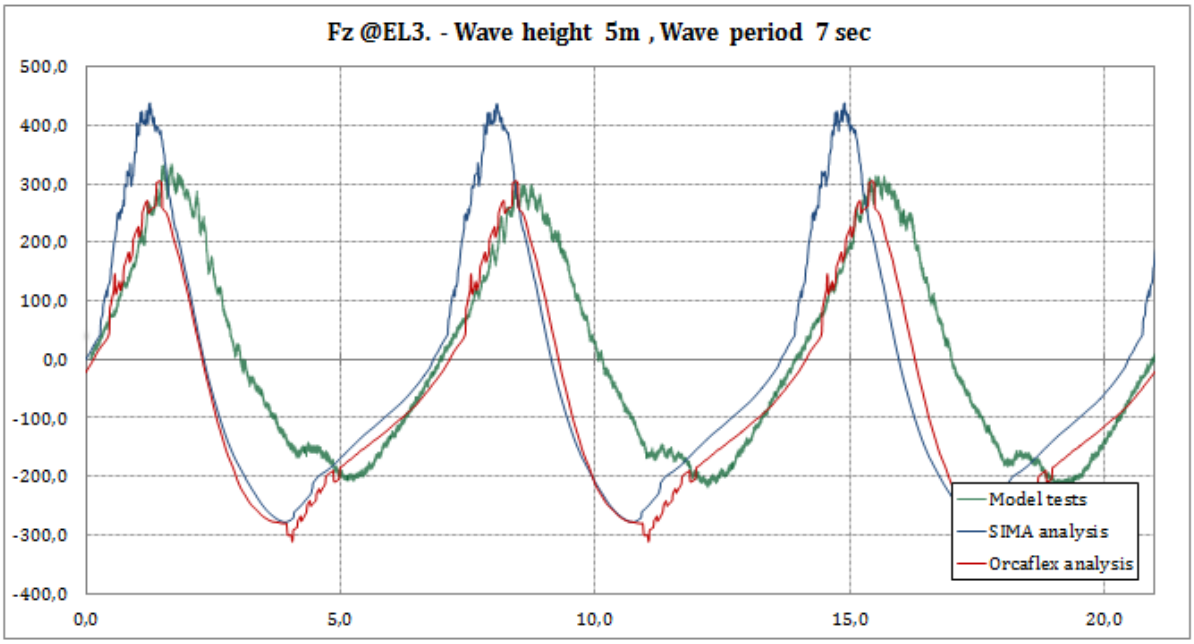
Fz @EL3. - Wave height 5m , Wave period 7 sec
500,0
400,0
300,0
200,0
100,0
0,0
-100,0
-200,0
-300,0
-400,0
0,0
5,0
10,0
15,0
20,0
Model tests
SIMA analysis
Orcaflex analysis

Case 8:

Fx

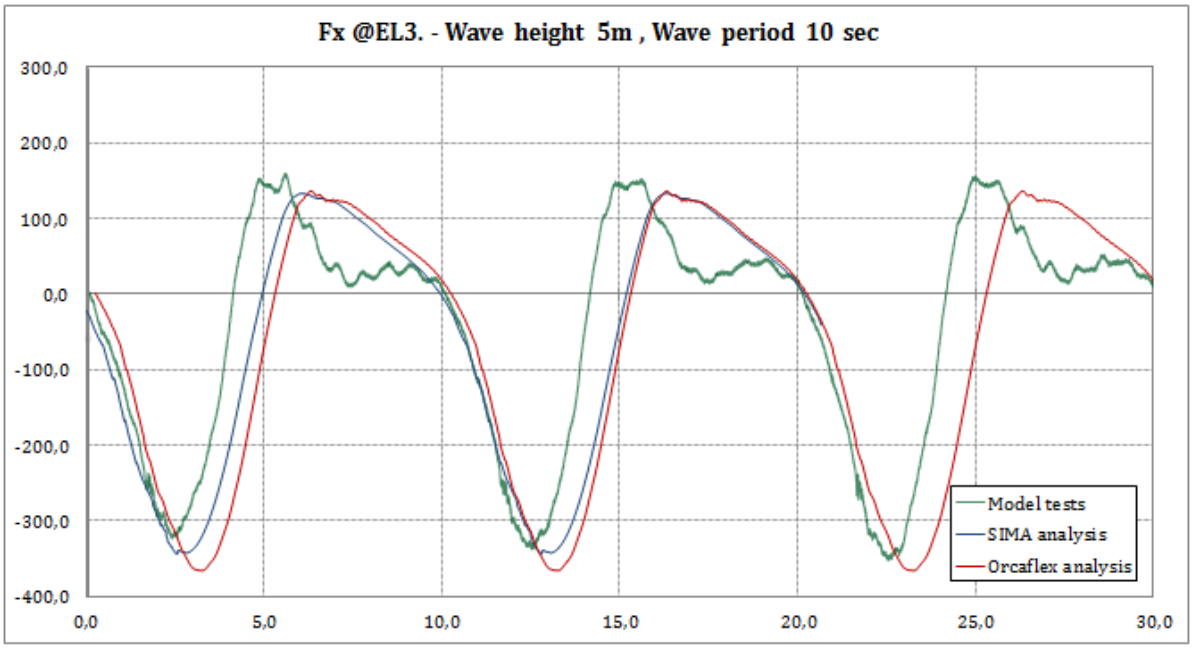
Fx @EL3. - Wave height 5m , Wave period 10 sec
300,0
200,0
100,0
0,0
-100,0
-200,0
-300,0
-400,0
0,0
5,0
10,0
15,0
20,0
25,0
30,0
Model tests
SIMA analysis
Orcaflex analysis

Fz

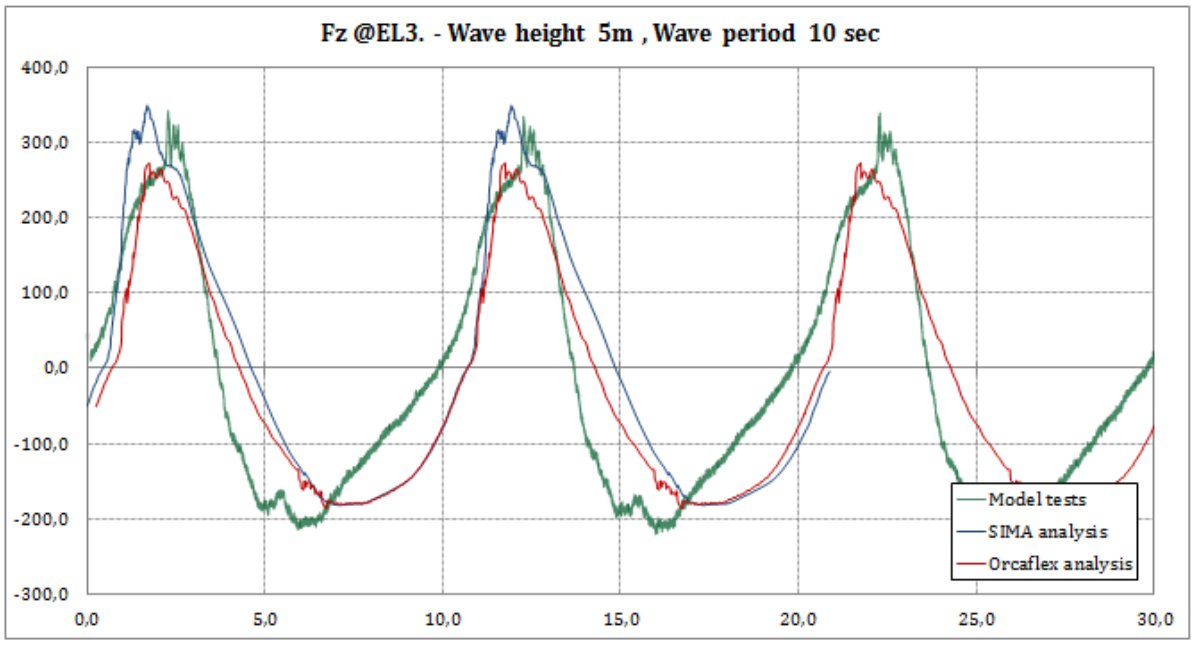
Fz @EL3. - Wave height 5m , Wave period 10 sec
400,0
300,0
200,0
100,0
0,0
-100,0
-200,0
-300,0
0,0
5,0
10,0
15,0
20,0
25,0
30,0
Model tests
SIMA analysis
Orcaflex analysis

Case 9:

Fx

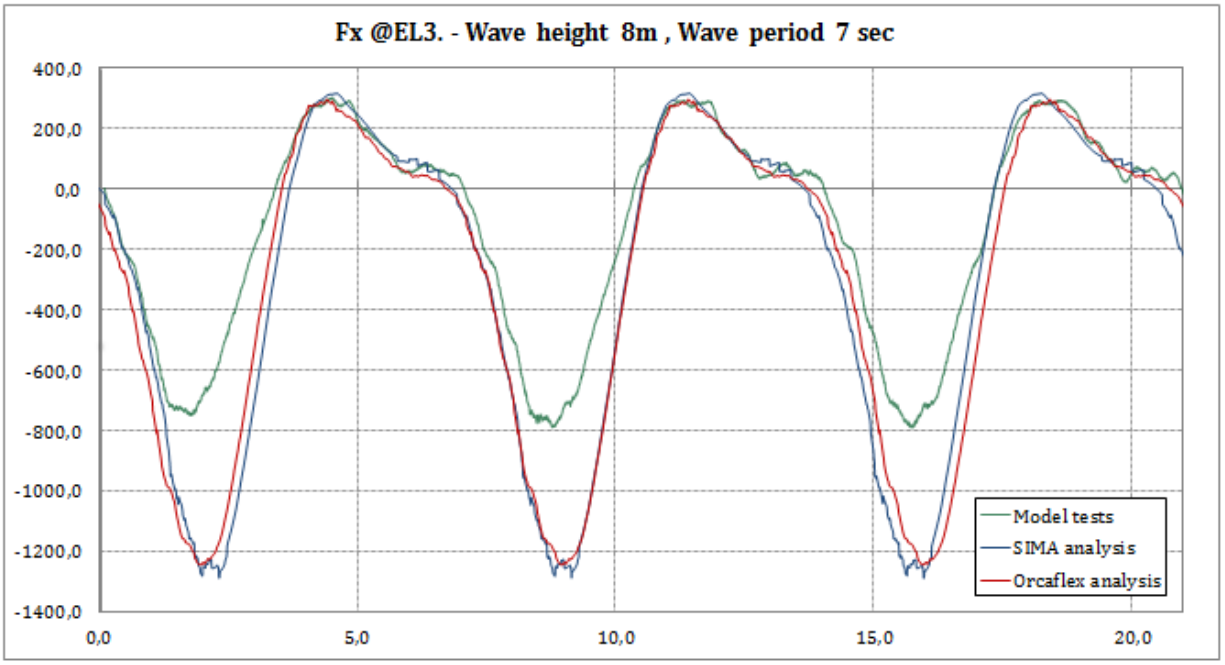
Fx @EL3. - Wave height 8m , Wave period 7 sec
400,0
200,0
0,0
-200,0
-400,0
-600,0
-800,0
-1000,0
-1200,0
-1400,0
0,0
5,0
10,0
15,0
20,0
Model tests
SIMA analysis
Orcaflex analysis

Fz

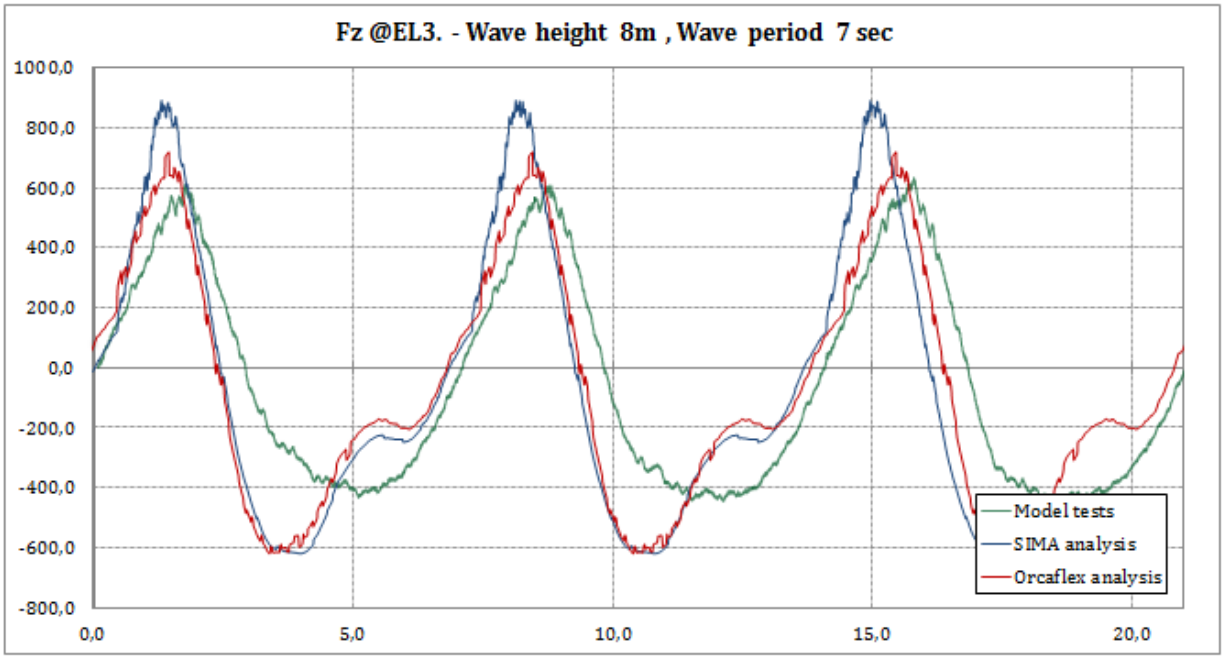
Fz @EL3. - Wave height 8m , Wave period 7 sec
1000,0
800,0
600,0
400,0
200,0
0,0
-200,0
-400,0
-600,0
-800,0
0,0
5,0
10,0
15,0
20,0
Model tests
SIMA analysis
Orcaflex analysis

Case 10:

Fx

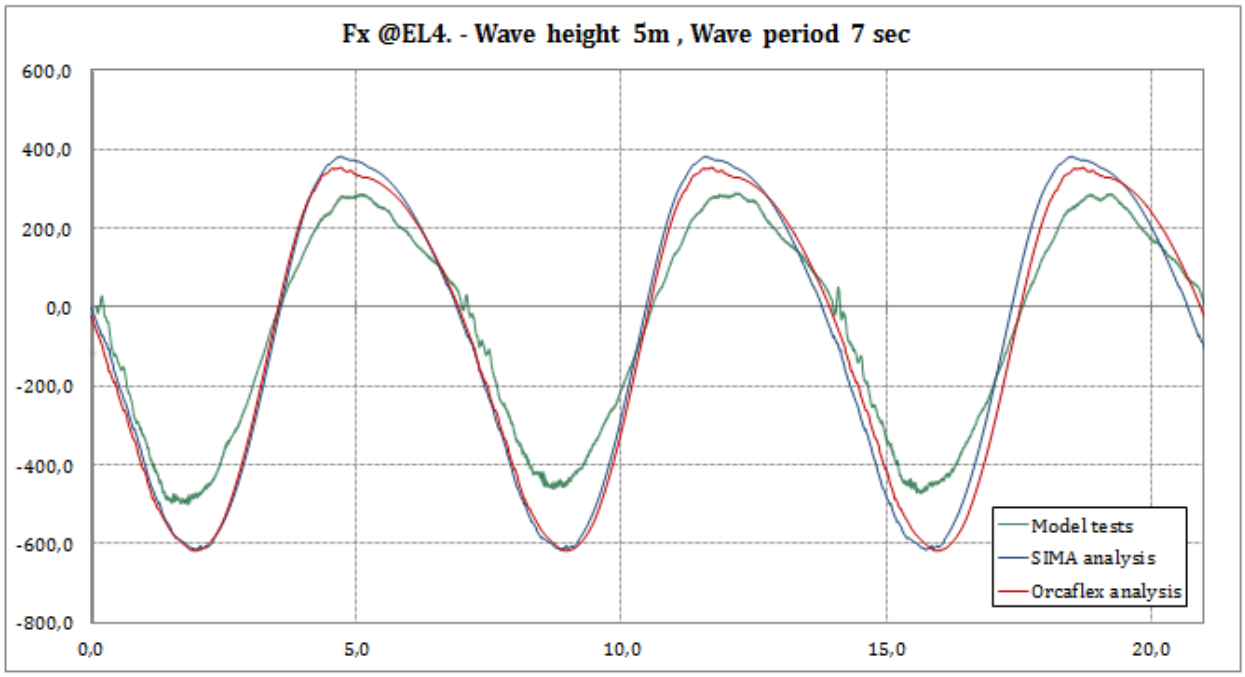
Fx @EL4. - Wave height 5m , Wave period 7 sec
600,0
400,0
200,0
0,0
-200,0
-400,0
-600,0
-800,0
0,0
5,0
10,0
15,0
20,0
Model tests
SIMA analysis
Orcaflex analysis

Fz

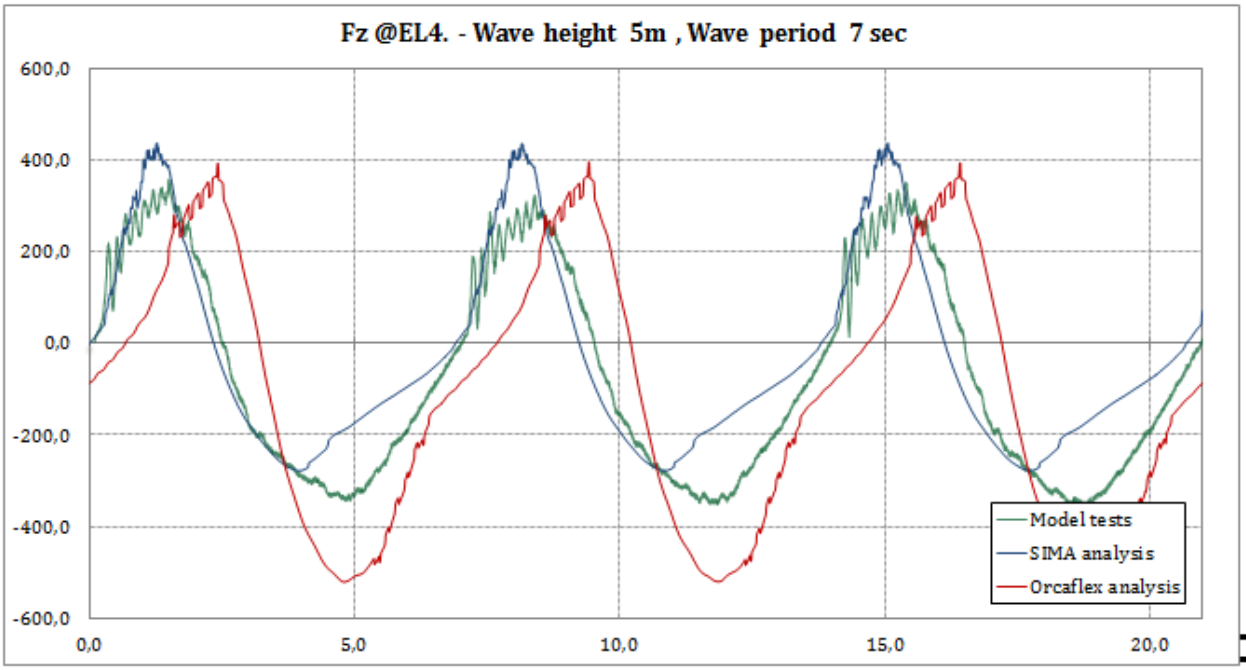
Fz @EL4. - Wave height 5m , Wave period 7 sec
600,0
400,0
200,0
0,0
-200,0
-400,0
-600,0
0,0
5,0
10,0
15,0
20,0
Model tests
SIMA analysis
Orcaflex analysis

Case 11:

Fx

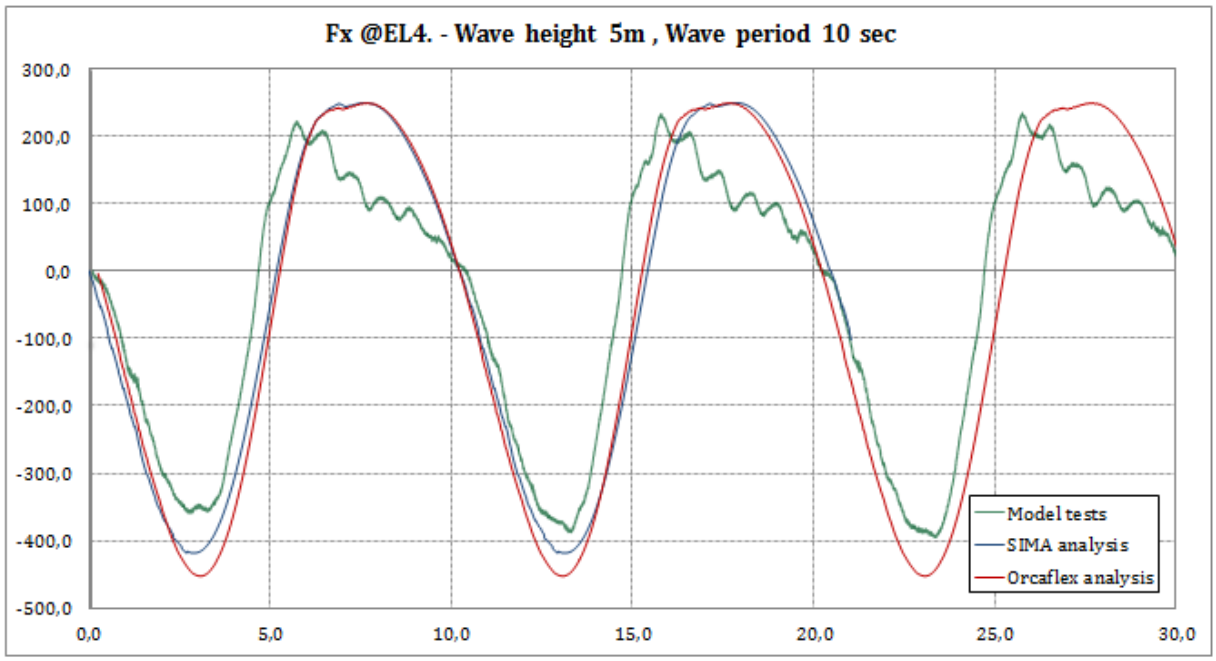
Fx @EL4. - Wave height 5m , Wave period 10 sec
300,0
200,0
100,0
0,0
-100,0
-200,0
-300,0
-400,0
-500,0
0,0
5,0
10,0
15,0
20,0
25,0
30,0
Model tests
SIMA analysis
Orcaflex analysis

Fz

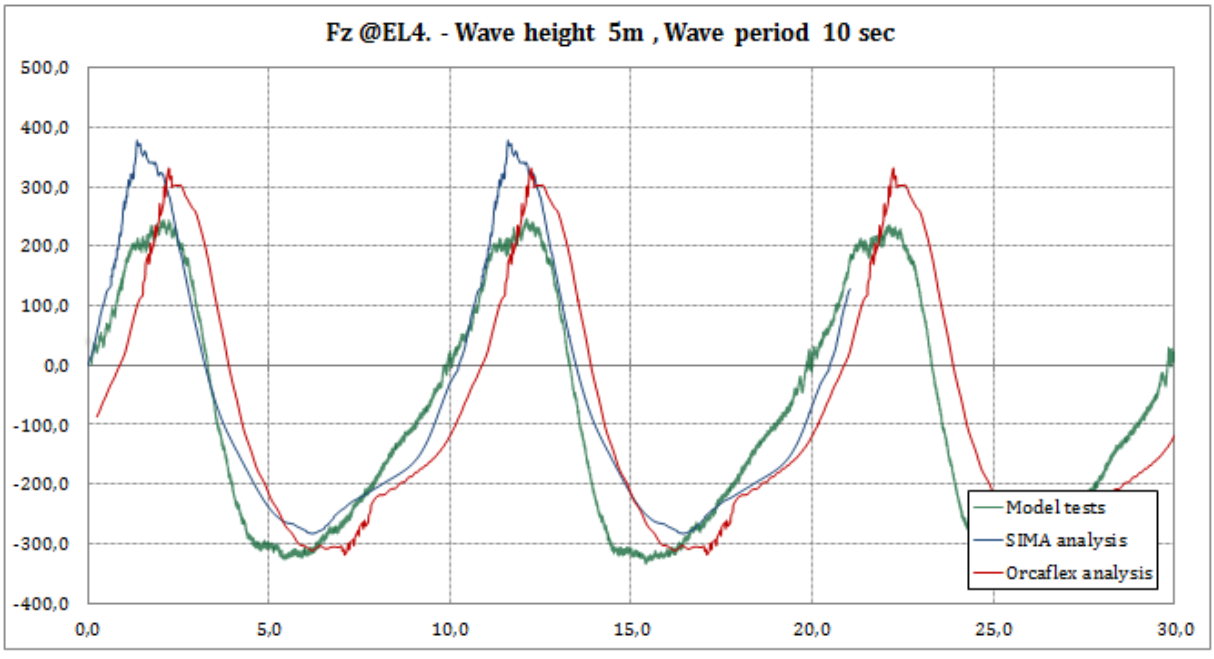
Fz @EL4. - Wave height 5m , Wave period 10 sec
500,0
400,0
300,0
200,0
100,0
0,0
-100,0
-200,0
-300,0
-400,0
0,0
5,0
10,0
15,0
20,0
25,0
30,0
Model tests
SIMA analysis
Orcaflex analysis

Case 11:

Fx

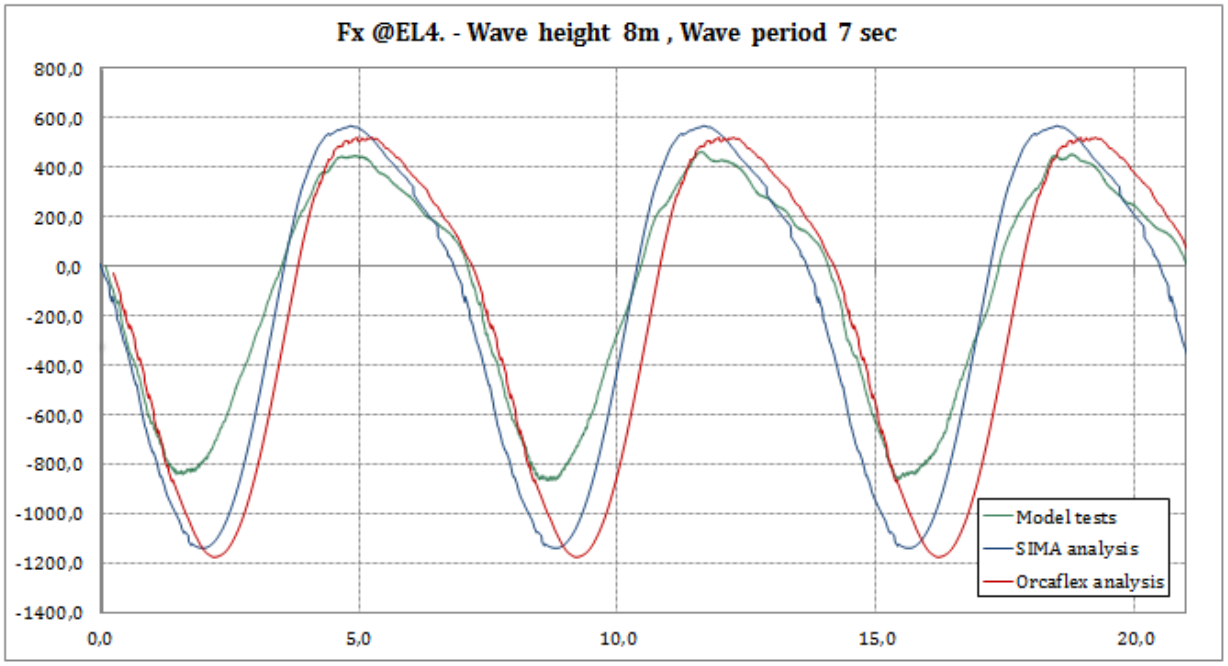
Fx @EL4. - Wave height 8m , Wave period 7 sec
800,0
600,0
400,0
200,0
0,0
-200,0
-400,0
-600,0
-800,0
-1000,0
-1200,0
-1400,0
0,0
5,0
10,0
15,0
20,0
Model tests
SIMA analysis
Orcaflex analysis

Fz

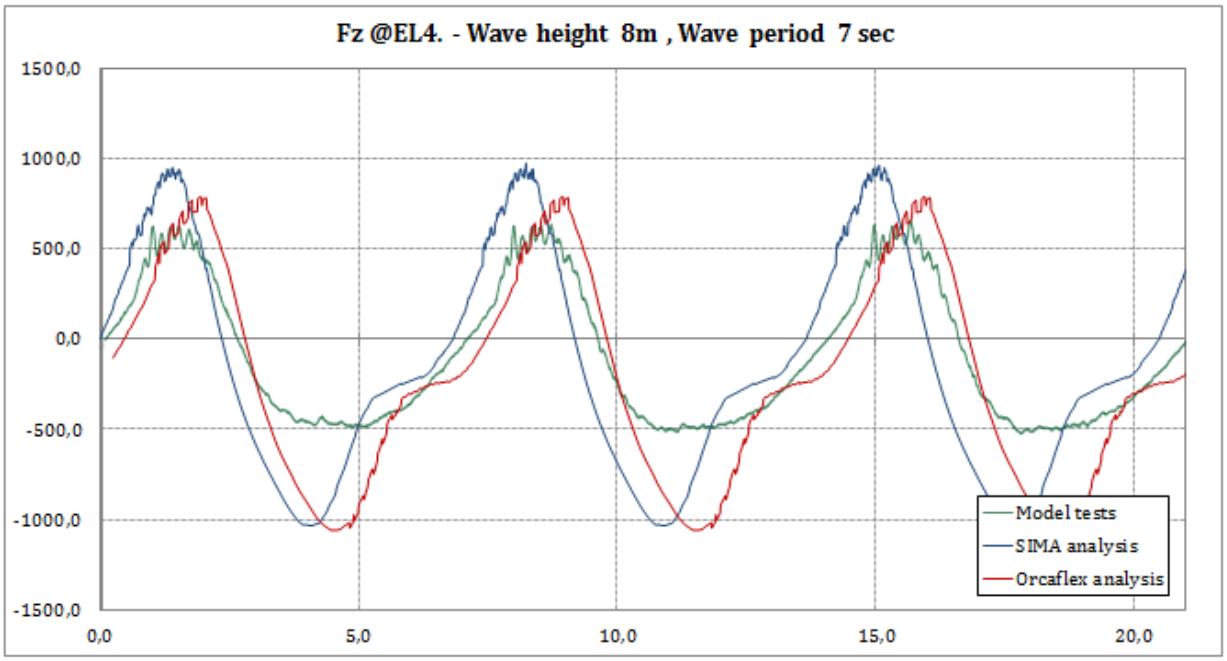
Fz @EL4. - Wave height 8m , Wave period 7 sec
1500,0
1000,0
500,0
0,0
-500,0
-1000,0
-1500,0
0,0
5,0
10,0
15,0
20,0
Model tests
SIMA analysis
Orcaflex analysis

APPENDIX 9: SUMMARY OF FORCE COMPARISON

Global Horizontal forces									
Project:	Master thesis - ASGARD Subsea Compression Module - Numerical Wave tests								
Test number	Elevation	Environment		SIMA-calculation		Orcaflex-calculation		Model test results	
		H [m]	T [s]	F_{Max}	F_{Min}	F_{Max}	F_{Min}	F_{Max}	F_{Min}
1	1	5,3	7,0	0,0	-182,4	0,2	-146,1	23,2	-120,6
4	2			41,3	-302,8	37,2	-295,4	49,7	-208,4
7	3			226,6	-561,7	211,3	-545,5	208,5	-414,6
10	4			380,3	-616,4	353,0	-618,5	294,1	-501,6
2	1	5,8	10,0	0,0	-121,0	1,1	-99,7	24,2	-150,6
5	2			30,4	-175,7	34,5	-190,2	72,0	-222,3
8	3			132,6	-344,6	136,2	-366,0	174,0	-355,5
11	4			249,8	-418,6	249,5	-452,9	235,1	-411,7
3	1	7,8	7,0	0,0	-484,0	1,3	-462,6	40,3	-365,3
6	2			51,3	-911,1	48,9	-811,3	88,3	-497,3
9	3			315,1	-1289,6	295,3	-1245,7	310,8	-792,4
12	4			566,5	-1140,6	518,6	-1177,0	462,9	-871,2

Global Vertical forces									
Project:	Master thesis - ASGARD Subsea Compression Module - Numerical Wave tests								
Test number	Elevation	Environment		SIMA-calculation		Orcaflex-calculation		Model test results	
		H [m]	T [s]	F_{Max}	F_{Min}	F_{Max}	F_{Min}	F_{Max}	F_{Min}
1	1	5,3	7,0	128,1	-2,2	237,3	-83,0	138,6	-46,9
4	2			355,5	-34,0	454,7	-118,9	347,0	-54,5
7	3			438,2	-278,1	304,7	-311,5	335,9	-222,1
10	4			475,8	-485,9	396,9	-521,2	367,2	-360,1
2	1	5,8	10,0	170,7	0,0	257,9	-61,4	173,7	-63,3
5	2			289,3	-0,3	393,4	-79,5	308,4	-94,7
8	3			350,0	-182,0	273,5	-186,5	343,3	-238,9
11	4			378,2	-282,7	331,8	-319,7	246,0	-342,6
3	1	7,8	7,0	317,1	-142,0	543,5	-325,9	323,9	-205,1
6	2			591,1	-254,7	678,3	-362,0	612,6	-247,0
9	3			890,9	-619,9	719,2	-619,8	653,3	-456,2
12	4			977,8	-1034,2	789,4	-1062,7	661,7	-526,8

APPENDIX 10: CORRESPONDANCE WITH ORCINA

Hi Anders,

This is clearly a very complex model, so it's going to be difficult to identify which particular forces are causing the drop in force that you are seeing in the WaterLevel 4.06m cases.

I therefore investigated the effect of removing some of the hydrodynamic loads in the model. I started of by suppressing the buoy hydrodynamic forces and found that the connection loads on the vessel did not change very much. So I then suppressed the hydrodynamics for the lines as well and was surprised to find that this too did not significantly affect the results.

I initially wondered if there was some difference in the way slam loads are ramped between the two programs, but found that suppressing the slam loads made very little difference. Similarly, I tried changing the height of the buoys to see if the ramping of buoyancy and hydrodynamic forces with proportion wet was responsible, but again there was no significant difference.

Consequently, I am drawn to the conclusion that the loads on the system are buoyancy dominated. Since the drop in load shown by your plots is fairly large, this suggests that there is some difference in the way buoyancy is calculated for partially submerged objects. I am reluctant to believe this as these forces are not difficult to calculate, but the evidence suggests otherwise, so further investigation would be worthwhile. Also, a model with all the buoys removed gave similar results to the full model, suggesting that the lines dominate the behaviour.

Rather than try to identify which effects are causing the differences in loads with the existing model with all its complexity, I would be inclined to construct much simpler models containing for example a single line or a single buoy attached to the vessel. I would also examine the various loads individually by switching them on and off. You can remove the buoyancy force for lines by setting their geometrical OD to be negligibly small and retain drag by setting a realistic drag diameter. However, it's not possible to have fluid inertia forces without displacement. So, I would suggest looking at the objects firstly with only buoyancy forces, then with buoyancy and inertia and finally with only drag applied.

regarding the comparison between calculation and experiment, I note that the Reynolds' number is very large for some of the lines in the model. For example Re for Pipe 44 is of order 1.0 E+9 or more over most of the line. It might be more appropriate to use Re dependent drag coefficients under these circumstances.

There isn't really a great deal more I can say. we don't have a copy of SIMO, so we are not in a position to carry out any comparisons ourselves, but I would strongly recommend running a set of very simple comparison cases to investigate the differences between the models. If these identify anything, we would very much like to be informed.

Best regards,

Colin Blundell

Orcina Limited,
Daltongate, Ulverston, Cumbria,

APPENDIX 11: COMPRESSOR MODULE AS BUILD BY OCEANIDE